Solar Energy 215 (2021) 266–310

Contents lists available at ScienceDirect

Solar Energy

journal homepage: www.elsevier.com/locate/solener

Review

A comparison and evaluation of innovative parabolic trough collector concepts for large-scale application

José Fredriksson [a,b,*], Martin Eickhoff [a], Lutz Giese [b], Michael Herzog [b]

[a] German Aerospace Center (DLR), Institute of Solar Research, Apartado 39, 04200 Tabernas, Spain
[b] University of Applied Sciences Wildau, Hochschulring 1, 15745 Wildau, Germany

ARTICLE INFO

Keywords:
Concentrated solar power
Parabolic trough collector
Innovation
Molten salt
Technical-economic evaluation
Parasitic consumption
Solar field costs

ABSTRACT

The present review defines the state of the art of parabolic trough collectors and identifies the concepts in the framework of innovation's requirements. These are the increase of operating temperatures and of the power plant's overall efficiency, as well as the cost reductions of the solar field by eliminating components and the reduction of parasitic power consumption (Pitz-Paal et al., 2007). The study investigates 34 collector concepts and classifies them according to their main structural features like mechanisms or materials. The categories include conventional collectors in Category A, collectors with alternative structure and sheet reflectors in Category B, with non-metallic materials like sandwich composite structures and concrete in Category C, with enclosed aperture in Category D and with fixed focus in Category E. For the technical-economic comparison, two conventional collectors vs. 14 innovations are analysed, following a design engineering method. The definition of a metric table defines the technical comparison criteria for those collectors suitable for thermo-oils or molten salts as heat transfer fluid. Results show that collectors operating with molten salts, instead of thermo-oil, have a significant techno-economic potential for utility scale application, for instance, the Molten Salt Trough, the UltimateTrough and the SkyFuelDSP (dispatchable solar power) as forerunners of their respective categories. Results show also that the inflatable Heliovis collector operating with thermo-oil has a relevant economic potential.

1. Introduction

Concentrated solar power technologies became of relevance with the first parabolic trough solar power plants after the oil crisis in the 1980's, when the hazard of an energy shortage was feasible. Today the struggle of securing energy supplies remains and as fossil energy resources gradually deplete, renewable energies represent the alternative pathway (Janotte, 2012). The last report of the International Energy Agency sums up the current energetic consumption coverage by source, where 79.5% are provided by fossil fuels and 17.2% from renewables. It states that a significant impact on the global climate can be the consequence, if the fossil energy consumption tendency does not change (Enriquez, 2017). In this context, the limitation of CO_2 and greenhouse gas emissions due to fossil fuels means, in fact, the greatest motivation to search for environmentally sustainable systems. To achieve this, mitigation of greenhouse gas emissions is the key strategy, which incentives the drastic reduction of current and future emissions caused by transport, industry, electricity generation and individual consumption of fossil energy (Janotte, 2012).

Solar thermal energy together with biomass and geothermal heat, correspond to only 4.1% of the global renewable sources share. Within the solar thermal branch, parabolic trough power plants remain with the greatest share of installed concentrating solar technologies. Worldwide it covers 66% of the concentrated solar power (CSP) projects, followed by solar towers (24%), Fresnel collectors (9%) and Dish/Stirling collectors (1%) (SolarPaces & IEA, 2019). All together are covering 5.8 GW of the worlds total energy consumption basis and in the near future additional power plants will supply further 3.8 GW (SolarPaces & IEA, 2019).

The Sun is the richest disposal source of renewable energies, where its radiation can be used by photovoltaic technology to directly generate electricity or by concentrated solar thermal-to-electric systems. On one hand photovoltaic technologies gained high importance in the market, due to the drastic decrease of its costs and the possibility to deploy solar fields at both, small and large scale in the megawatt range. With this, the

* Corresponding author.
E-mail addresses: eng.fredriksson@gmail.com (J. Fredriksson), martin.eickhoff@dlr.de (M. Eickhoff), lutz.giese@th-wildau.de (L. Giese), michael.herzog@th-wildau.de (M. Herzog).

https://doi.org/10.1016/j.solener.2020.12.017
Received 4 May 2020; Received in revised form 7 December 2020; Accepted 8 December 2020
Available online 16 January 2021

Nomenclature

Latin letters

A_{col}	collector aperture area [m^2]
A_{eff}	effective aperture area [m^2]
A_{loop}	collector loop aperture area of [m^2]
A_{rec}	receiver projected area [m^2]
a	aperture width of collector [m]
C_g	geometrical concentration ratio [–]
$cos(\theta_i)$	cosine losses [–]
c_p	specific heat capacity factor [J/kg·K]
d_{ci}	receiver's cover inner diameter [mm]
d_{co}	receiver's cover outer diameter [mm]
d_{ri}	receiver tube's inner diameter [mm]
d_{ro}	receiver tube's outer diameter [mm]
DNI	Direct Normal Irradiance [W/m^2]
E_u	useful exergy production [–]
E_s	exergy flow of the solar irradiation [–]
f	focal length [m]
f_m	mean focal length [m]
$G_{b,ap}$	direct irradiance on the collector's aperture [W/m^2]
G_{im}	radiant flux at the focal line [W/m^2]
H	solar field cost of collector concept [€/m^2]
$H_{baseline}$	baseline cost, i.e. UltimateTrough [€/m^2]
$H_{M,min}$	market lowest achievable cost [€/m^2]
l_{col}	collector module length [m]
l_{loop}	loop length [m]
M	mass [kg]
$\dot{m}_{HTF}$	mass flow of heat transfer fluid [kg/s]
$\dot{m}_{design}$:	mass flow at design point [kg/s]
n	number of obstacles [–]
n_c	number of evaluated criteria [–]
P_{el}	electric power [W_{el}]
$P_{pump,el}$	electric power consumption of the HTF pump [W_{el}]
p_{max}	maximal value of total of points [–]
$p_x, \bar{p}_x$	value of criteria x and mean values [–]
$\dot{q}_{loss}$	specific thermal losses [W/m]
$\dot{Q}_{con,abs}$	concentrated absorbed power [W_{th}]
$\dot{Q}_{eff}$:	effective thermal energy [W_{th}]
$\dot{Q}_{loss}$	thermal losses [W_{th}]
S, S_f	centre of mass, centre of mass on focal axis [–]
$S^{\hat{A}'}, S^{\hat{A}'\hat{A}'}$	centre of mass of an element [–]
T	torque [Nm]
T_{amb}	ambient temperature [K]
$T_{in,SF}$	inlet temperature in solar field [°C]
$T_{out,SF}$	outlet temperature in solar field [°C]
$\dot{V}_{HTF}$	volumetric flow of heat transfer fluid [m^3/h]
X	technical value [–]
Y	economic value [–]

Greek Symbols

α	absorptance [–]
β	solar field cost levelling factor [–]
γ	intercept factor [–]
Δp	overall pressure drop [bar]
$\Delta p_{crossover}$	pressure drop in crossover components [bar]
Δp_{HTF}	pressure loss in the solar field [bar]
$\Delta p_{obstacles}$	pressure drop in obstacles [bar]
$\Delta p_{receiver}$	pressure drop in the receivers [bar]
ΔT	temperature difference [K]
ε	emittance [–]
η_{clean}	cleanness efficiency factor [–]
η_{col}:	collector thermal efficiency [–]
η_{end}	end loss efficiency factor [–]
η_{ex}	exergy efficiency
η_{length}	effective length factor [–]
$\eta_{loss,pipe}$	pipeline thermal losses
$\eta_{opt,peak}$	peak optical efficiency [–]
$\eta_{parasitic}$	parasitic consumption [%]
η_{PB}	power block efficiency
η_{pump}:	heat transfer fluid pump efficiency [–]
η_{SF}	solar field efficiency [–]
η_{shade}	shade loss efficiency factor [–]
$\eta_{solar-to-electric}$	solar to electric efficiency of solar power plant [–]
$\eta_{torsion}$	losses due to structural mechanical torsion [–]
η_{track}	losses due to imperfect tracking [–]
Θ_T	torque angle from the mid-plane [rad]
θ_i	incidence angle
λ	friction coefficient for a turbulent stream [–]
$\xi_{90°}$	pressure loss coefficient for 90°-elbows [–]
ρ_{mean}	mean density of heat transfer fluid [kg/m^3]
ρ	tracking angle [rad]
σ_{spec}	standard deviation of specular reflectance [–]
τ	transmittance [–]
ψ	rim angle [°]

Acronyms

BOP	balance of plant
BO-PET	biaxial orientated polyethylene terephthalate
C&I	commercial and industrial
CSP	concentrated solar power
CNT	carbon nanotube
DLR	Deutsches Zentrum für Luft- und Raumfahrt
DSG	direct steam generation
ENEA	Ente Nuove tecnologie Energia e Ambiente
Eq.	Equation
EOR	enhanced oil recovery
ET	EuroTrough
ETFE	ethylene tetrafluorethylene
HCE	heat collector element
HS	heated steam
HTF	heat transfer fluid
MS	molten salt
MWCNT	multi-wall carbon nanotube
N.A/n.a.	not available
NREL	National Renewable Energy Laboratory
LCOE	levelized cost of energy
LF	linear Fresnel
O&M	operations and maintenance
PS	Polystyrol
PTC	parabolic trough collector
PTR	parabolic trough receiver
PU	Polyurethane
PVC	polyvinylchloride
PVD	physical vapour deposition
SAM	system advisor model
SCA	solar collector assembly
SCE	solar collector element
s-diagram	strength diagram
SEGS	Solar Electric Generating Systems
SF	solar field
Skal-ET	scaled EuroTrough
SWCNT	single-wall carbon nanotube
TO	thermal oil
UHPC	ultra-high performance concrete
UT	UltimateTrough
VDI	Verein Deutscher Ingenieure/ Association of German Engineers

price of photovoltaic power installations decreased between 2005 and 2014 from 40 ct/kWh to 9 ct/kWh and even to 4–6 ct/kWh at adequate solar conditions (ISE, 2015). On the other hand, CSP experienced a market breakthrough in the beginning of the 2000s, mainly due to the integration of solar thermal storage blocks in the solar field, which enables the disposition of energy to the grid even after sun hours. Thus the first power plant in Europe *Andasol 1* produced energy for 27 ct/kWh in 2006 and future prices target 6.6 ct/kWh[1] in 2021 within a hybrid power plant project (PV + CSP) in Dubai *DEWA* (SolarPaces & IEA, 2019). Despite this, solar thermal power plants carry significantly higher financial investments and risk in comparison to photovoltaic deployments.

In conventional parabolic trough power plants, around 38.5% of the investments are driven by the solar field (IRENA, 2012). Even though significant tariff reductions were achieved and projected, the potential of further reducing the costs and enhancing the performance of solar power plants is possible: first by up scaling effects, second by increasing operational temperatures and subsequently the global efficiency, and third through reduction of components in the solar field (Ruegamer et al., 2014). For these reasons, the present review investigates the different types of current innovative parabolic trough collector concepts that have the potential to meet these requirements. It also compares those technologies that can enhance the cost efficiency of solar plants with the implementation of molten salt as heat transfer fluid.

The review starts with a general description of the state of the art essential components for a parabolic trough collectors. In Chapter 3 a categorization between conventional and innovative technologies is summarized highlighting the main attributes for each of them. Chapter 4 presents the technical evaluation criteria with a respective analysis. The chapter includes also the metric guidelines and the evaluation matrix methodology proposed in the present review.

2. State of the art

Parabolic trough collectors belong to line focusing systems with a one axis tracking mechanism. They concentrate the solar energy by reflecting direct normal irradiance into the collectoŕs focal line. At this height, a selective coated and vacuum isolated receiver absorbs the thermal energy into the streaming heat transfer fluid (HTF) from the inlet to the outlet of the tube as shown in Fig. 1. This heat is transferred rather into a steam cycle to drive a steam turbine or it is led into the storage block. This additional storage block gives solar power plants the characteristic of energy dispatchability, which enables the access to electrical power in the absence of sun.

Harvesting of the solar energy to yield designed operational temperatures happens in the solar field. State of the art solar fields operate with an input temperature $T_{in,SF} = 295^{\circ}C$ and an output temperature $T_{out,SF} = 400^{\circ}C$ (Schenk & Eck, 2012). Extensive modular series of parallel collector rows called loops give shape to the solar field. Header and piping interconnections complete the circuit between the loops, the storage system and the power block.

The smallest unit in a solar field is the Solar Collector Element (SCE) or collector module. The composition of a loop has a number of solar collector assemblies (SCA), which is the series of adjacent collector modules driven by a single drive. The description of the SCA is what is understood, as the collector in a loop and this is precisely the focus of the present review. Subsequently, a number of SCAs form a collector loop. Fig. 2 shows the loop subdivision within a solar field at the example of a HelioTrough. The number of SCE, SCA units and loop dimensions, can vary depending on the implemented collector, yet the definitions remain general.

The size of the solar field depends on the selected design point (or rated power output) of the plant. If one considers a plant with a thermal storage system, there is another parameter influencing the size of the solar field. For example, it is possible to enlarge the solar field in such a way that its thermal power output is far above than the thermal power output that the power block can convert into electrical energy (Günter et al., 2011). The additional power is directed into the thermal storage and can be used to generate additional energy during periods when solar radiation is not available or scarce. This storage system helps define the rated power of the plant. The ratio between the size of the solar field and the rated output power plant is expressed as the “solar multiple” of the power plant (Günter et al., 2011). More precisely, the solar multiple (SM) is the ratio between the thermal output of the solar field at the design point and the thermal output required for the power unit operating at full load. There is a direct relationship between the SM and the size of the storage tank: larger solar fields (in relation to the nominal power of the power block) require a larger storage tank. This factor is relevant for economical, technical and even political decisions, since the same power block can generate more electric power over the year.

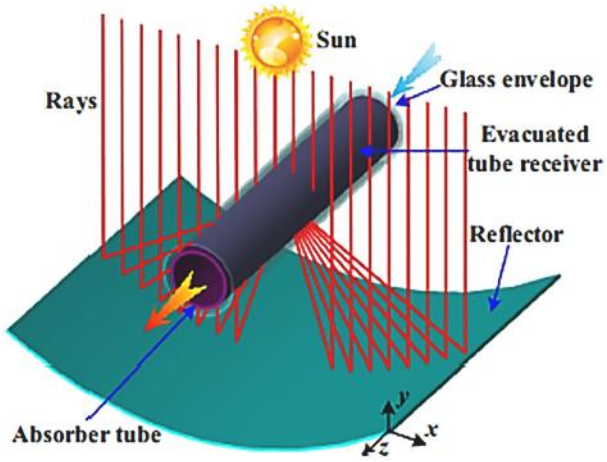

Fig. 1. Concentration of the solar energy at the focal point of a parabolic trough collector (Vijayan & Kumar, 2017).

Fig. 3 a) shows a state-of-the-art utility power plant, Noor I in Morocco, with an installed gross capacity of 160 MW_{el} and 3 h of thermal storage. Another example in Fig. 3 b) is the first European plant Andasol I in Spain with a designed gross capacity of 50 MW_{el} and 7.5 h of thermal storage.

Both examples work with thermal oils in the solar field block, with molten salts in the storage and with a Rankine Cycle in the balance of plant. This configuration is the conventional way of operating the system and a scheme can be seen in Fig. 4. This configuration yields a power plant efficiency between 35% and 38% with a living steam temperature between 375°C and 385°C at 100 bar pressure at the inlet of the main turbine (Enriquez, 2017).

In order to improve the efficiency of the plants and to target investment cost reductions, first investigations have been made to implement molten salts as HTF in the solar field (Maccari et al., 2015; Eickhoff et al., 2015). This medium, which is already been implemented in the storage tanks, would allow the extraction of the thermal exchanger between the solar field and the thermal block, as shown in Fig. 5. The direct connection of these two blocks and the properties of the medium enable solar field outlet temperatures up to 550 °C. Connected to a Rankine power cycle, the solar plants efficiency increases between 43.3% and 46% with a steam temperature between 535 and 550 °C at a pressure of 250 bar at the inlet of the main turbine (Ruegamer et al., 2014; Enriquez, 2017). This is a good practical example of Carnoťs principle, which describes that the maximum operating temperature of the thermodynamic cycle has a direct impact on the net efficiency of the cycle.

[1] 7.3$ct/kWh converted in Euro currency.

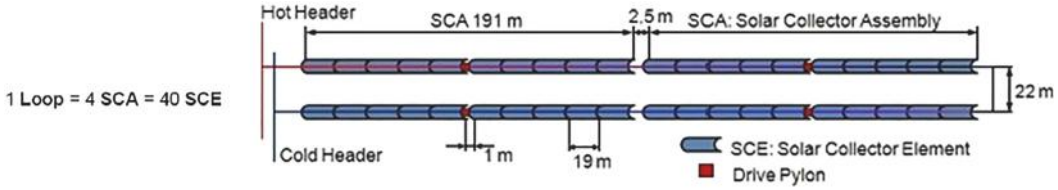

Fig. 2. HelioTrough loop segmentation and dimensions (HelioTrough, 2019).

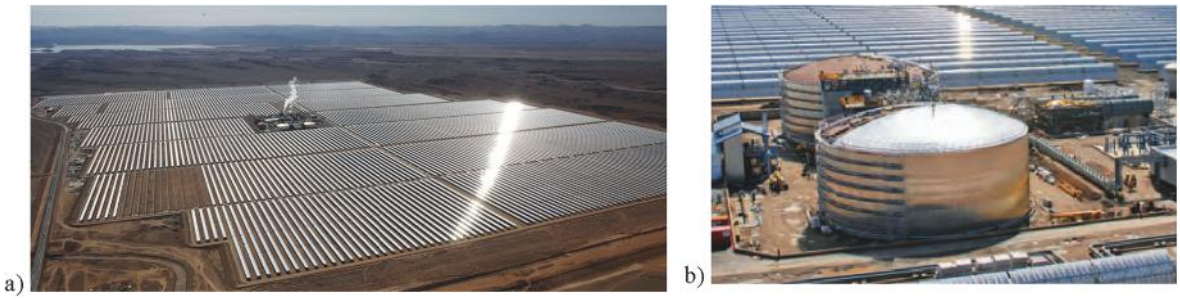

Fig. 3. a) Noor I Solar Plant, Ouarzazate (Edevane, 2016) b) Thermal storage tanks at Andasol1, Spain (Solar Millenium AG, 2008).

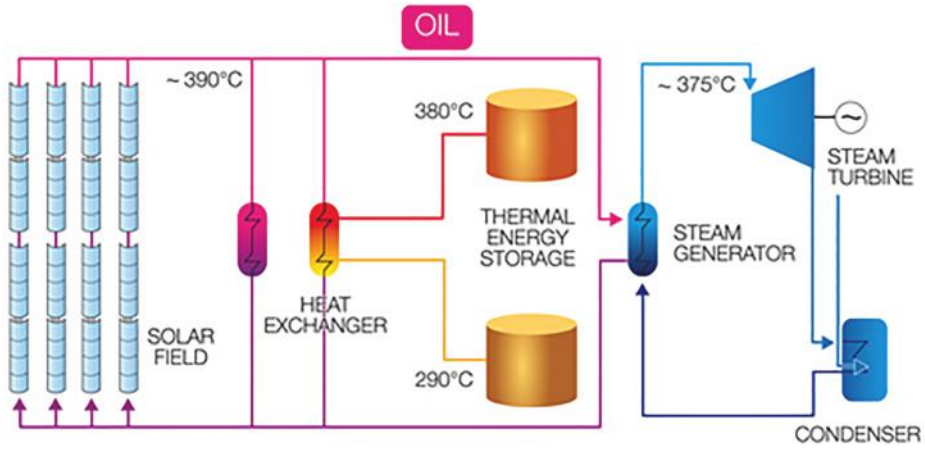

Fig. 4. Solar thermal power plant with parabolic trough collectors and thermal oil as HTF in the solar field (ArchiemedeSolarEnergy, 2019).

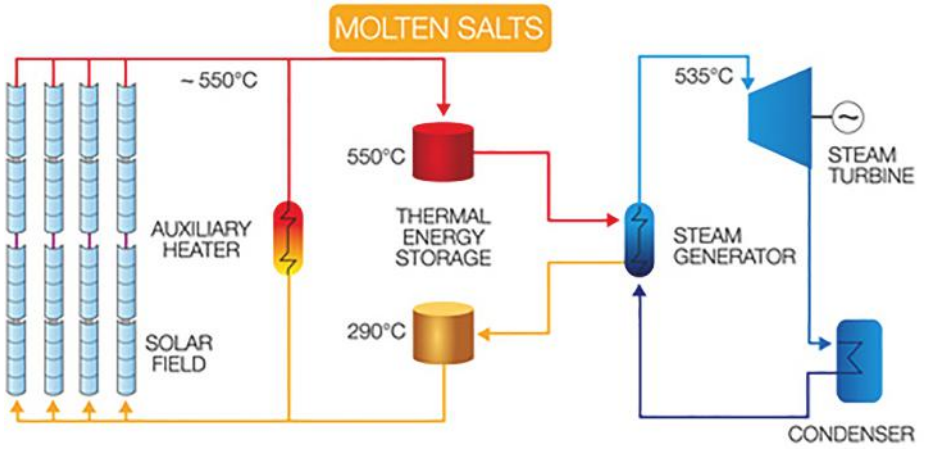

Fig. 5. Solar thermal power plant with parabolic trough collectors and molten salt as HTF in the solar field (ArchiemedeSolarEnergy, 2019).

Alongside the use of molten salt as a promising solution for linear industrial plants, there is the integration of Brayton cycles with super critical carbon dioxide (see Fig. 6). This new generation of plants is constrained to the development of supercritical fluids. Studies on the Brayton cycles show that they are a viable means of increasing the net efficiency of the plant and allow the reduction of solar field costs and optimization of the aperture area (Enriquez, 2017). This configuration was designed in 1967 and adapted for the use in solar plants over the years with carbon dioxide (CO_2) in a supercritical state as reviewed in the following sources (Neises & Turchi, 2014; Ahn et al., 2015). Thanks to the high density of the working fluid compared to the water vapor in the Rankine cycles, the reduction of both turbineś and compensators dimensions, and subsequently of the required civil works, are feasible. An example of the proposed configuration implements a synergy between both solutions: the use of solar fields using molten salt as heat transfer fluid and supercritical CO_2 power cycle.

The development of special components such as turbines, compressors, coolers, piping and heat exchangers, have high requirements to tolerate the exhaustive corrosion caused by the medium, in addition to the high pressure at 250 bar of the Brayton cycle (Dyreby et al., 2014). Commercially different companies are developing these components at an advanced technology readiness level, for example: Heatric and Norwich (Enriquez, 2017). Simulation studies conclude that this synergy between molten salts in the solar field and a Brayton power cycle can achieve a net plant efficiency up to 46.84% with a possible turbine inlet temperature of 550 °C at 250 bar pressure. The specific configuration to get these values requires recompression with main compression intercooling systems (Enriquez, 2017). The same author published a possible plant net efficiency of 50.85% assuming a turbine inlet temperature of 650 °C for the same configuration.

These three configurations presented, are intended to demonstrate the state of the art and two promising directions for the implementation of linear collectors for utility solar plants, namely molten salts solar fields and a synergy with supercritical CO_2 Brayton power cycles. Each of these configurations involves a specific design of the solar field that directly influences the technical and economic parameters of a plant, either by optimizing the necessary effective collection surface or by implementing other heat transfer media. Collectors are an element of development that contribute to a large part of the techno-economic characteristics of a plant. Beyond the size of the solar field and the thermal storage, the collector units have an essential task in the solar field: They first collect and concentrate the input energy of the entire process. More precisely, their specific components define the effectiveness of the solar energy concentration process into the system. Depending on their use, each of them fulfils a series of mechanical, physical and economical requirements. Specific collector designs differ in aspects such as aperture width, concentration ratio, reflector materials, support structure, receiver design and loop configuration (Janotte, 2012). The total optical and thermal performance of a collector, result out of the optical efficiency and the thermal losses of these components respectively (Röger et al., 2014). Fig. 7 gives an overview of the components that are relevant in the definition of a collector at the example of an EuroTrough.

The review focuses from here on providing details about the collector components and their properties that influence the technical performance. Throughout the chapter on the state of the art, certain innovations are mentioned for each of the points presented.

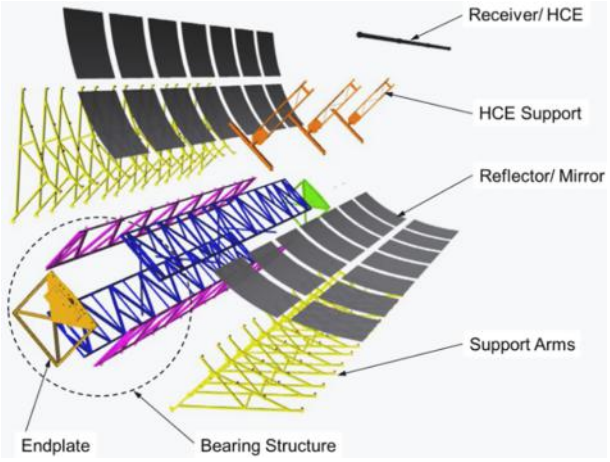

Fig. 7. Main components of a parabolic trough collector at the example of an EuroTrough collector (GIZ, 2014).

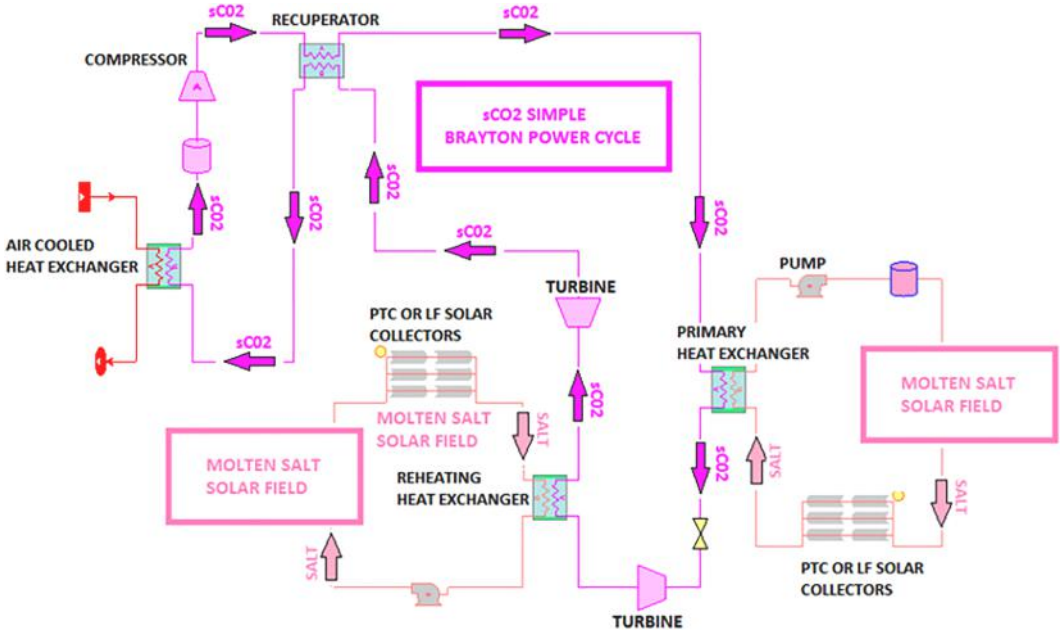

Fig. 6. Solar thermal plant with linear collectors and Brayton power cycle with supercritical CO_2 in a simple configuration with heat recuperation (Enriquez, 2017).

2.1. Geometry and concentration ratio

Parabolic troughs concentrate the incident direct normal irradiance on its focal line. Fig. 8 shows a symmetric parabolic collector and a receiver at focal distance. The analytical representation of the parabola is described in Eq. (1) according to the x/y-system shown in Fig. 8:

$$y = \frac{1}{4f}x^2 \tag{1}$$

Four important parameters define the collector's geometry: aperture width, rim angle, focal length and collector length. Only two of the first three parameters are necessary to determine the size and shape of the parabolic trough collectors as seen in Eq. (2) (Bellos and Tzivanidis, 2018).

$$\psi = \tan^{-1}\left(\frac{8\cdot\frac{f}{a}}{16\cdot\left(\frac{f}{a}\right)^2 - 1}\right) \tag{2}$$

However, the rim angle alone is sufficient to determine the shape of the cross-section of a collector. This means that parabolic troughs with the same rim angle are geometrically similar (Günter et al., 2011). This parameter affects the concentration ratio and the irradiance on the absorber tubes, so it cannot be too small neither too large. Another parameter is the geometrical concentration ratio as given in Eq. (3). The concentration ratio considers the radiant flux at the focal line and the direct irradiance on the collectoŕs aperture area. A simplification of this is the ratio of the collector aperture area to the projected receiver area. The last description is more common and known as the geometrical concentration ratio, considering the receiver and collector length as equal ($l_{col} = l_{rec}$):

$$\mathbb{C}_g = \frac{A_{col}}{A_{rec}} = \frac{a\cdot l_{col}}{d_{ro}\cdot l_{rec}} = \frac{a}{d_{r0}} \tag{3}$$

In conventional parabolic trough collectors a rim angle around 80° is generally used and a concentration ratio of about 82 (expressed as 82 'suns').

2.2. Mirror materials

Mirror materials have the task to concentrate more than 90% of the incident solar radiation on the absorber tube, requiring high specular reflectance and high geometrical precision. Silver and aluminium materials are commonly used due to their highly reflective properties. Their manufacturing and maintenance should contribute to an economically viable option, while offering long time durability and resistance against UV-radiation, breakage, soiling and abrasion.

The optical reflectance (ρ) of a surface is a parameter, indicating the amount of incident solar irradiation that is reflected by this surface. There is a distinction between these two extreme types of reflection: the diffuse scattering reflection in the whole hemisphere (ρ_{hem}) and the specular reflection (ρ_{spec}) (Meyen et al., 2009). The latter one obeys the law of reflection, according to which the incident angle equals the reflected angle of the light beam. Considering irregularities or slope errors of the mirror surface, a certain range of tolerance is defined for this parameter. It is measured with specular reflectometers, which allows an angle of acceptance (σ_{spec}) at 25 mrad (Meyen et al., 2009). For CSP applications, the parameter values are weighted with the solar spectrum, which result in the *solar weighted hemispherical reflectance* (ρ_{SWH}) and the *solar weighted direct reflectance* (ρ_{SWD}). The last one is of relevancy since it indicates the expected amount of sunlight that can hit the absorber (Meyen et al., 2009).

2.2.1. Thick glass

First commercial collectors implemented mirror facets (thickness: 4–5 mm) with a silvered back layer. The low iron-content in the glass increases the light transmission. Panels of that kind demonstrated their initial optical qualities after more than 15 years of operation. The manufacturing of these facets has been enhanced and industrialized over the last 30 years with the increasing number of solar fields. Their specific price per square meter has dropped up to 44%, where current estimates are around 16 €/m^2 (Krüger et al., 2018). Measurements and practical experience have shown the superior quality of silvered glass mirror reflectors compared to alternative materials (Meyen et al., 2009). A large number of conventional collectors use thick glass mirror facets.

2.2.2. Thin glass

These reflectors demonstrated excellent optical qualities, durability, lightweight and cost reduction potential. The material offers a higher degree of flexibility, but it is a sensitive material towards breakage. It requires to be embedded on a rigid structural surface, for instance, with a proper adhesive material. Because of their proven number of benefits these reflectors are been used in some of the innovative concepts (e.g. SL4600+, ToughTrough, Split Mirrors and MS-Trough). Further research investigates the use of ultra-thin flexible glass reflectors with a thickness of 100 μm and the standard coating structure. This product is nevertheless not commercially available by now (Krüger et al., 2018).

2.2.3. Aluminized reflectors

They are based on an aluminium substrate, commonly applying high-purity aluminium as the reflective layer followed by a protective top coat. The performance on reflectivity and durability has been too insufficient to get the breakthrough for large-scale CSP application. They are nevertheless thanks to the low weight, an economical alternative and studies show the potential of optical improvements (DLR et al., 2018). Later studies have demonstrated an optimized layer system in comparison to commercially used reflectors. In this example, the solar direct reflectance increased from 82.6% to 92.3% by using a reflective silver coating and silicon nitride (Si_3N_4) as top layer (Krüger et al., 2018).

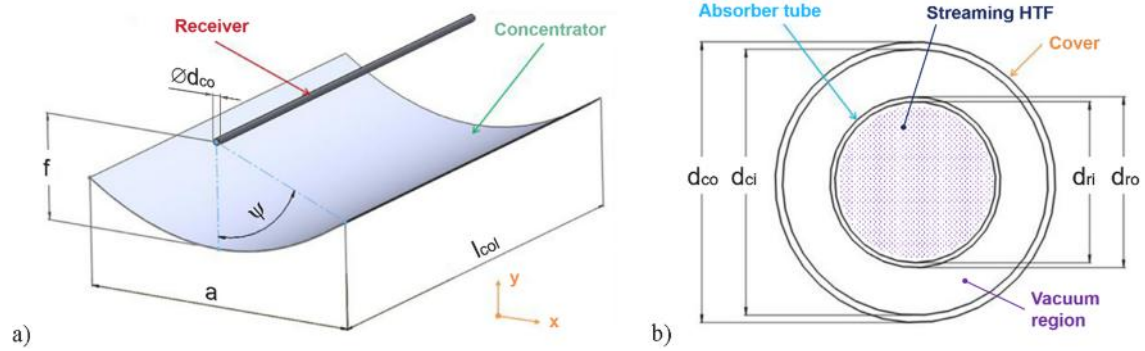

Fig. 8. a) Geometrical parameters of a parabolic trough collector b) "cross-section of the evacuated receiver tube" (Bellos and Tzivanidis, 2018).

2.2.4. Polymeric films

Since the 1990s, this type of reflectors have been optimized in terms of optical performance and longevity. Polymeric films also have been compared to glass and aluminium reflectors. Results show that the smoothness of the surface is not sufficient to reach the values of glass mirrors in terms of specular reflection. In fact, they show a beam deviation of 0.9 mrad in an experimental comparison study to glass with less than 0.3 mrad (Meyen et al., 2009). This means that polymeric films are characterized by a wider beam deviation from the expected incident focal range than glass mirrors.

Even though aluminium coated and polymeric film reflectors have been implemented, their main challenge to overburden is that of longevity. Both are front surface reflectors, which cause a higher exposition of the reflective surfaces to the environment. From this follows a faster decrease of the specular direct reflectance of these materials (Meyen et al., 2009).

2.3. Receivers

Receivers have the task to absorb the incident radiation and gain the thermal energy into the heat transfer fluid. Receivers for operational temperatures greater than 300 °C use commonly vacuum isolated tube to enhance the thermal performance (Eduardo Zarza, 2012). In this case, the vacuum isolated glass envelope covers the absorber tube inside, which is made of stainless steel or carbon steel. The purpose to implement evacuated receiver tubes with a residual gas pressure of less than $\leq 10^{-3}$ mbar is precisely to mitigate the convection losses that occur in the concentration process (SCHOTT Solar CSP GmbH, 2013). In an operational solar field, heat losses occur in the receivers and the heat transfer fluid pipes. These losses depend on the temperature difference between the heat transfer fluid and the surrounding.

Technology improvements to reduce thermal losses and to increase resistance against glass breakage were developed. On one hand, when thermal oils are used in the system during an operation period, the fluid tends to expel hydrogen molecules (H_2). These molecules scatter through the metal tube into the cavity under vacuum. As a result, the vacuum is deteriorated and the “hot tube phenomenon” occurs, involving overheating of the tube and causing an increase in thermal losses of up to a factor 6 (SCHOTT Solar CSP GmbH, 2013). An early solution to this phenomenon was the implementation of ’getters’ in the cavity under vacuum to absorb those H_2 molecules achieving better longevity and thermal performance. New models, as in Fig. 9b, have also implemented noble gas capsules (e.g. Xenon) with the same purpose. This approach enables a return to the initial thermal performance after more than 25 years of use.

On the other hand, the bellows at each end seal the receiver and serve as mechanical compensators to the dynamic thermal expansion of the steel tube. In the majority of collector concepts, the receiver is a movable component through the entire assembly, while not only it is tracking the sun, but also when it thermally expands between cold state and operational state. The thermal expansion of the tube approximates a length difference of 0.5 m for each 100 m of installed receiver at a temperature of 400 °C. Each receiver segment, usually of 4 m long, has these bellows as shown in Fig. 9. In the beginning, this was a technical challenge, as the glass-metal junction had to compensate for the different thermal expansion coefficients. Due to the different heat states of the glass (around ambient temperature) and the tube (at operating temperature), the risk of breakage of the insulation glass was higher. Other causes of breakages are natural vibrations caused by strong winds or even by the impact of flying objects taken with the wind (Wang, 2019).

The main requirements for receivers are high absorption of the light and low emissivity of the thermal radiation. To achieve this, special treatments are essential for the single elements. The glass envelope is made of borosilicate, for instance, to attribute high transmittance (τ) levels up to 96%. Receivers also require low reflectance rates, for which an anti-reflective coating is applied.

The absorber tubes have a denominated selective coating, since optical behaviour parameters on the surface can be adjusted (or selected). In the case of absorber tubes, the absorptance (α) must be high for one spectral range, namely the solar spectral range ($0.25\ \mu m \leq \lambda \leq 2.5\ \mu m$), and its emittance ($\varepsilon$) must be low for another spectral range, namely the infrared range ($3\ \mu m \leq \lambda \leq 50\ \mu m$) to reduce thermal radiation losses (Günter et al., 2011). The first layer of the coating is metallic and high reflective in the infrared range. It is typically made of Molybdenum (Mo), Aluminium (Al) or Copper (Cu). The following layer consists of a Cermet material, which is composed of a ceramic matrix and embedded metallic nano-particles, for instance Mo-Al_2O_3 or Mo-Si_2O (Usmani & Harinipriya, 2015). On top, the antireflection ceramic layer consists of oxides like Al_2O_3 or Si_2O (see Fig. 10).

Current receivers achieve absorptance values of the solar radiation between 0.95 and 0.96 and lower values of 0.09–0.10 in emissivity of the thermal radiation at 400 °C. These results correspond to receivers dimensioned for thermo-oils. Molten salt receivers can have a surface emissivity value of 0.10 at operational temperatures of 600 °C (Archimede Solar Energy, 2012). A selective coating is more difficult to design once temperatures rise, since there is a larger overlap between the thermal emission spectrum and the solar spectrum (Ambrosini, 2015).

Absorber diameters vary between 70, 80 or 90 mm with a glass diameter of 115–125 mm. The diameter selection has an influence on the intercept factor. It describes the portion of reflected light hitting the absorber. A big diameter can increase the intercept factor, but it possesses at the same time a larger surface area. This would subsequently increase thermal losses at high temperatures. That is why smaller diameters have an advantage regarding thermal performance, but this demands a higher geometrical and optical accuracy from the collectors.

There are other type of receivers under research and development, aiming to excel current technology standards from an economic-technical point of view. Among the many alternatives, Fig. 11 shows three concepts: the V-cavity receivers as one efficient alternative for high temperature applications (Chen et al., 2015), a receiver suited for air as heat transfer medium (Good et al., 2013) and a receiver with an insert type to induce specific flows of the HTF, thus enhancing the thermal performance. To mention further inventions, there are variations of cavity receivers (Bortolato et al., 2016; Liang et al., 2018; Chen et al., 2012; Bellos and Tzivanidis, 2018), flat absorbers with an asymmetrical reflector (Bortolato et al., 2016) and approaches with different fin design combinations to reduce pressure losses. These receivers have not reached commercial maturity, yet they are important approaches to mention as promising thermal performance improvements. Since these efforts focus on the enhancement of specific and detailed receiver collector element, the present study will focus on conventional vacuumed receivers to maintain the scope of the study. In the interest of the reader, the authors recommend the “alternative designs of parabolic trough solar collectors” from Bellos and Tzivanidis, 2018 for a deeper overview on this matter (Bellos and Tzivanidis, 2018).

2.4. Heat transfer fluid

The heat transfer fluid (HTF) is the fluid circulating in the solar field cycle and transports the thermal energy to the power or storage block. The type of HTF determines the operational temperature range of the solar field and so the maximum power cycle efficiency that can be obtained (Price et al., 2002). Some requirements on HTFs are listed in Table 2.

First power plants at Solar Electric Generating Systems (SEGS) used **mineral oil** as HTF in the solar field and simultaneously as storage fluid. Due to the high flammability of this medium and the operational temperatures limitations up to 300 °C, it was substituted by organic oils enabling a higher thermal stability at higher temperatures (Price et al., 2002; Günter et al., 2011). Currently organic **thermo-oils**, a compound of biphenyl ($C_{12}H_{10}$) and diphenyl-oxide ($C_{12}H_{10}O$), are the most frequented HTFs with over 25 years of application. They satisfy the

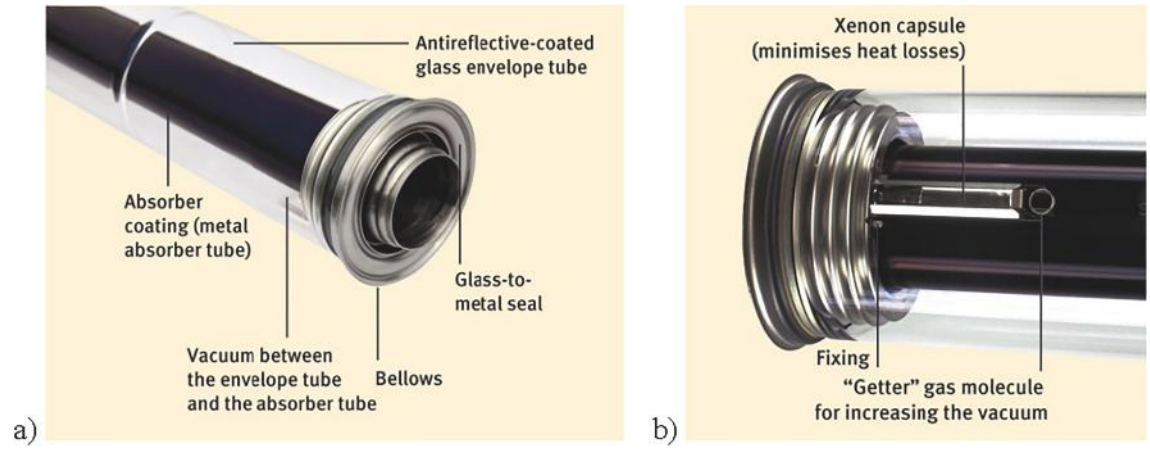

Fig. 9. a) Components of a receiver tube at the example of a PTR70 Schott receiver b) Integrated elements to enhance longevity and performance [source: Schott AG]

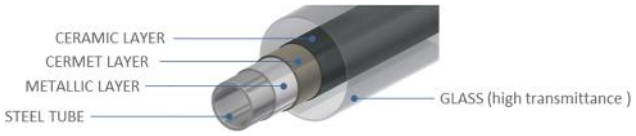

Fig. 10. Multi-layer coating of the absorber tube.

majority of the aspects listed in Table 2, starting with a low freezing temperature at about 12 °C, a high heat capacity and maximal operating temperatures at 400 °C (Günter et al., 2011). However, for higher temperatures than that, thermal decomposition starts to occur. This deteriorates the consistency and properties of the medium due to the formation of gases and volatile compounds. Research with biphenyl and diphenyl-oxide fluids show the forming of coke-like products at temperatures between 400 °C and 465 °C (Jung et al., 2015). In practical operating systems, periodical replacement is therefore necessary due to the aging of the fluid (Jähning, 2005). Thermo-oils are available in large amounts, but at high costs. They are also deficient in flammability and environmentally more harmful than other possible media. Current **synthetic oils** remain under research to improve the thermal stability at higher temperatures, to lower the freezing temperature and to make the price more affordable.

Other media are **molten salts**, which are salt mixtures heated to operate in their liquid phase. They have succeeded in CSP as storage medium, due to their low price and good thermodynamic properties, which enhance some of the technical advantages versus thermal oils. This HTF, aside of being accessible and available, it has high thermal stability, high density, good thermal/electric conductivity and relative low viscosity (Baudis, 2001). Nitrate salts can operate at 550 °C with a thermal stability up to 600 °C, for instance, with *Solar Salts* composed of a binary salt mixture containing 60% sodium nitrate ($NaNO_3$) and 40%

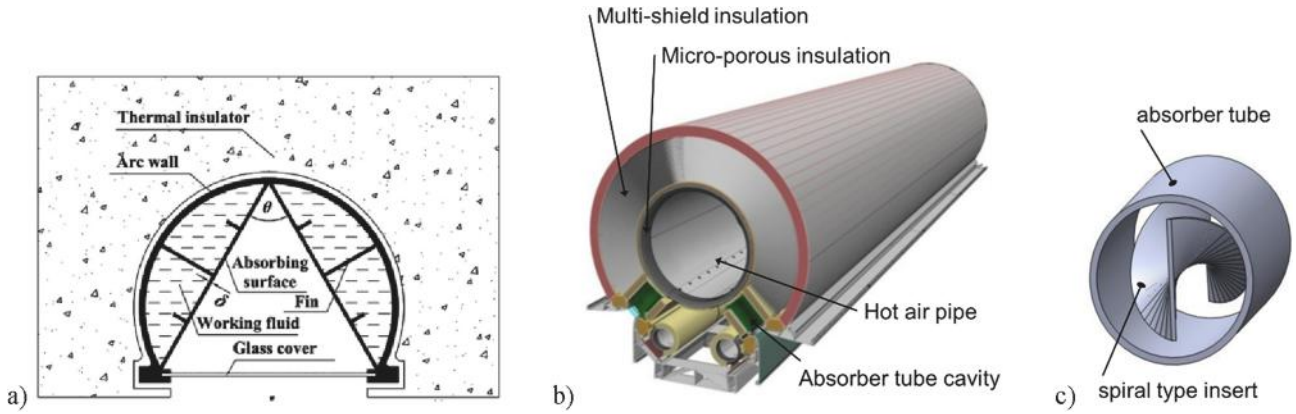

Fig. 11. a) V-cavity receiver with fins and thermal insulation, Lic.-Nr: 4,402,660,122,330 (Chen et al., 2015), b) Airlight receiver (Good et al., 2013), c) Twisted insert inside the absorber tube, Lic.-Nr: 4,403,060,850,043 (Bellos and Tzivanidis, 2018).

Table 1
Overview on current reflector materials for parabolic tough collectors.

Property	Thick glass	Thin glass	Aluminized reflector	Polymeric film reflector
Solar weighted hemispherical reflectance	93.5%[1]	93.0–96.0%[3]	86.0–90.0%[4]	92.5–94.0%[2,5]
Solar weighted direct reflectance	95.5%[1]	96.0%[3]	79.0–92.3%[4]	87.4–95.0%[2,5]
Durability	Very good	Very good	To be improved	To be improved
Cost[3] (€/m^2)	16	13–36	< 18	9–13
Issue:	breakage	breakage, handling	hemispherical and direct reflectance	direct reflectance, longevity

[1]Datasheet (Flabeg, 2009), [2]S.Meyen (Meyen et al., 2009); [3]ASME-Journal of Solar Energy Engineering (Price et al., 2002); [4]ConSol Project (Krüger et al., 2018); [5]ReflechTech datasheet (Skyfuel, 2017).

Table 2
Heat transfer fluid requirements (Günter et al., 2011).

Requirement	Motive
• High evaporation temperature	The HTF must be liquid and operated under manageable pressure. The HTF cannot evaporate at the high temperatures in the solar field: except for DSG applications, since it aims saturated/superheated steam state of the medium.
• Low freezing temperature	No freezing protection measures are necessary, if temperatures in the solar field drop.
• Thermal stability	The HTF needs to withstand operation temperatures and avoid thermal cracking. Operating temperatures are constrained to this requirement.
• High heat capacity	To favour the storage and transportation of high amounts of thermal energy
• Low viscosity	Reduces important pumping energy
• Low investment cost and Availability	Cost savings of the final LCOE and of logistic efforts
• Environmental compatibility	Common responsibility
• Low flammability & Low risk of explosion	Reduction of operational fire hazards

potassium nitrate (KNO_3). Its volumetric heat capacity is reasonable and its vapour pressure is very low, allowing storage under atmospheric pressure and eliminating the cost of thick walls for the storage tank (Wagner, 2012). For applications that require temperatures above 600 °C, the options are limited to chloride and fluoride salts. These salts are more stable than the nitrate salts. Chlorides and fluorides can operate to slightly higher temperatures up to 900 °C. These salts also have higher melting points between 300 and 500 °C, which increases the risk of the salt freezing. In addition, chlorides and fluorides are extremely corrosive, especially at high temperatures. As a result, they require expensive construction alloy materials, which makes the investment substantially expensive (McMullen, 2016). These properties, limit their implementation for linear concentrating systems, but also the fact that commercial receivers are constrained due to the tubés selective coating to operate at temperatures of 560 °C (e.g. type HCEMS-11 from Archimedes Solar Energy & Schott receivers) (Enriquez, 2017). It is also important to note that the benefit of the Solar Salt (nitrate) is that it is the same medium used in the thermal storage tanks, so large quantities need to be secured. The price of this medium has therefore a great economic impact.

The use of molten salts as heat transfer fluid suggests a direct storage system as an alternative power plant design concept (i.e. solar field and storage block in one cycle). Follow to that the heat exchanger between the blocks is negligible. The great advantage of molten salts is the cost effective use of storable thermal energy. This design could reduce the expenses on thermal storage costs by 65% and increase, not only the storage temperature difference up to 2.5 times, but also the steam cycle efficiency to $\geq$ 40% (Kearney, 2003). The use of molten salts as HTF has been demonstrated on a 5 MW_{el} solar plant in Sicily by Archimede Solar Energy. A further large commercial power plant has not been deployed up to date since some disadvantages of molten salts could be considered a risk. Above all, the high freezing temperatures of the fluid at 227 °C (Wagner, 2012) could affect key components like receivers, pipelines, valves and pumps by salt solidification. Daily drainage concepts of the fluid (Eickhoff et al., 2015), recirculation of the fluid (Kearney, 2003) or heat trace systems in the receivers are current technical options to maintain the fluid above the freezing temperature. Further research and test are still undertaken.

Another accessible heat transfer fluid is **water/steam** to target direct steam generation (DSG). It is composed of a single cycle, where the HTF of the solar field is the same circulating in the Rankine cycle. Demineralized **water** is heated by the collector loops into steam and again to water in the same cycle. DSG still remains under research, though the working principle was demonstrated at the Plataforma Solar de Almeria on the DISS project at 100 bar steam pressure and temperatures of 500 °C (Feldhoff et al., 2014).

Other novel thermal working fluids are oil-based or water-based fluids combined with selected nanoparticles. They are so-called nanofluids, where some nanoparticles samples are: "Cu, CuO, Al, Al_2O_3, TiO_2, SiO_2, ZnO, Au, SiC, CeO_2, MWCNT, SWCNT, CNT, etc." (Bellos and Tzivanidis, 2018). Research shows thermal and optical performance benefits with their implementation. The enhanced thermal conductivity leads to an efficient thermal gain and flow rate of the fluid. At the same time, the particles increase the viscosity of the medium and cause a higher work demand of the pumping system, thus increasing the parasitic losses of the system. Studies show enhancement in the thermal efficiency of 8.5% with Water/Al_2O_3 (Subramani et al., 2017), of 7.6% with Syltherm 800/Al_2O_3 (Mwesigye et al., 2015) and of 4.3% with Oil/Al_2O_3 (Bellos et al., 2016). The high cost of the fluid, the increment of parasitic losses, the thermal instability, the toxicity and chemical and mechanical erosion, are limitations for their use at utility scale and further research is still ongoing. Literature shows the potential to enhance the thermal performance through single element modifications and its practical limitations (Bellos and Tzivanidis, 2018).

3. Parabolic trough collector concepts

The chapter highlights the characteristics of various collectors, some of them of commercial implementation and others of innovative approaches in the Research & Development stage. The purpose is to identify similar aspects of the manufacturing, assembly and the working mechanism. The categories help to elaborate a collector genealogy according to their main functional characteristics, and offers a good overview for the reader of existing parabolic trough collector concepts. A categorization of the collectors aims to classify them under following aspects:

- Bearing structure
- Reflector type
- Structure materials
- Innovative features.

This classification is influenced neither by performance properties nor by the heat transfer fluid of use. The authors opt rather for a more general classification and identify two main branches of collectors: the conventional and the innovative concepts. Innovative concepts of parabolic trough collectors are understood according to (Pitz-Paal et al., 2007). Innovative concepts will:

(i) "Increase the power generation efficiency, mainly through increasing operating temperatures
(ii) Reduce solar field costs by minimizing components costs and optimizing optical design
(iii) Reduce operational consumption of water and parasitic power."- *EASAC, 2011* (European Academies Sciences Advisory Council (EASAC), 2011)

Conventional collector concepts are classified in Category A and are further subdivided by their main body structure. The Categories from B to E contain the innovative concepts as shown in Fig. 12.

3.1. Category A: Conventional collectors

Parabolic trough collectors within this category follow the same concept defined by their components. Their specific elements and mechanisms are for example:

- Silvered glass reflector facets, about 4 to 5 mm thickness with a specular reflectance of 93.5% and more than 15 years durability.

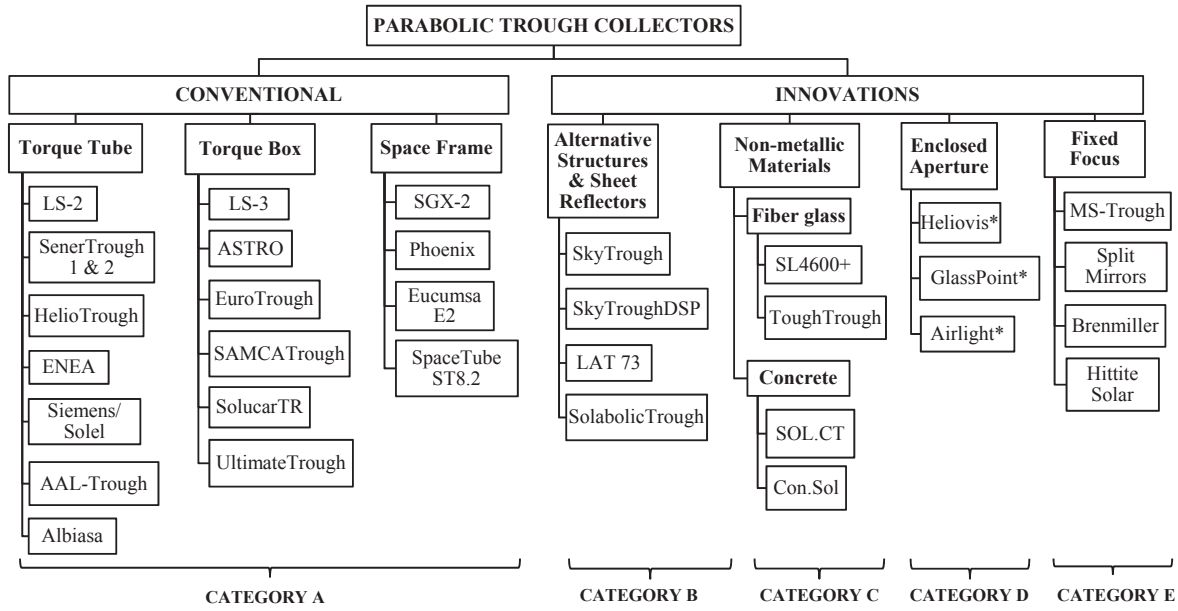

Fig. 12. Conventional and innovative parabolic trough collector concepts for large-scale application categorized according to their prevalent feature. *Collector shares properties belonging to another category.

- Vacuum insulated receivers, with stainless steel tubes and respective selective coating. They are usually of a maximum length of 4 m. Modern receivers are suitable for other heat transfer fluids at higher temperatures and pressures.
- Hydraulic or geared drive system with a tracking axis bellow the vertex of the parabolic cross-section. The rotary axis is built coaxial to the centre of mass axis as an optimization to reduce the loads on the drives.
- Central torque unit, from which further arms extend to support the mirrors and the heat collector elementś supports (HCE). Central torque units in this category are double torque box, torque box, torque tube and space frame. The last minimizes assembly costs and achieves lighter structures with standardized frame components (see Fig. 13).
- Assembly jigs installed on-site rather in the open sky or in an assembly hall. With the jigs, accurate mounting of the central body and the arms is achieved up to a structure tolerance of 0.5 mm.
- Flexible interconnection elements such as ball-joints or flex-hoses. These elements suffer from frequent breakdowns during operation and tend to have low resistance against high pressure (see Fig. 14).

Fig. 15 shows a timeline with an overview of the collectors and their respective modulés dimensions. Solar field efficiency and economic feasibility calculation models conclude that higher concentration ratios can lead to a significant reduction of elements per square meter. The scaling effect of the collectoŕs mirror aperture reduces, for example, the implementation of elements like pipelines, receiver tubes, pylons and drives among others. It is important to keep in mind that larger apertures are subject to stricter requirements in accuracy and robustness of their structure.

The successful deployment of solar fields using several of Category A concepts for energy production established the state of the art for modern solar power plants in the global market, making them indispensable for this study. Category A include the technological advances that aim a cost reduction, for example the standardization of components, simpler assembly structures, manufacturing methods and logistics. A baseline for a solar field cost is drawn by the EuroTrough (Skal-ET) collector with a total of 230 €/m^2 in the example of 50 MW Andasol and similar solar power plants (Schiel, 2011). Elements included in the cost estimation are later specified.

3.1.1. LS-1, LS-2, LS-3

These collectors developed by LUZ Industries, demonstrated the parabolic trough technology for large-scale energy production in modern times. Between the 70́ s and 80́ s there were attempts to introduce the technology to operate at temperatures up to 260 °C, which proposed

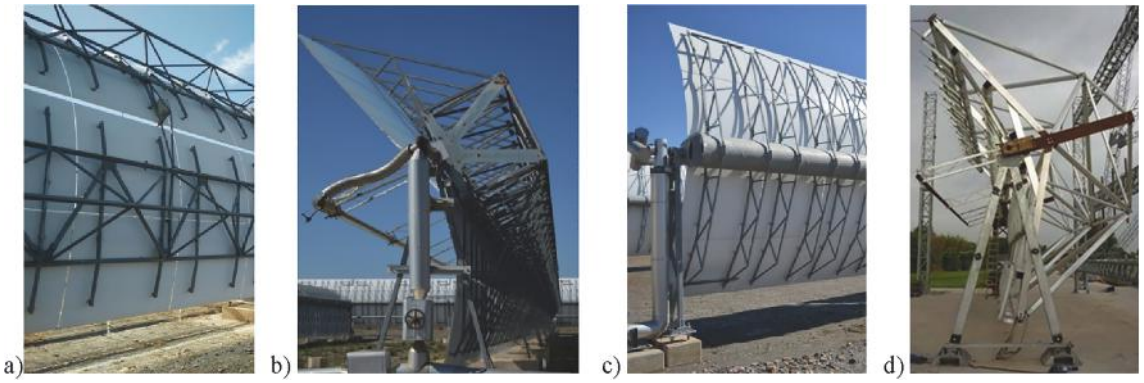

Fig. 13. a) Double torque box b) torque box c) torque tube d) space frame (Abengoa Solar, 2013).

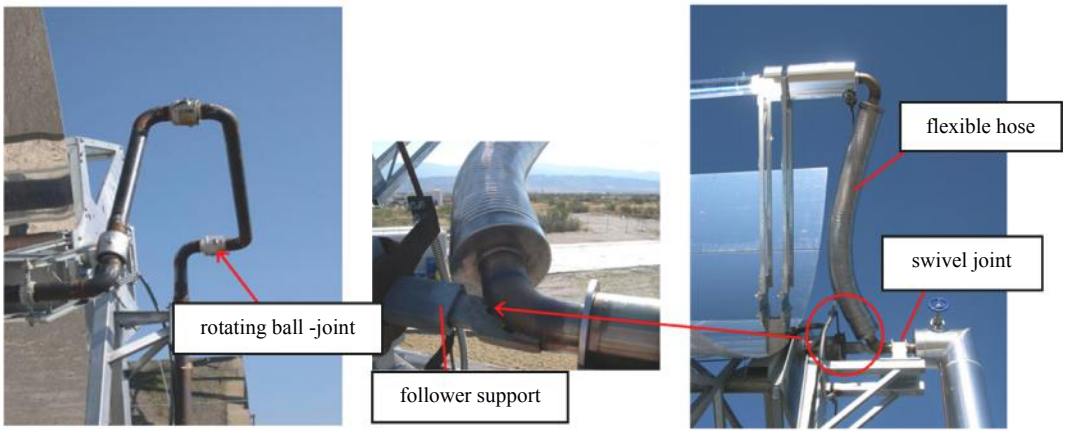

Fig. 14. Flexible interconnection elements (Eickhoff, 2010).

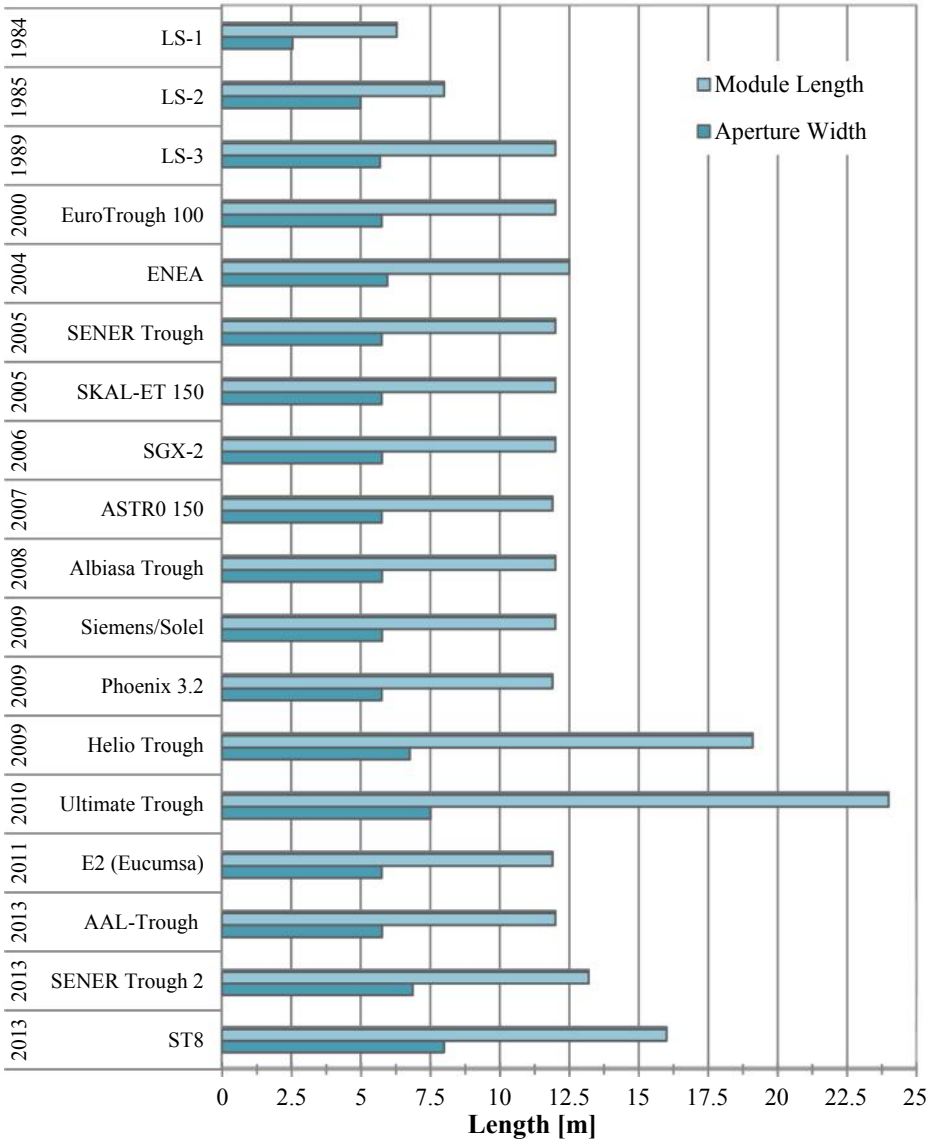

Fig. 15. Time line of conventional collector concepts and modulés dimensions.

a use for industrial process heat generation. Due to the degree of complexity and challenges to conceive a new technology at industrial scale, there was not much response by investors. The main reasons were the high initial cost, the long-term return of investment and the affordable fossil energy. Nine solar stations (SEGS I-IX) were built despite this at larger dimensions in the Mojave Desert, California, USA. Each of them designed as a hybrid plant with a backup firing from natural gas, yet with solar energy as primary source (CIEMAT et al., 2001). The first solar fields SEGS I -II used the models LS-1 and LS-2, both with a central steel torque tube and cantilever arms to support the glass mirror facets (see Fig. 16). The LS-2 and LS-3 were developed in order to up scale the concentration factor and aperture area. An LS-3 solar collector assembly was composed of 8 modules, each of 12 m length. The structure of the LS-3 represented a better resistance against bending and torsion according to LUZ.

3.1.2. EuroTrough

The EuroTrough collector developed in the year 2000. The main motivation was to introduce a novel collector with optimized performance at low cost, after the success stated at SEGS. The central torque box structure can be seen in Fig. 17. It is comprised of a pre-galvanized steel profile frame of about 1.4 m × 1.5 m over the collector´s length. On this structure 28 profiled arms (14 on each side) of the same material are mounted to support the 4 times 7 mirror facet lines. The structure is reinforced with endplates at each end, which rest on the bearing pylons and contribute to the torque transmission over the adjacent modules. At the same time the receiver supports are assembled to the upper part of the torque box, where ~ 4 m long receivers are mounted on-site. The EuroTrough was designed according to the geometrical dimensions of the LS-3. (CIEMAT et al., 2001).

3.1.3. HelioTrough

The HelioTrough was completed in 2006 and tested in a 400 m loop in 2009 at SEGS V, Kramer Junction. Its technical qualification character and production facilities are taken from the bench market of the Skal-ET (scalated EuroTrough). Its design, however, shares similarities with the LS-2, which also uses a central torque tube with cantilever arms (see Fig. 18). The aperture width and module length increased with the HelioTrough development, to increment the effective aperture area and reduce the amount of components per square meter. The 48 parabolic mirrors concentrate the light on a 90 mm diameter receiver, thus the cross section allows a 60% higher mass flow at same flow velocity, with related higher heat gain at constant pressure drop (Riffelmann et al., 2009).

The aperture is optimized by eliminating the gaps at pylons level between the modules. This allows a continuous aperture, which reduces the implementation of components such as crossover assemblies along the SCA. Adjustable joints on the support structure for the thick glass reflectors enable the positioning of these elements, thus enhancing the optical efficiency. In addition, a new concept of drive and bearing pylons has been developed. It facilitates an uninterrupted transmission of the torque through the entire solar collector assembly. The collector's centre of gravity has been designed at the height of the torque tubes rotational axis with the assistance of the visible counter weights at the back part of the collector. This aims to overcome the influence of permanent torsion and the stress on elements like bearings and drive units. (Riffelmann et al., 2009)

3.1.4. Ultimate Trough

The UltimateTrough is characterized by its large aperture and length (7.51 m × 24 m) (see Fig. 19). It saves up to 23% of the solar field cost in comparison to the EuroTrough (Riffelmann et al., 2013). Further advantages apart from the cost savings are the increased optical performance and the reduction of assembly parts (Schiel, 2011).

The torque box is oversized up to about 1.85 m × 1.85 m from which 24 arms extend to each side. These cantilever arms support the mirrors in 4 rows per 12 mirror of about 2 × 2 m per facet. A gap between the outer and inner mirror rows alleviates frontal and lateral wind loads, reducing them up to 30% (Riffelmann et al., 2013). It is important to note that its large size and rigid structure are dimensioned to prevent deformations that could degrade the optical efficiency of the collector. Since the centre of gravity and the rotation axis are located under the vertex of the parabola, a continuous mirror aperture through the solar collector assembly is achieved. At structural level, by means, at the joining between the steel structure and the mirrors a tension free junction is carried out to allow high variance and reduce the hazard of glass breakage (Riffelmann et al., 2013). Glass and steel are the main materials used in this collector. The selected steel for the hollow profiles was chosen to enable a worldwide accessibility with the common type S235 (Balz & Schweitzer, 2015). Regarding the assembly technology the "clinching method"[2] was firstly applied to build the torque box structure, reducing more than 50% of bolts and nuts in the solar field and offering a possible high automation degree, where assembly jigs remain necessary.

3.1.5. Siemens/Solel

The collector design combines the LS-3 concept dimensions and uses a torque tube as the LS-2 collector (see Fig. 20). In 2009, Siemens provided the collectors for the operational Lebrija solar power plant (50 MW) in Spain (Günter et al., 2011).

3.1.6. SGX1 & SGX2

Already in the early 2000′s space frame structures composed of extruded aluminium profiles were an approach to build collectors (Price et al., 2002). The collector line proposes an advanced development within the conventional collectors' category. It targets a lighter and standardized concept with agile assembly process, production and transportation logistics. The evolution of this concept led to the optimized SGX-1, implemented in the 1 MW solar plant Saguaro, Arizona, and SGX-2, implemented in the 64 MW Nevada Solar One plant (see Fig. 21). With the space frame concept it is possible to achieve SCAs from 100 m to 150 m in length per drive, for which fewer fasteners and welding works are required. The use of special profiles and knots offers an improved alignment of the reflective mirrors.

3.1.7. SenerTrough 1 and 2

Both collectors, SenerTrough-1 & SenerTrough-2, use a torque tube along the module, where the second represents an up-scaled version of + 25% of the SNT-1 (see Fig. 22). The main feature of these collectors are the cantilever arms, manufactured with thin sheet stamped technology that provides the parabolic shape and the support points for the mirrors. This achieves lighter structures and high precision and repeatability in the manufacturing process. This subsequently favours the geometrical accuracy and cost reduction of the solar field. The elements such as the torque tube, the arms and the heat element collectors' supports are made of carbon steel, due to its good strength ratio value (Sener, 2018). Similar designs can be appreciated in the ENEA collector.

3.1.8. ENEA

The ENEA collector was designed to demonstrate the implementation of molten salt in the solar field at the 5 MW_{el} Archimede Power Plant in Sicily. The design of the trough possesses a central torque tube with cantilever arms made of metal sheets similar to the Sener collectors (see Fig. 23). The latter are cut in the form of the parabola and have additional stamped circular patterns, providing rigidity and lightweight to the structure. Moreover, it implements thin glass mirrors on special aluminium honeycomb facets, which provide a sufficient stiffness to produce very large panels, which simplify the assembly process (Vignolini, 2009). The collector uses specially developed receivers type

[2] Its origins are found in the automotive industry assembly lines.

Fig. 16. a) LS-1 b) LS-2 c) LS-3 collectors at SEGS (GIZ, 2014).

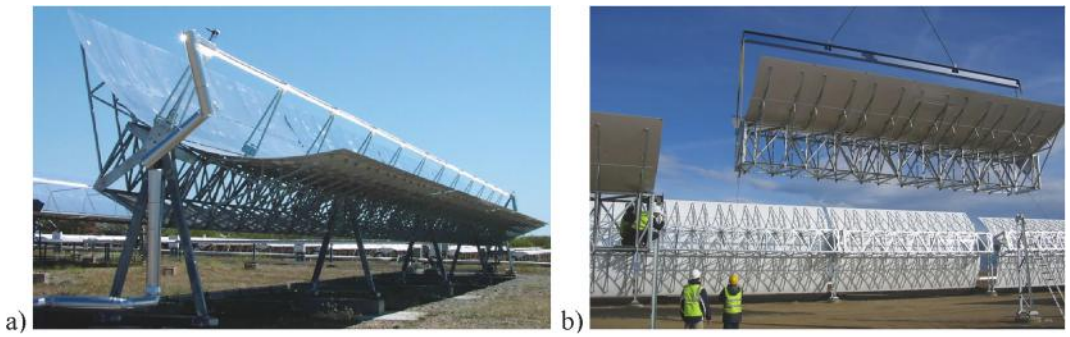

Fig. 17. a) EuroTrough prototype at the Plataforma Solar de Almería [source: Plataforma Solar de Almeria]. b) Skal-ET installation at the Andasol 1 Solar Power Plant [source: Solar Millennium AG]

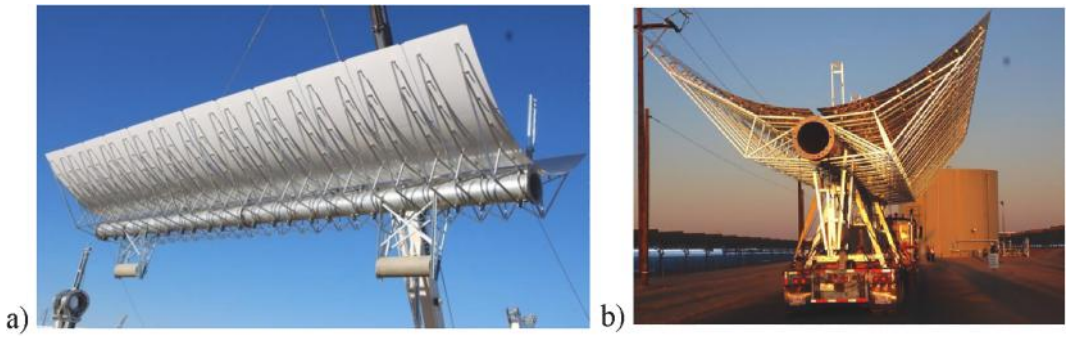

Fig. 18. a) HelioTrough collector module (length = 19,1m, width = 6,77 m) during assembly (Schiel, 2011). b) Module transportation from the assembly hall to the loop (Schiel, 2011).

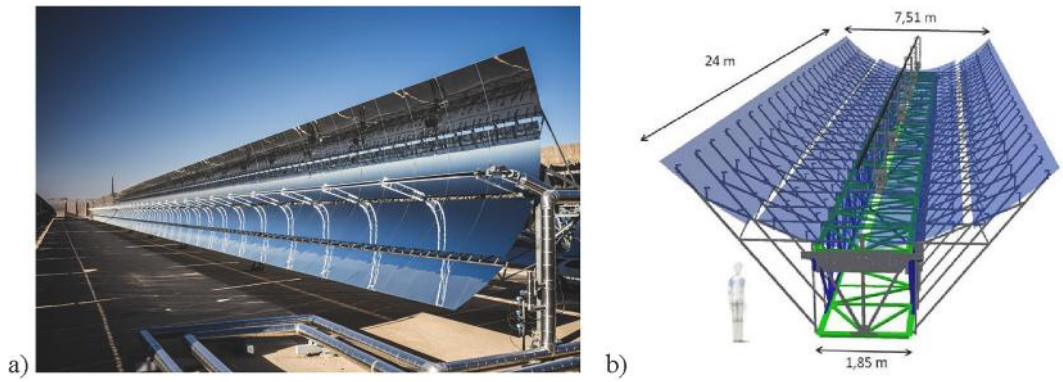

Fig. 19. a) Installed Ultimate Trough (sbp, 2012) b) torque box and dimensions (schlaich bergermann partner, 2013)

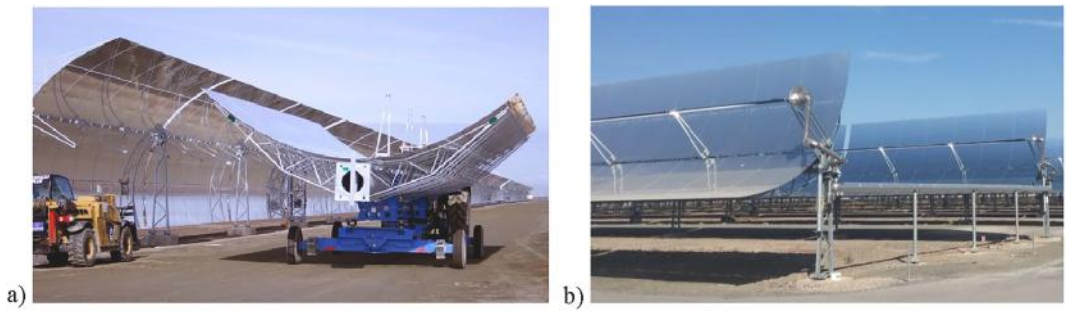

Fig. 20. a) Siemens/Solel Collector on the 50 MW Solar power plant Lebrija 1 (Siemens, April 13th, 2010). b) Installed trough loops (Soleval Termosolar, 2016).

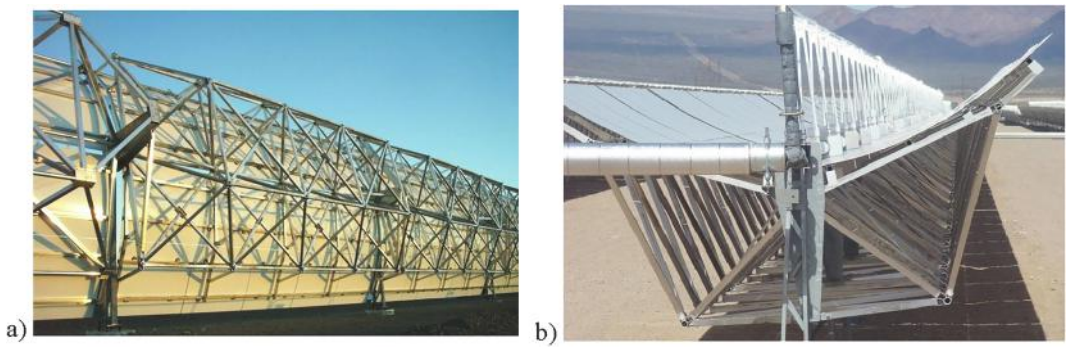

Fig. 21. a) and b) SGX-2 extruded aluminium profile space frame collector at 64 MW Nevada Solar One solar power plant (Speciality Structures and Installations, 2017).

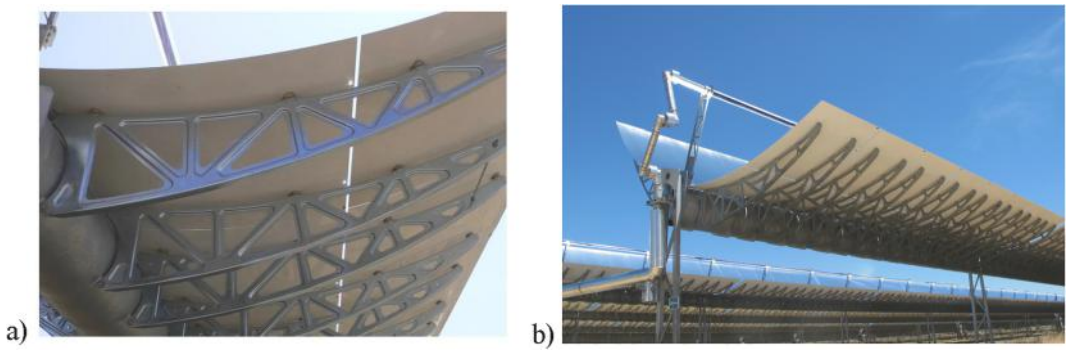

Fig. 22. a) SenerTrough stamped cantilever arms connected to the central torque tube and supporting mirrors. b) Scaled up SenerTrough 2 collector module. It follows the previous concept (GIZ, 2014).

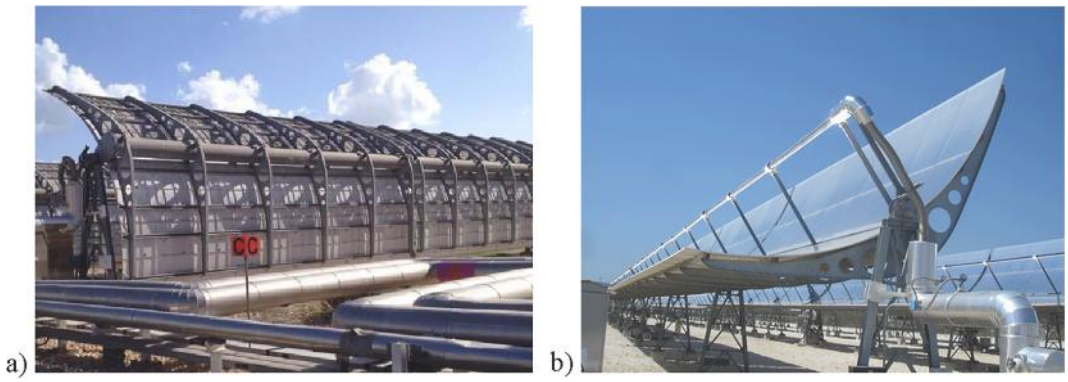

Fig. 23. a) Back and b) front ENEÁs parabolic trough (Yokohama, 2010).

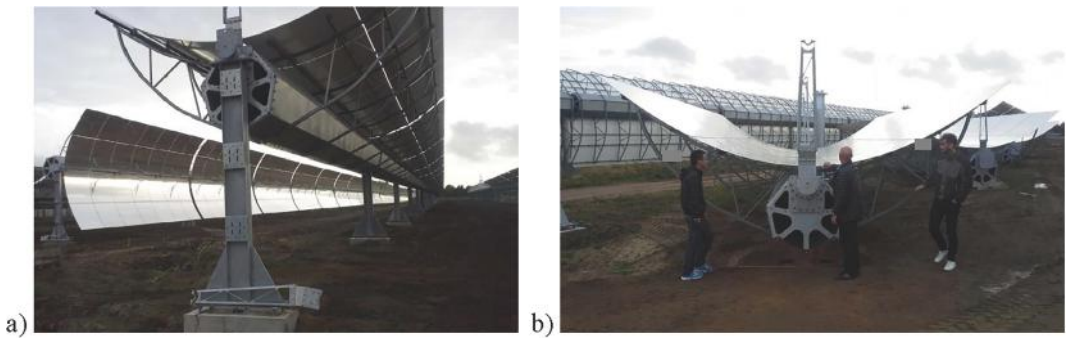

Fig. 24. a) Alternative torque tube structure and fundament. b) Wing design of the cantilever arms (Perers, 2016).

HCEMS-11 which operate with the fluid salt mixture of potassium- and sodium nitrate (40% KNO_3 60% $NaNO_3$) from 270 °C up to 550 °C at a design pressure of 8.5 bar (Archimede Solar Energy, 2012).

3.1.9. AAL-Trough (Gen.4.0)

The collector CSP uses a central torque tube unit and a 'wing design' for the cantilever arms as seen in Fig. 24. The torque tube has an hexagonal shape, composed of two bent metal sheet sections along the module. The cantilever arms bring support together with longitudinal steel profiles to the glass mirrors.

3.1.10. ASRT0

The ASTR0 collector is very similar to the EuroTrough (see Fig. 25). It has a torque box design with low cost steel profiles and implements fasteners instead of welds in its structure. One of the very few changes is the reduction of the number of cantilever arms and the use of longitudinal purlins to support the reflector panels. Installations of this collector are in Spain (e.g. Solnova) and northern Africa. The performance is similar to the EuroTrough, with a minor cost reduction (Abengoa Solar, 2013).

3.1.11. Phoenix (3.2)

The Phoenix collector follows Abengoa Solar series line of development (see Fig. 26). Requirements for this generation were set to achieve an economic concept in terms of manufacturing, materials and process of assembly, while maintaining an acceptable optical performance. Consequently, torsion stiffness, alignment and resistance to wind loads are targets in the concept. The space frame structure is made out of 80% aluminium with steel torque arms enabling 60% higher torsion stiffness than that of the ASTRO collector (Abengoa Solar, 2013). Furthermore, the assembly time is reduced to around one fifth. The optical performance was approved within the generation 3.2 and attains ~ 10% cost reductions compared to the previous ASTRO collector (Abengoa Solar, 2013).

3.1.12. E2 (Eucumsa)

The E2 or Eucumsa is a variation of the Phoenix design composed of a steel space frame structure (see Fig. 27). It requires a jig alignment of the mirrors and contains improved purlins for their mounting on the steel structure. One reference project is the 280 MW Solana Generating Station in Arizona. Another one is the 100 MW KaXu Solar One in South Africa.

3.1.13. SpaceTube (ST8.2)

The SpaceTube8.2 (ST8.2) built by Abengoa Solar in 2013 has the largest aperture within Category A with 8.2 x16 m dimensions (see Fig. 28). Under the "Sunshot Initiative" of the US Department of Energy the company strives not only to develop this large aperture collector, but also to improve different production and assembly elements of their predecessor designs. Further manufacturing optimization of the collectors sub-structures, lower input material costs and mechanized production are the target for its development. The project named "SolarMat" reports an estimated of 91.83 $\$/m^2$ for specific collector costs (O'Rourke et al., 2015). The SpaceTube's frame eliminates welded assemblies and large jig alignments, thus reducing specialized manpower. Its manufacturing and fabrication apply stamping techniques and the assembly comprehends an automated process that achieves an accurate mounting of the parts. The latest version of this collector is the ST8.2. For this line innovative approaches in its structure were also tested, for example the use of composite panels as reflecting components and also adaptations for the use of molten salt as HTF. The implementation of this model is to be applied in the Mohammed bin Rashid Al Maktoum Solar Park, in Abu Dhabi. It is a 950 MW hybrid project, where 700 MW will be based on CSP and 250 MW on photovoltaic.

3.2. Category B: Alternative structures & sheet reflectors

In category B there are concepts derived from the structural advances of conventional collectors. Included are collectors with space frames and

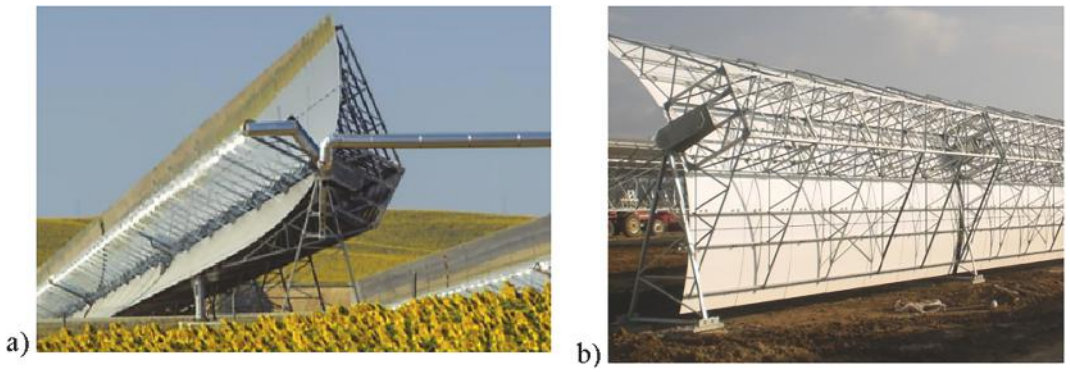

Fig. 25. ASTR0 collector by the company Abengoa Solar, 2007 (Abengoa Solar, 2013).

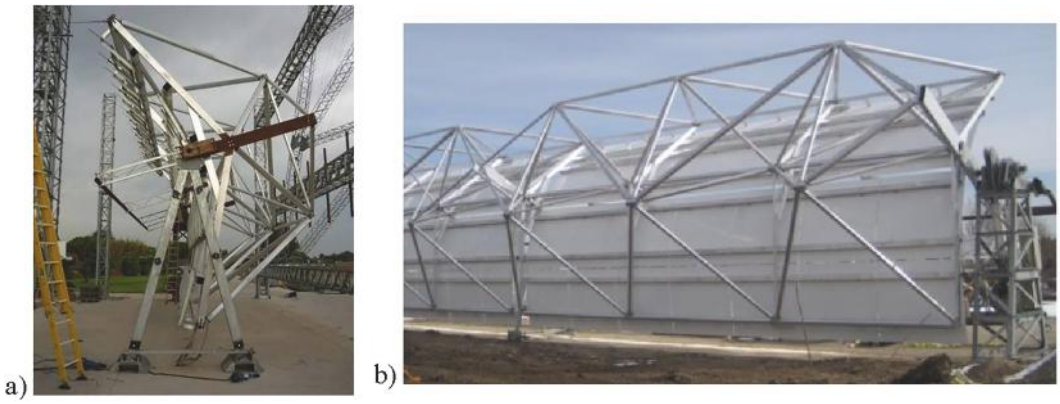

Fig. 26. a) Final structural space frame of the 3rd generation. b) Phoenix Gen 2.0 forerunner of the Phoenix 3.2 with a space frame structure (Abengoa Solar, 2013).

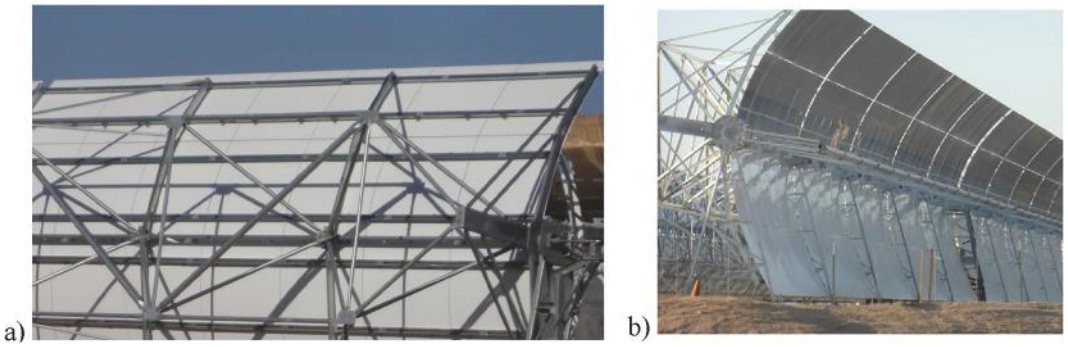

Fig. 27. a) E2 collector back view of the space frame (GIZ, 2014) b) front view (Own Creation, 2013).

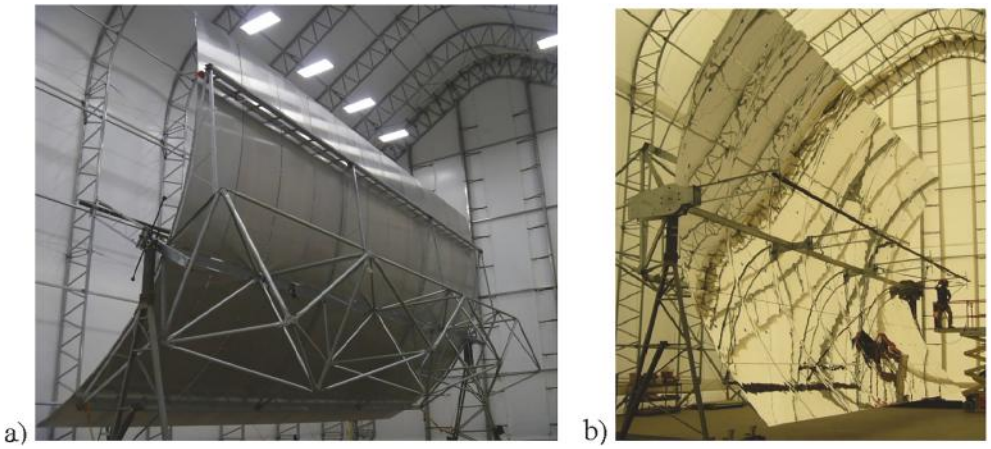

Fig. 28. a) ST8 Space Tube with glass mirrors and b) with composite panels (Abengoa Solar, 2013).

an alternative metallic structure that seek to lighten the weight and reduce the elements per square meter. These collectors aim for a significant costs reduction per module without adjudicating the characteristic performance.

More important than the structural implementation of metals such as aluminium, is the reflector material that replaces the conventional thick glass panels. Among them polymeric reflective films and coated aluminium sheets are found. Each of these has not only different optical properties, but also other needs of maintenance, assembly and durability properties. Glass mirrors make around 13% of the costs of a solar field and weight around 10 kg/m^2, e.g. RP2 Flabeg type facet. Aluminium reflectors, e.g. ALMIRR, can weigh 4.8 kg/m^2 with 4 mm thickness and similar to polymeric films, which are in nominal thickness 0.1 mm, attached to an aluminium sheet surface.

Thanks to the standardization of the profiled tubes and connection nodes, the installation of these collectors does not require assembly jigs. Their structure also allows a more efficient assembly in terms of workmanship (cranes, men power…), reducing the installation expenses.

3.2.1. *SkyTrough & SkyTroughDSP*

The US-American company SkyFuel developed a line of parabolic trough collectors targeting a significant cost reduction trough standardized lightweight structures and the utilization of reflective polymer films (see Fig. 29). SkyFuel developed an adhesive reflector, called ReflecTech, to substitute the commonly used glass mirror panels. This foil is glued onto aluminium sheet rolls, which are slide into precision

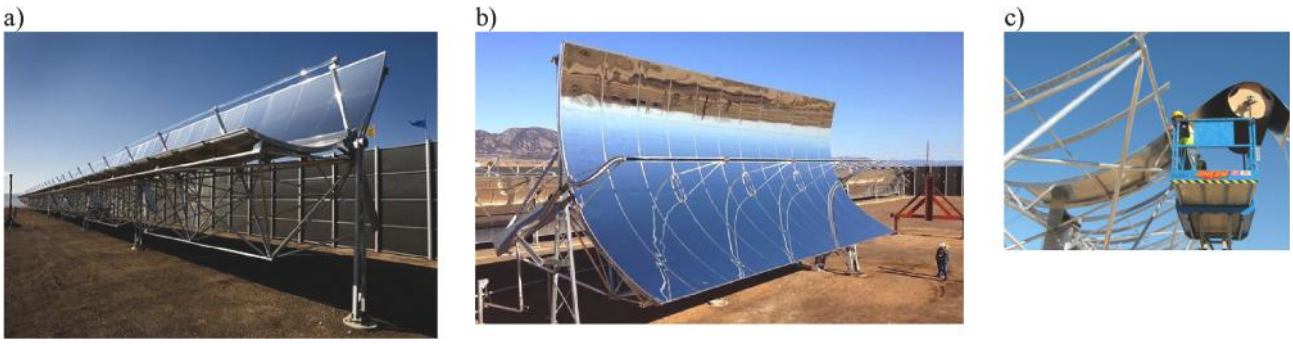

Fig. 29. a) SkyTrough Parabolic Solar Concentrator in Arvada (Laezman, 2009) b) SkyTroughDSP (HeliosCSP, 2015) c) Reflectors been installed in a SkyTroughDSP collector (SkyFuel, 2017a,b).

ribs in the structure, thus giving the parabolic shape. The SkyFuel Company developed also the SkyFuelDSP (Dispatchable Solar Power) collector with a specific collector cost of 100 $/m^2 (Schuknecht et al., 2018).

In 2010, the first collector was the SkyTrough. It attained a 36% cost reduction in comparison to a EuroTrough 150 collector (Mason & Reitze, 2013). The SkyTroughDSP, follows the same previous design, yet with 30% scaled up aperture dimensions and with the suitability to operate with molten salts as HTF. Both collectors use a space frame structure of aluminium tubes (Al 6051) (Kurup and Turchi, 2015) and exploit the lightness of the design to alleviate the requirements on the holding structure and drive mechanism. These collectors have been implemented in small scale applications and demonstration loops. Currently the company SkyFuel aims to build the Chabei 64 MW Molten Salt Parabolic Trough Power Station in the South East China.

3.2.2. *Large aperture trough (LAT 73)*

The LAT 73 is a development of 3 M and Gossamer Space Frames. It has an aluminium space-frame structure and uses a reflective polymer film called Solar Mirror Film 1100. Dan Chen, Business Manager of 3 M, claimed in an interview a 25% solar field cost reduction with the LAT 73 in comparison with conventional concepts (3M & Gossamer Space-Frames, 2012). It uses over 40% fewer components, which result in around 20% material cost savings, adding to that the absence of assembly-jigs and more simple assembly steps (3M & Gossamer Space Frames, 2012). For example, the installation of one of 20 reflectors is alone stated at 3 man-minutes per facet (see Fig. 30b). Furthermore 20% less receivers and pylons are needed as a consequence of the larger aperture and concentration ratio.

3.2.3. *Solabolic trough*

The SolabolicTrough implements a torque box and profiled truss arms with roll-ups at each end for the mounting of the coated aluminium sheet reflectors (see Fig. 31). The reflectors are tensed into the ideal parabolic shape with cables and springs. Two main challenges were encountered after the prototype phase. First, an ideal optical alignment was not achieved after tensing the cables in their position, due to the expansion of the cables and the sliding of the connecting points (Adel, 2018). Second, the requirements on the springs were constraining the proper tensile distribution on the truss. A special manufacturing of these springs was needed in order to fulfil their corresponding function, yet for the intention of the concept, this would mean an increase in complexity and costs (Adel, 2018).

The concept suggested a 20% weight reduction per unit aperture area and a 35% reduction of a solar field costs in comparison to a conventional solar collectors' field. A parabolic trough of 10 m aperture was assumed for the cost estimation, yet the practical implementation was still constrained to the two facts mentioned above (Adel, 2018).

3.3. *Category C: Non-metallic materials*

This category presents parabolic trough collectors implementing (i) composite sandwich structures and (ii) high performance concrete materials. While the first subdivision (i) focuses on the parabolic aperture structure, the concepts with concrete (ii) suggest an overall casting of the main body and the support structures. These collectors require a different line of manufacturing, transport and assembly process. The use of alternative materials aims a breakthrough in costs reduction with concrete as a cost efficient and worldwide accessible material. Furthermore, the enhancement of the geometric parabolic accuracy and

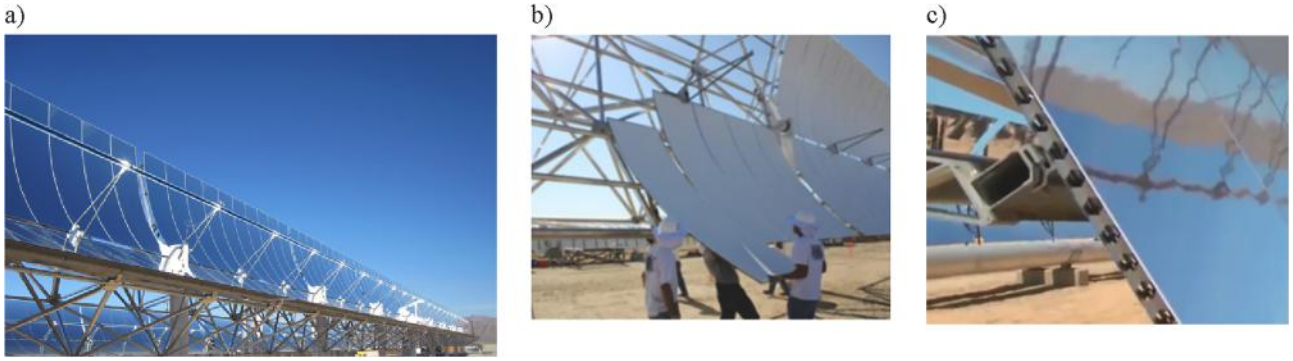

Fig. 30. a) Large Aperture Trough at a pilot loop in SEGS I, b) Reflector panel mounting and c) detail of panel to structure connection [credits: 3 M, Sunshot Initiative].

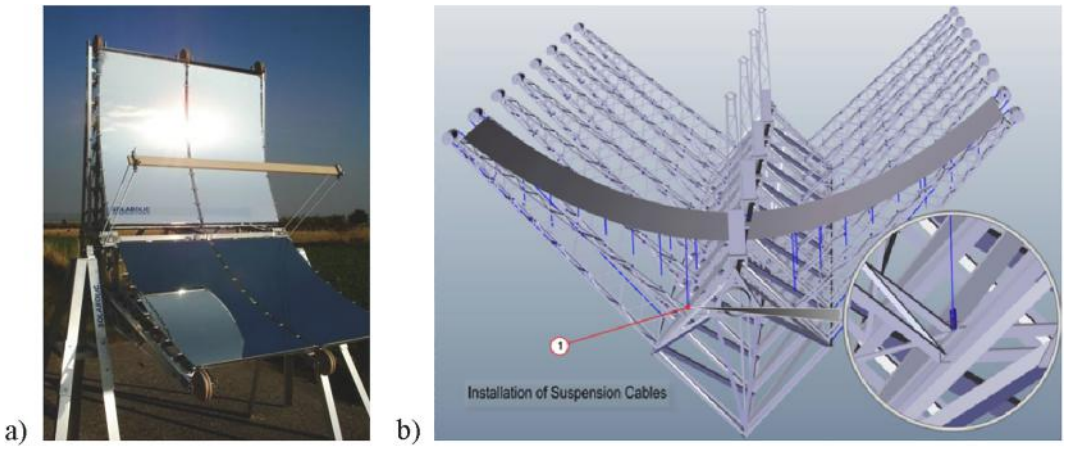

Fig. 31. a) Physical model (Adel, 2015) b) Torque box and truss arm structure with emphasis on the installation of the springs and suspenders (Adel, 2015).

Table 3
Densities and Youngs moduli of diverse materials (Krüger et al., 2018).

Material	density [kg/m^3]	Youngs Modulus [GPa]
Steel	~7850	210
Aluminium	~2710	70
Sandwich Composite (et. Schapitz 2011):	~ 1460	25.25
i. Fiberglass	25	1.7
ii. Foam	2500	70
iii. Thin glass		
Ultra-High Performance Concrete-(UHPC) e.g. Nanodur®, Ductal®	~2510	0.045–0.053

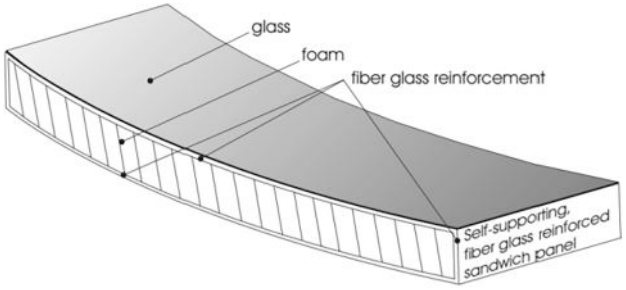

Fig. 32. Self-supporting fibreglass reinforced sandwich structure (Blümner, 2012).

resistance towards strong winds should also be favoured with the composite materials. Table 3 sums up the density values of the here alluded materials.

(i) *Fiberglass sandwich composite structures*

This subdivision includes the Solarlite SL4600+ and the ToughTrough collector. In general, the elements are a three-layered sandwich composite. The outer layer is a mat of fibreglass and resin, which encloses an inner core usually of polystyrene (PS) or injectable polyurethane (PU) foam, as seen in Fig. 32. In both cases, the structure results in an increased bending stiffness, where epoxy resin is used in the case of a PU core (Krüger et al., 2018). In addition to the higher stiffness, the production of sandwich composites has the advantage that the mirror material is incorporated during the manufacturing process. For this purpose, an adhesive technology is applied. Furthermore, the reverse side of the composite is equipped with a UV-stable protection to avoid the materials degradation.

(i) *High performance fiber reinforced concrete*

This subdivision includes the SOL.CT and the ConSol collectors. The Airlight collector corresponds also to a further concept with this properties section, but it is sorted in 3.4 Category D: Enclosed Aperture Collectors due to its prevalent characteristic of an enclosed aperture. Ultra-high performance concrete (UHPC) is commercially used for architecture and civil infrastructures, which require great durability and tensile strength. For the application on parabolic trough confectioning specific machinery is needed, e.g. mixture machines for concrete processing, transportation cranes and molding elements. Due to the intended apertures and large size elements, a production hall is required, which should also be big enough to enable the storage of the pieces while hardening.

3.3.1. *Solarlite 4600+*

The German company Solarlite developed collectors that implement sandwich composites of fiberglass and resin with a hard foam in the core of the structure (see Fig. 33). It uses flexible thin glass reflectors glued on the surface. A torque tube assumes the torsion forces and it has additionally three pairs of steel stamped sheet arms to support the parabolic body. The combination of the light weight composite and partial steel structure amounts a specific weight of 19 kg/m^2 (Prahl, 2009). According to the manufacturer, the optical efficiency is 75% (Solarlite GmbH, 2010). Solarlite informed that a new generation is in perspective with a larger aperture (5.77 m) and a steel/glass design including composite panels and enhanced optical performance. A former version of this collector was deployed for direct steam generation (DSG) and operates the first 5 MW_{el} power plant of its kind in Kanchanaburi, Thailand.

3.3.2. *ThoughTrough*

ToughTrough GmbH developed innovative solar reflector panels using composite sandwich materials, steel and thin glass (see Fig. 34). Beyond this, the highly automated and precise manufacturing process derived from the aeronautical and automotive sectors, aim a better performance, lightweight and higher stiffness. Its design for industrial scale manufacturing achieves a 25% cost reduction in comparison to existing models (Stancich, 2012). The main reduced costs drivers include −25% in foundations and more than −25% in the mirror shell, collector frame and pylons together, according to CEO Carsten Holze (Stancich, 2012).

The prototype consists of a torque tube and four continuous longitudinal segments of their parabolic facets. They are mounted on steel

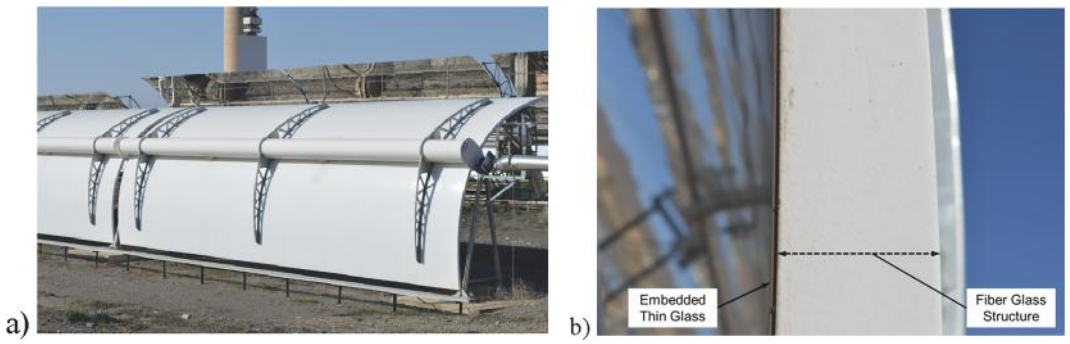

Fig. 33. a) Solarlite SL 4600 + at the DISS facility to demonstrate the Direct Steam Generation (DSG) process, Plataforma Solar de Almería, b) Parabolic shape integrating fiberglass and foam in the core. Photos taken at PSA 2019.

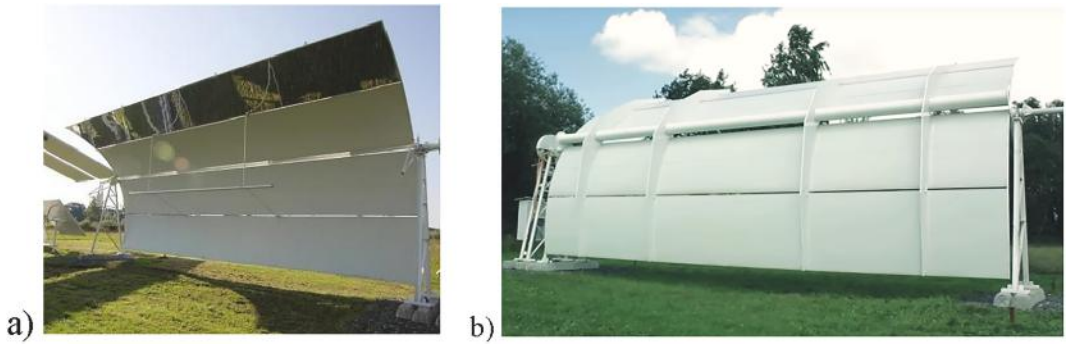

Fig. 34. a) Prototype parabolic trough using ToughTrough mirror technology; b) Backside of the prototype module [Credit: toughTrough GmbH, Lübtheen in Mecklenburg-Vorpommern, 2011 May]

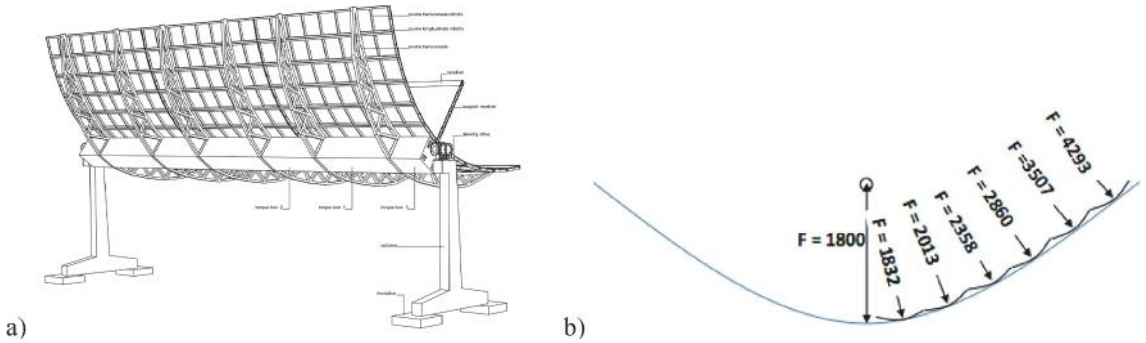

Fig. 35. a) Concrete structure with segmented torque box, pylons, transversal beams and parabolic frame, b) Integration of cold bent mirror plates (AltoSolution, 2018).

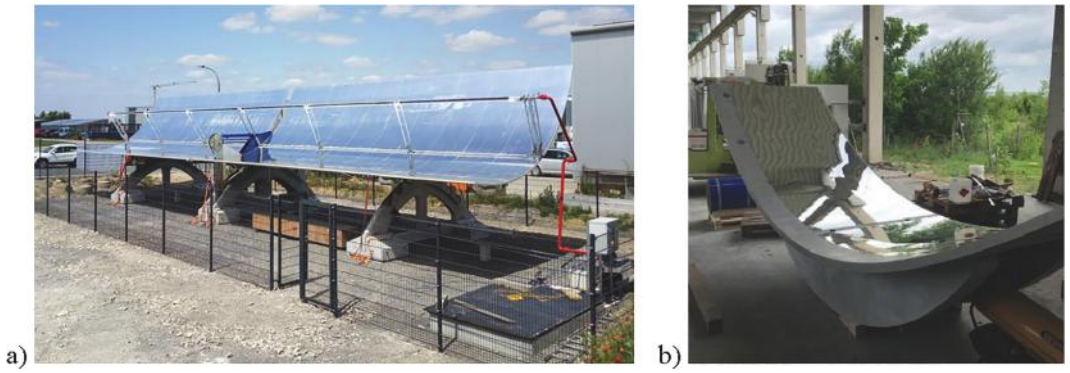

Fig. 36. a) Demonstration of a two modules prototype operated with a central gear motor, b) Laminated concrete surface segment with a flexible silvered aluminium reflector (Krüger et al., 2018).

arms which extend from the central body. Those facets can be customized from a length of 1.7 m to 18 m and a width of 1.6 m. The structure is based on a front layer of thin glass, followed by a core of polyurethane (foam of roughly 25–50 mm thickness), which is enclosed within a steel/fiberglass composite back layer (toughTrough, 2018). In comparison to the EuroTrough design 50% of mass reduction is achieved and around 1 ton less of weight per module (Stancich, 2012).

3.3.3. Sol.CT

Alto.Solutions presents a collector concept composed of ultra-high performance concrete (UHPC) precast elements. Its configuration is analogue to a conventional collector, which uses a torque box and transversal support structures for the mirrors. The latter correspond to another innovative feature of their concept, since it uses mechanically cold bent mirror plates instead of conventional glass facets.

Fig. 35 b) shows the schematic cross section of a final installed contour of the adjacent mirrors. The flat plate glass has a thickness of 2–3 mm and uses a silver reflective layer with 94% reflectivity (Alto-Solution, 2018). A new design will use facets of 1 × 1 m to reduce optical errors. A pilot plant with 1500 m^2 aperture is coming soon according to the manufacturer. Regarding the optical and thermal efficiency, data is limited, since a prototype has not been completed yet. Furthermore a slewing drive unit is integrated for the tracking mechanism. Alto.Solutions estimate specific collector costs at 69 €/m^2 and a reduction of 40% for a solar field cost based on SAMs database (Alto.Soultions, 2018).

3.3.4. ConSol

The ConSol (Concrete Solar Collector) project represents a different approach using alternative high performance concrete material (see Fig. 36). The prototype is composed of on-site casted elements partly of Nanodur® and partly of normal strong concrete C35/45 with a shell thickness of 3.5 to 5.5 cm. The reflectors are silvered coated aluminium sheets, which are adhered to the concrete shell with a double-sided adhesive tape. The reflectance of the mirrors was measured at 92.3%. The intercept factor in zenith position of only 46% could be adjusted up to 86% by repositioning the 70 mm diameter receivers (Krüger et al., 2018). The expected value for the light´s deviation is a consequence of the uncertainty of the material´s widening in the casting process. About the drive mechanism, a central unit for a row of adjacent collectors was discarded, since simulations showed insufficient resistance towards torque loads induced by wind. Specific solar field costs with ConSol are estimated at 261 €/m^2. Projected improvements in the design aim material cost reductions from 76 €/m^2 to 38 €/m^2 (Krüger et al., 2018).

3.4. Category D: Enclosed aperture collectors

The collectors of this category differentiate from the conventional ones, since they include a type of translucent cover above the aperture area. Different configurations and materials like polymeric membranes or glass types have been developed as an adaptation to certain regions of the world. Those are particularly environments with strong winds, high rate of humidity and heavy air due to dust, sand or pollution. These conditions mean exhausting maintenance work of the collector's components and a significant drop of the performance due soiling layers in the reflectors and absorber tubes. Moreover resources like water could be less accessible in such an environment, for instance in a desert region in the Middle East. In fact, these collectors could not be considered a technology of application, if it was not for their adapted solutions to the environment. They also give an alternative perspective on the implementation of technology and contemplate the use of heat transfer fluids like air, steam and oil for different industrial processes that propose a significant saving of CO_2 emissions.

None of the collectors follows a specific design, but rather overflows to new approaches in order to adapt them to the enclosed aperture. The main curiosity of the concept focusses on the optical performance, since placing a layer in front of the collecting area cause additional optical effects. A general assumption on these collectors is based on a lower optical efficiency in comparison to the conventional collectors. The reflectance, transmittance and absorbance constrained by the covering materials, are the main reasons.

3.4.1. Airlight

The Swiss company Airlight developed a large aperture collector based on fibre reinforced concrete and an inflatable polymer membrane as structural material (see Fig. 37). The latter includes a reflective polymer film, which is glued in a parabolic shape. Its application was developed for industrial process heat production as well as for electricity generation. A pilot power plan between 2012 and 2014 used an alternative storage unit with a special container filled with gravel (Airlight Energy, 2015a,b). The receiver of this collector is adapted for air as heat transfer fluid, which corresponds to a further special feature. The air flows through the collector in large sized pipelines and arrive at the inlet with 250 °C and 570 °C at the outlet of the collector.

An assumption of a thermal-to-electric conversion efficiency of 35%, expects a negligible parasitic loss of 1.8% of the power output, consumed by the fans circulating the process air. (Good et al., 2013). The performance of this collector is reduced, first due to transmission and reflection losses, second to inaccuracies of the reflective layer and third due to fluctuating inflation pressure of the membranes (Bader, 2011). The ideal radiative flux at the receiver aperture is reduced by 8.5% due to transmission losses introduced by the concentrator top membrane, and by an additional 6.3% because of reflection losses on the mirrors (Bader, 2011). Summing up, the collector is based on materials like concrete (rapid hardening high performance), stainless steel, rocks, and the membranes of: BO-PET as reflective layer, ETFE as translucent external film and PVC as bottom layer.

3.4.2. HelioTube

The Austrian company Heliovis AG developed the HelioTube collector (see Fig. 38). The materials used for the structure are based on steel and aluminium. The inflated tube is composed of a transparent ETFE layer, a reflective membrane of PET and a complementing base

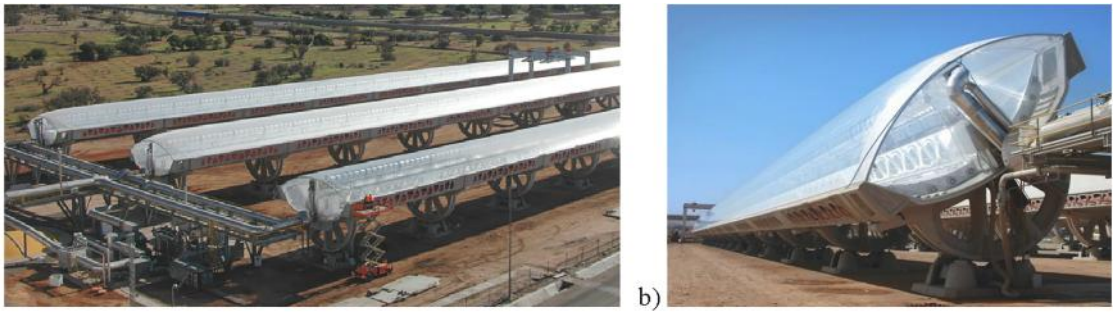

Fig. 37. a) Deployed Airlight collector in the pilot plant Ait Baha, Morocco, 2014, b) Wide and enclosed aperture of the collector with its body structure made of precast concrete elements (Airlight Energy, 2015a,b).

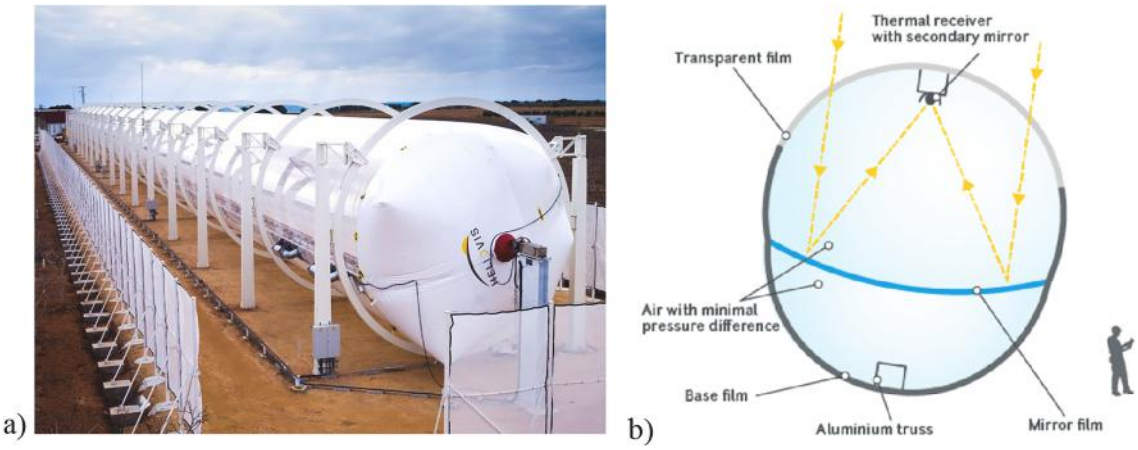

Fig. 38. a) Pilot HelioTube collector (Energy Globe World Award 2017), b) scheme of the two segments inflated tube and main components (Heliovis AG, 2018).

film of PVC. The mirror film separates two segments being inflated at different pressures, thus shaping the parabolic layer, which has its focal point at the upper extreme of the circle. Here a secondary mirror is implemented. A collector is dimensioned with a 9 m in diameter and a length of continuous 220 m. Its implementation is suitable for DNI values above 1900 kWh/m^2 (Heliovis AG, 2018). It is claimed that temperatures up to 400 °C can be reached and also a thermal capacity of 1 MW$_{th}$ for each tube. A solar field cost reduction of 50% (Bermadinger et al., 2019) can be possible compared to conventional PTC systems, due to the advantages in automated manufacturing, transporting and maintenance procedures.

3.4.3. GlassPoint

In 2012 GlassPoint demonstrated the housed collectors in a large scale pilot plant for enhanced oil recovery (EOR) in the south of Oman. Its capacity delivered 7 MW$_{th}$ steam energy, averaging 50 tons of output steam per day. Today they are completing a 1.000 MW$_{th}$ (1GW$_{th}$ steam energy) solar field for this application named Miraah with an equivalent of 6.000 tons of output steam per day. By enlarging the solar field the natural gas consumption for steam production shall be lowered to 20%. The gas resources would be used only at night or when solar energy is not available. The aperture field of GlassPoint is enclosed in an advanced agricultural greenhouse, where the collectors and the fixed receivers are suspended and driven by steel rods from the ceiling (Bierman et al., 2013). Inside the structure, collectors get protection from the present environment at sites with strong winds, sand and humidity (see Fig. 39).

The aluminium reflectors are embedded in a lightweight parabolic honeycomb structure, which enables a drive cable system to operate as tracking mechanism with 0.01 degrees of accuracy. Today a mirror panel weighs 1.2 kg/m^2 (Bierman et al., 2017). The mirror panels including the frame of the first collector weighted 4.2 kg/m^2. The peak efficiency at zenith angle 0° and DNI 950 W/m^2 is estimated between 66% and 68% in a hot state considering 2% of losses due to soiling, possible roof structure shadowing, glazing losses and the use of non-vacuumed receivers (Bierman et al., 2013). GlassPoint assures that these losses are compensated by the zero operational wind speeds and the soiling removal system. In regard to the efficiency of the new generation information was limited, but this new collector implements evacuated receivers and represent 99.9% intercept factor at the focal point. An automated cleaning device was developed, which operates daily at least on half of a roof and once every night with full recaptured washing fluid. Due to dust deposition, the operational performance of the pilot plant showed a drop of 12% of the efficiency during a sandstorm (Bierman et al., 2013).

3.5. Category E: Fixed focus

In a fixed focus collector, the stationary focal axis along the module features the main characteristic. These collectors place the receivers on the focal axis and coaxially to it, the rotary axis of the parabolic concentrators. Collectors of other categories, usually have their rotary axis at the vertex of the parabolic structure or slightly below, making the absorber tube to rotate together with the whole concentrator, as schematized in Fig. 40 a). For this reason, flexible connections like ball or swivel joints are required in those collectors at each end.

A fixed focus collector instead, can eliminate these components since no movement influences the absorber tubes and non-flexible elements can be used at the end of their solar collector assembly, by means of direct welded or flanged piping connections. This specifically targets the elimination of parts that represent frequent breakdowns in solar power

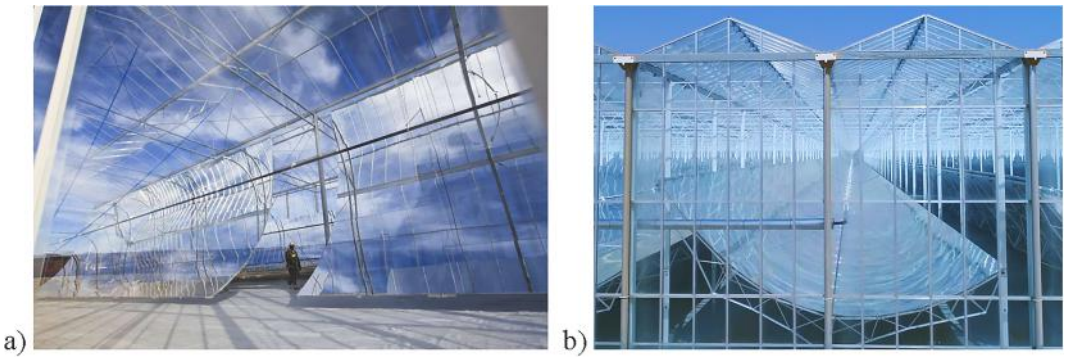

Fig. 39. a) Pilot plant of suspended parabolic collectors and receivers in an advanced greenhouse structure, b) Collector row at the Miraah project with additional V-truss structure on the back of the mirror panels (GlassPoint, 2019).

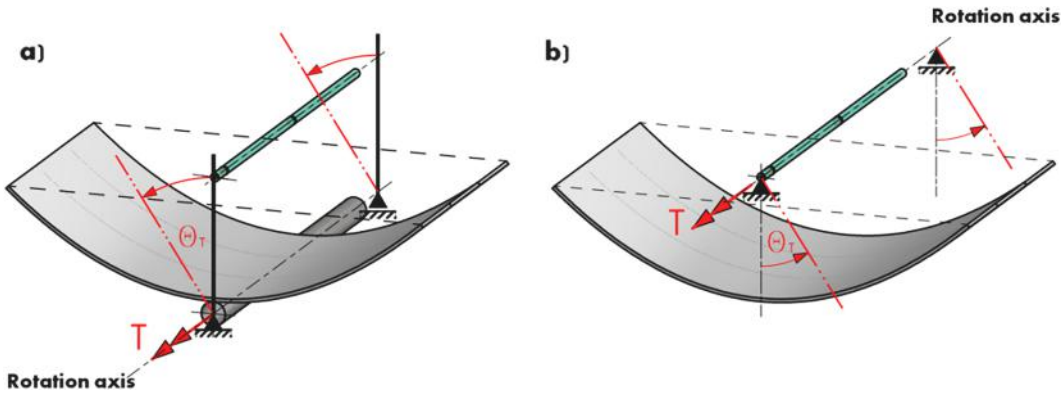

Fig. 40. a) *Conventional configuration:* The rotational axis is coaxial to the torque unit of the collector (e.g. torque tube) b) *Fixed focus configuration:* The rotational axis coincides with the focal line of the parabola at receiver's height.

plants. The capital cost of these amount 8% of the total share in a conventional solar field, including: material, assembly and installation cost (Schiel, 2011). A failure of a joint could lead to important flammable leakages causing fire accidents as happened at Andasol on 15th December 2009.

The movability of the absorber tube has been one limitation for the use of molten salts as heat transfer fluid and also for direct steam generation, due to the high operational temperatures and process pressure. Therefore, this concept offers the potential to increase the solar field's efficiency and reduce the specific solar field component costs and O&M costs.

In *conventional collectors* of Category A an optimized solution to alleviate the constant torque load on the structure, is that of placing the collectors centre of mass on the rotary axis (e.g. UltimateTrough, HelioTrough). This is also possible for the fixed focus concept, even though the rotary axis is constrained to the focal line. The requirement in this case is a meticulous mass distribution of the structures components, in order to achieve this particular coaxial alignment. If the requirement is fulfilled the torque load at receivers height would be mitigated, as well as the induced deformations at the end of the collector. The advantage of the fixed focal design is therefore the feasibility of building longer solar collector assemblies.

Fig. 41 shows two case sketches regarding the centre of mass on a fixed focus collector. The centre of gravity at the estimate position can be influenced by the parabolic geometry for example with the variation of the rim angle. In this case a rim angle of less than 90° ($\Psi < 90°$) is exemplified, not meaning the restriction for $\Psi \geq 90°$.

Fig. 41 a) shows the parabola's centre of mass at point S, where the gravitational force F_G induces the toque load with important influence especially at the end of long collector rows. In this case, the stiffness requirements in the structure are high, as well as the rigidity of drive units and bearings. Fig. 41 b) shows the parabolic structure with a shifted centre of mass at the focus S_f by adding a mass M. At the point $\dot{S}$ acts the force F_M with the aim of equalizing the load of F_G at now named $\acute{S}$. In this case, the parabolic trough structure balances around the centre of mass point for any value of Θ and the permanent torque load in the structure is mitigated.

3.5.1. Hittite solar

The Turkish collector from Hittite Solar Energy was developed to operate with superheated direct steam generation (DSG) up to 500 °C. The main motivation was to present a collector that could operate without constant breakdowns of the piping connectors. Their approach was to fix the receiver on the rotating tracking axis and to balance the collectors' centre of mass on it (see Fig. 42). This explains the counterweight above the receivers. The parabolic surface is embedded on a semi-circular structure with profiled and stamped metal sheet parts. The outer circumference serves as the support of the modules on guidance wheels at ground level. About the torque unit, a metal space frame between the semi-circular support units is responsible for its transmission,

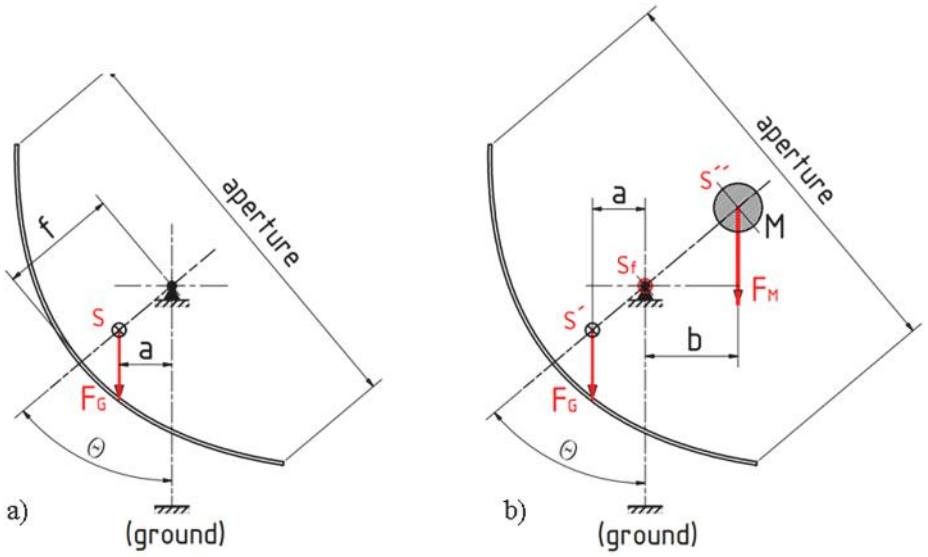

Fig. 41. Mass distribution in a fixed focus parabolic trough with the rotation axis on the focal axis.

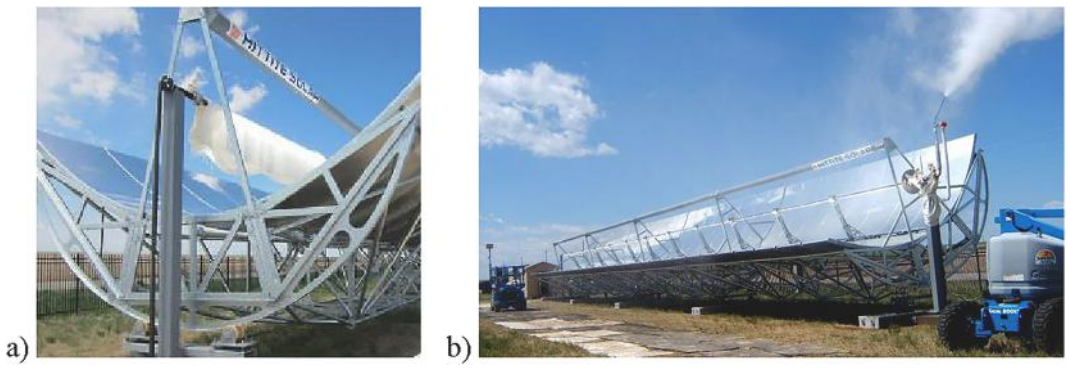

Fig. 42. a) Hittite Solar fixed focus collector with counterweight and b) solar collector row (Fairly, 2016).

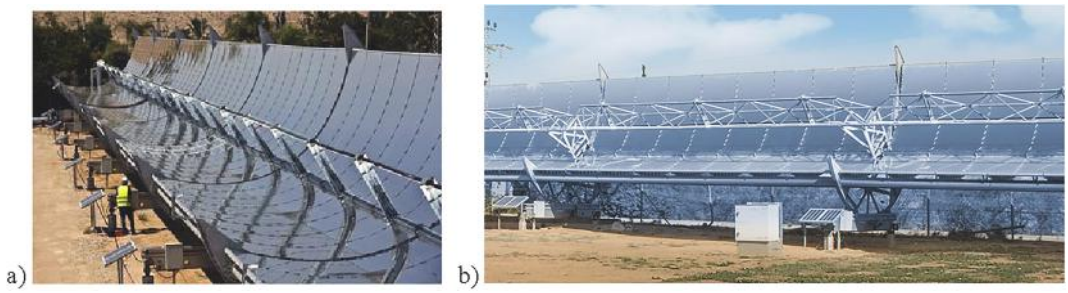

Fig. 43. a) Prototype with continuous receiver along the solar collector assembly at the Negev Desert, Israel (Reuters, 2014) b) Collector with an alternative V-Truss structure as heat collector element support (Brenmiller Energy, 2019).

which also brings support to the modules reflectors. It uses thin glass reflectors laminated on aluminium sheets with a thickness of 1.5 mm. The collector with a an aperture of 6 × 46 m has been tested four times until an output of 200 kW_{th} with steam (Fairly, 2016).

3.5.2. Brenmiller

The Israeli parabolic trough of Brenmiller Energy was developed mainly for direct steam generation (DSG) and uses fixed absorber tubes (see Fig. 43). The modules are directly connected to the next circular frame, and no welding assemblies are necessary. This frame is composed of pre-galvanized parts with an outer circular frame and an inner parabolic frame that has its focus at the geometrical centre of the outer circular profile. The centre of mass, however, is not located on the focal line. Each of these support structures is equipped with a motorized drive, which act as the modules bearings. The synchronization of these units is aimed to bring a constant torque through the SCA to reduce the angular error. A pair of torque tubes, supporting the tempered glass reflectors, is mounted for torque transmission at each end of the circular frames (Brenmiller et al., 2016). These reflectors are mounted with engineered clips, which propose an innovative method for mirror alignment (see Fig. 44).

The concept requires a jig assembly post for the torque tubes, the space frame and mirrors. With a so-called floating' solar field structure, land levelling is not necessary. The collectors are mounted on bases connected by rails. This way the collector modules are rolled to their respective position. Further technical data (e.g. dimensions, performance and costs) are limited since the troughs' line of development was discontinued and will remain in that stage, due to R&D priorities of Brenmiller´s main technology (Lipman, 2019).

3.5.3. Split mirrors

Scientists of the DLR. designed the Split Mirrors in 2009 as shown in Fig. 45. The mirror facets have a similar architecture as in the Solarlite SL4600+ collector and estimate 30% of specific mass reduction. The concept proposes a decentralized drive system with various smaller units (thus lower rated torque is required) along the solar collector assembly and aims good resistance behaviour towards wind loads, as the flow passes straight forward through the collector's gaps. The improved

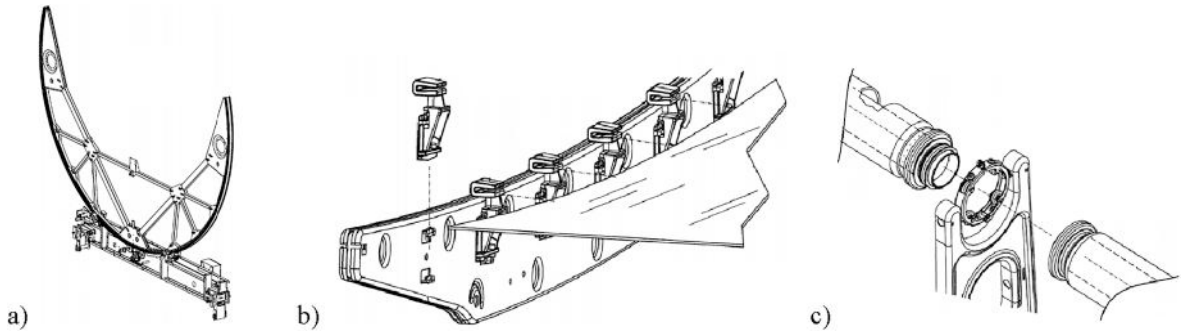

Fig. 44. a) Circular frame mounted on the support and drive bases, b) clamping method concept for mirror support and alignment, c) Illustration of the receiver tubes bearings at the HCE proposing a direct flange (Brenmiller et al., 2016).

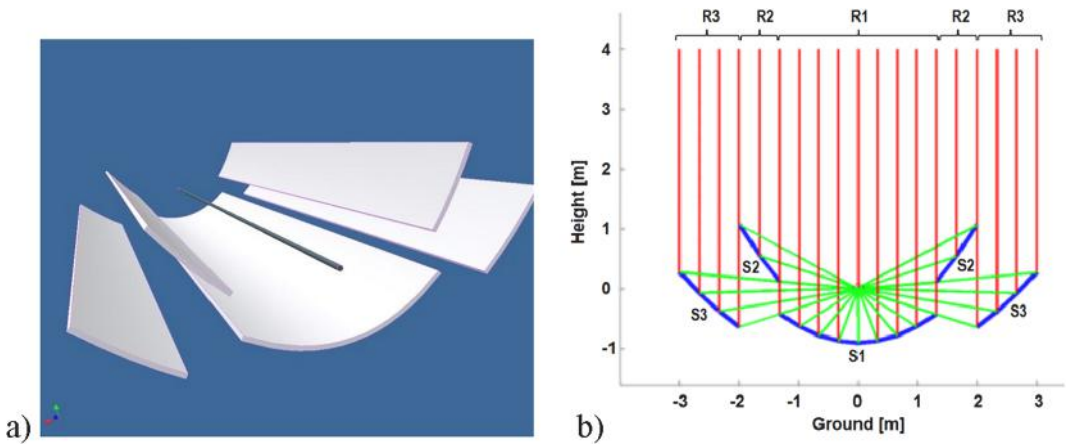

Fig. 45. a) 3D concept of the fixed focus collector with segmented parabolic aperture (Prahl & Pfahl, 2009), b) Ray's path on a cross-section of the fixed focus parabolic trough (Prahl, 2015).

optical performance results nevertheless at the expense of using more glass per square meter with a calculated increase of 19% compared to EuroTrough. A rough calculation results on a 20% drop of the solar field material costs in comparison to the EuroTrough (Prahl, 2009).

An interview with the inventor of the concept pointed out challenges regarding the holding structure of the facets (Prahl, 2019). It should be configured as simple as possible; neither to cause an overburden of weight nor shadings on the aperture that could drop the collector's performance. Further aspects still require R&D, like the heat collector element supports and the receiveŕs interconnection bearings on the pylons to achieve longer assemblies. In a development stage, while parabolic trough collectors are adapting to molten salts as heat transfer fluid, this concept possesses the potential to be considered as an alternative for this applications. Due to its stagnating advance of practical realization, the collector concept´s performance and costs can only be described by numerical and analytical studies so far.

3.5.4. MS-Trough (Molten Salt)

The MS-Trough is a fixed focus collector concept for the special use of molten salt as heat transfer fluid developed by experts of the DLR. A scaled prototype (1:4) demonstrated the functionality of the concept and remains under development. Fig. 46 b) shows the location of the torque tubes above the focal line, which collaborates to the proper mass distribution of the design. Similar to a see-saw the torque tubes are connected by an arm with welded holders and turn in the middle around the centre of mass. Since the components' distribution allocates the centre of mass on the rotary axis, the collector remains at balance in any angular position. The structure itself also suggests a new kind of assembly, for which special jig assemblies would be required on site. One collector has several 200 m long concentrator units that can be tracked and focused individually. This concept enables a continuous solar collector assembly of 1000 m length. Two key components for this realization are innovative solutions: firstly, special bearings for the receivers are featured at the pylons, which function as a connection between the tubes and separate the receivers from the movable collector shell. Secondly, these tubes are mounted under a continuous sliding rail between the pylons through the entire SCA. These elements compensated the thermal expansion of the tubes during operation. The continuous row of absorbers without the flexible transition and end joints not only reduces investment and maintenance costs, but also thermal losses. The positioning of the parabolic mirrors with a narrow mean focal length contributes to a good optical performance, since the reflected sun beams travel a shorter distance, reducing deviations until the focal point. State of the art optical performance of ~ 75–80% can be achieved with the geometrical facets´ accuracy with an aperture of about 7 m (Lüpfert, 2015). Thin glass reflectors of 1 mm thickness are combined with a thin sandwich material panel of reinforced fiberglass and foam. This structure contributes to the lightweight, stiffness and geometrical precision of the concept.

3.6. Technical data overview

Tables 4–8 sum up technical data of the collector concepts with indications on materials, structures, HTF and special features. Thermo-oils (TO) include here: mineral, synthetic and silicone oils. There are further indications for applications with air, molten salts (MS) and Heated Steam (HS) (i.e. demineralized water as high-pressure steam).

4. Value analysis and evaluation

4.1. Comparison criteria

With the definition of the state of the art parabolic trough collectors and their relevant components, the next step is to conduct a value analysis with a comparative character. In the following subsections, the collectors are compered on specific criteria. The definition of these criteria is made from a techno-economic perspective.

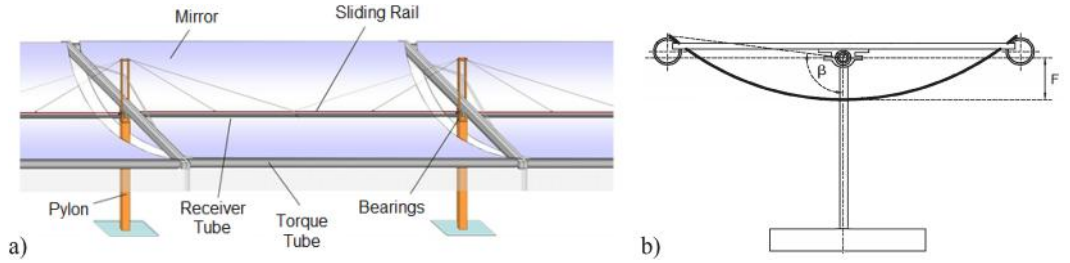

Fig. 46. a) MS-Trough collector and components with a fixed receiver along the modules (DLR, 2019), b) pair of torque tube units on each end (Eickhoff, 2018).

Table 4
Overview of Category A: Conventional parabolic trough collectors.

Collector	Bearing Structure	Aperture [m]	SCE Length [m]	SCA Length [m]	Rim Angle [°]	Focal Length [m]	Geometric Concentration [-]	Peak Optical Efficiency [-]	Absorber Tube Diameter [mm]	Heat Transfer Fluid	Reference
LS-1[1]	torque tube	2,55	6,3	50,2	–	0,94	61	71	40	TO	SEGS I-II
LS-2[1]	torque tube	5,00	8,0	47	80	1,49	71	76	70	TO	SEGS I-VII
LS-3[1]	V-truss framework	5,70	12,0	99	80	1,71	82	74	70	TO	SEGS VII-IX
EuroTrough/ SKAL-ET[1,2]	torque box	5,76	12,0	100/ 150	80	1,71	82	75	70	TO	SEGS V/ Kuraymat/ Andasol
ASTR0 150[3]	torque box; no wildings	5,76	11,9	–	–	–	–	–	–	TO	Solarnova, Spain/ North-Africa
Phoenix 3.2 [3]	aluminium space frame w/steel torque arms	5,76	11,9	–	–	–	–	–	–	TO	Solnova
Eucumsa [3]	steel space frame	5,76	11,9	125	–	–	–	–	–	TO	Solana, Arizona/ South Africa
SpaceTube ST8.2 [3,4]	space frame	8,00	16,0	–	–	–	–	–	–	TO	SolarTAC, CampoSol
ENEA [5, 6]	torque tube	5,96	12,5	100	~77	1,8	75–80	–	–	MS	Archimede Power Plan
SGX-2 [5]	aluminium space frame	5,77	12,0	150	–	–	82	–	70	TO	Saguaro, Nevada Solar 1
Sener Trough [5]	torque tube, stamped cantilever arms	5,76	12,0	150	80	1,7	82	–	70	TO	Extresol, Spain
Sener Trough 2 [5,6]	torque tube, stamped cantilever arms	6,87	13,2	–	–	–	86	–	80	TO	Valle 2, Cádiz, Spain
HelioTrough [5,]	torque tube	6,77	19,1	191	90	1,71	76	81	90	TO & MS	Test Loop SEGS Blythe, USA
Ultimate Trough [7, 8]	torque box	7,51	24,0	247	90	1,95	94	80 (75.5)	90 (70)	TO (MS)	Harper Lake, USA/Saudi Arabia, Duba
Solel/ Siemens [5]	torque tube	5,77	12,0	99	–	–	–	–	–	TO	Lebrija, Spain

Sources: [1] (Price et al., 2002); [2] (Lüpfert et al., 2003); [3] (Abengoa Solar, 2013); [4] (O'Rourke et al., 2015); [5] (Günter et al., 2011); [6] (GIZ, 2014); [7] (Riffelmann et al., 2013); [8] (Ruegamer et al., 2014).

Table 5
Overview of Category B: Alternative structures & sheet reflectors.

Collector	Bearing Structure	Aperture [m]	SCE Length [m]	SCEs per SCA [#]	SCA Length [m]	Rim Angle [°]	Geometric Concentration [-]	Reflector Type	Peak Optical Efficiency [-]	Absorber Tube Diameter [mm]	Heat Transfer Fluid	Reference
SkyTrough[1,2]	aluminium space frame	6,0	13,9	8	115	82,5	75	polymeric film ReflechTech'	76	80	TO	Protoype SEGS II
SkyTrough DSP[2]	aluminium space frame	7,0	17,7	8	148	82,5	87,5	polymeric film ReflechTech	75	80	MS, TO	Chabei, China
LAT 73[3,4]	aluminium space frame	7,3	12,0	16	192	84,8	104	polymeric film 3 M 1100	77	70	TO	Dagett, SEGS I
Solabolic Trough[5]	torque box, profiled arms	5,8	12,5	12	150	~82.0	72	aluminium sheet	–	80	TO	Segment Prototype

Sources: [1] (Günter et al., 2011); [2] (SkyFuel, 2017a,b); [3] (GIZ, 2014); [4] (3M & Gossamer Space Frames, 2012); [5] (Adel, 2018).

4.1.1. Optical performance

Parabolic trough collectors convert only a fraction of the incident solar energy into useful heat due to present optical and thermal losses. The absorbed thermal energy $\dot{Q}_{eff}$ at the receiver's end results out of the amount of concentrated absorbed power $\dot{Q}_{con,abs}$ under consideration of present heat losses $\dot{Q}_{loss}$ (Schenk & Eck, 2012).

While $\dot{Q}_{con,abs}$ is constrained by the collectors optical properties, the additional heat losses occur in the receiver mainly due to radiation and a

Table 6
Overview of Category C: non-metallic materials.

Collector	Bearing Structure	Aperture [m]	SCE Length [m]	SCEs per SCA [#]	SCA length [m]	Rim Angle [°]	Geometric Concentration [-]	Reflector Type	Peak Optical Efficiency [-]	Absorber Tube Diameter [mm]	Heat Transfer Fluid	Reference
Solarlite SL 4600+[1,2]	torque tube, sandwich composite panels	4,6	12	10	120	87,6	66	laminated thin glass	75	70	HS	Kanchanaburi, Thailand
Tough Trough[3]	torque tube, sandwich composite panels	–	–	4	–	–	–	laminated thin glass	–	–	TO	Prototype, Mecklenburg-Vorpommern,
SOL.CT[4]	concrete	2 / 6 / 9	12	4	–	–	–	cold bent thin glass	–	–	TO	–
ConSol[5]	concrete	5,77	12	12	144	80,0	82	coated aluminium	67	70	TO	Demonstration, Germany

Sources: [1] (Günter et al., 2011); [2] (Solarlite GmbH, 2010); [3] (toughTrough, 2018); [4] (AltoSolution, 2018); [5] (DLR et al., 2018).

Table 7
Overview of Category D: enclosed-aperture collectors.

Collector	Bearing Structure	Aperture [m]	SCE Length [m]	SCEs per SCA [#]	SCA Length [m]	Rim Angle [°]	Focal Length [m]	Geometric Concentration [-]	Reflector Type	Peak Optical Efficiency [-]	Absorber Tube Diameter [mm]	Heat Transfer Fluid	Reference
Airlight[1,2]	fibre reinforced concrete and inflatable polymeric membrane	9,7	212	1	212	74	3,3	70	polymeric film	61	140	Air	Ait Baha Pilot Plant, Marocco
GlassPoint[3,4]	cabled suspended mirrors, fixed receiver	7,6	8	12	180	89	2	109	coated aluminium	68	70	HS	Berry Petroleum, MIRAAH, Oman, Kuwait, California
Heliovis HelioTube[5,6]	inflatable polymeric membrane tube, with metal frames	8	220	1	220	67	3	80	polymeric film	71	80	TO & HS	Mercajucar, Spain

Sources: [1] (GIZ, 2014); [2] (Airlight Energy, 2015a,b); [3] (Glass Point Solar, 2013); [4] (Bierman et al., 2013); [5] (Bermadinger et al., 2019); [6] (Heliovis AG, 2018).

Table 8
Overview of Category E: fixed focus collectors.

Collector	Bearing Structure	Aperture [m]	SCE Length [m]	SCEs per SCA [#]	SCA Length [m]	Focal Length [m]	Geometric Concentration ratio [-]	Reflector Type	Peak Optical Efficiency [-]	Absorber Tube Diameter [mm]	Heat Transfer Fluid	Reference
Hittite Solar [1]	space frame & semi-circular structure supported on ground	6	12	6	72	–	75	thick glass	–	80	HS	Demonstration SCA
Brenmiller[2]	double torque tube, circular frame & profiles	–	–	–	–	–	–	thick glass	–	–	TO	Demonstration SCA
Split Mirrors[3]	truss frame, fibre glass and resin, foam	6	12	12	144	0.98 (mean)	86	thin glass	75	70	TO & MS	None
Molten Salt Trough[4]	double torque tube, thin sandwich composite	7.8	12	66	1000	1.2	110	thin glass	78	70	MS	Prototype Tabernas, Spain

Sources: [1] (Fairly, 2016); [2] (Brenmiller et al., 2016); [3] (Prahl & Pfahl, 2009; Blümner, 2012); [4] (Lüpfert, 2015).

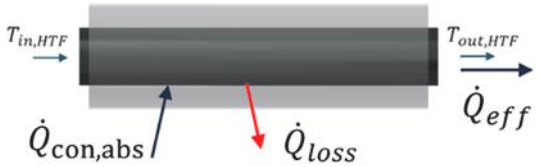

Fig. 47. Heat balance on receiver with evacuated glass envelope.

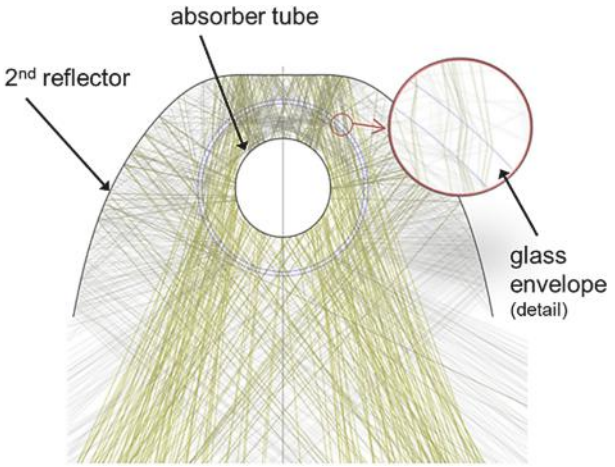

Fig. 48. Ray tracing study on the secondary reflector and receiver with n = 500 rays (Bermadinger et al., 2019).

small fraction to convection:

$$\dot{Q}_{\text{eff}} = \dot{Q}_{con,abs} - \dot{Q}_{\text{loss}} \tag{4}$$

It is possible to calculate the amount of solar energy that is absorbed into the receivers as expressed in Eq. (4). The heat balance is shown in Fig. 47. The direct normal irradiance is delimited by the dimensions of the aperture area, thus the fraction of useful power is its value times the effective aperture. Its value is also reduced in dependence to the inclination, which contains cosine losses and the angle modifier factor. Further optical losses occur, which are expressed as efficiencies (Schenk & Eck, 2012):

$$\dot{Q}_{con,abs} = \text{DNI}\cdot\cos(\theta_i)\cdot A_{\text{eff}}\cdot\eta_{\text{opt,peak}}\cdot\text{IAM}(\theta_i)\cdot\eta_{\text{shad}}\cdot\eta_{\text{endloss}}\cdot\eta_{\text{clean}} \tag{5}$$

- η_{shad}: considers optical losses due to shading of the sunrays before they hit the mirrors.
- $\eta_{endloss}$: Refers to the collector end losses of beams that do not hit the absorbers due to the non-perpendicular incidence of the suńs radiation. In between adjacent modules, the end losses retained since the next collector catches the reflected light of the previous one. This factor is commonly contained in the IAM. Optical modifications like booster reflector technologies are a feature to mitigate these losses, thus improving the collector's performance. These components are

Table 9
Peak optical efficiencies of different parabolic trough collectors.

Category	Collector	$\eta_{opt,peak}$	Category	Collector	$\eta_{opt,peak}$
A	EuroTrough (Skal-ET)	0.75[1]	D	Airlight	0.64[7]
	UltimateTrough	0.80[2] (0.76*[2])		GlassPoint	0.68[8]
B	SkyTrough	0.76[3]		Heliovis	0.63[9]
	SkyTroughDSP	0.75[4]	E	Hittite Solar	n.a
	LAT73	0.77[5]		Brenmiller	n.a
C	SL4600	0.75[6]		Split Mirrors	0.75[10]
	Tough Trough	n.a		MS-Trough	0.78[11]
	Sol.CT	n.a			
	ConSol	0.67[6]			

*Using molten salt as HTF.
Sources: (Lüpfert et al., 2003)[1] (Ruegamer et al., 2014)[2], (SkyFuel, 2017a)[3], (SkyFuel, 2017b)[4], (Raush & Chambers, 2014)[5], (Krüger et al., 2018)[6], (Good et al., 2013)[7], (Glass Point Solar, 2013)[8], (Bermadinger et al., 2019)[9], (Blümner, 2012)[10], (Lüpfert, 2015)[11].

additional vertical reflectors at the end of the collector rows, which capture those lost beams and reflect them back into the absorbers. Resent research has shown enhancement in both optical and thermal performance with the implementation of this feature (Bellos & Tzivanidis, 2019).

- η_{clean}: Refers to the cleanness of the mirrors and receivers, regarding dust, soiling or humidity.

Peak optical efficiency – Optical losses occur even at optimal direct normal irradiance. This happens when the sun is perpendicular with respect to the collector area, or in other words, when the incidence angle is$\theta_i = 0^{\circ}$. Eq. (6) estimates the peak optical efficiency when the fluid is close to ambient temperature, meaning that no thermal losses are present in the system. From Eq. (5) it is possible to write:

$$\eta_{\text{opt,peak}} = \frac{\dot{Q}_{con,abs}}{A_{\text{eff}} \cdot \text{DNI}} \tag{6}$$

assuming a state without shade, end losses and optimal cleanness. Another definition is given in Eq. (7) where other factors are taken into account like the optical properties of the mirrors, receivers and the structural accuracy (Eickhoff et al., 2014). With this equation, the optical deviations are included to estimate the peak value.

$$\eta_{\text{opt,peak}} = \rho_{\text{tot}} \cdot \gamma \cdot \tau \cdot \alpha \cdot \eta_{\text{length}} \cdot \eta_{\text{track}} \cdot \eta_{\text{torsion}} \tag{7}$$

Each of these factors can be improved in order to achieve a better optical efficiency. One practical example is the implementation of a secondary reflector to improve the intercept factor on the receivers.

Table 10
Ranking of reflector types for large scale application of parabolic troughs.

Rank	1.	2.	3.	4.
Reflector Type	Thin glass	Thick glass	(i) polymeric reflector (ii) enclosed coated aluminium	(i) enclosed polymeric reflector (ii) coated aluminium

They consists in using an auxiliary secondary reflector to capture those deviated beams after the primary parabolic mirror. A commercial example is the Heliovis collector, which implements a secondary reflector at receiver level and can achieve a concentration ratio of 100 times (Bermadinger et al., 2019). Secondary reflectors can redirect those optical errors from the primary mirror.

It has to be taken into account that implementing an additional mirror, increases the number of surfaces where the beams are reflected, absorbed and emitted. An orientation displacement of the mirror can cause as well further deviations. From the studied commercial collector only Heliovis implements this optical modification as seen in Fig. 48.

In most of the commercial collectors the peak optical efficiency is explicitly given. From Category A the UltimateTrough is chosen as a reference for the comparison versus the innovations. This collector is one of the new developments of its category and it is used as comparison reference in other studies. It enables therefore access to more information than other collectors, since more data can be acquired. For this reason, the UltimateTrough is chosen as a reference state of the art thru the chapter.

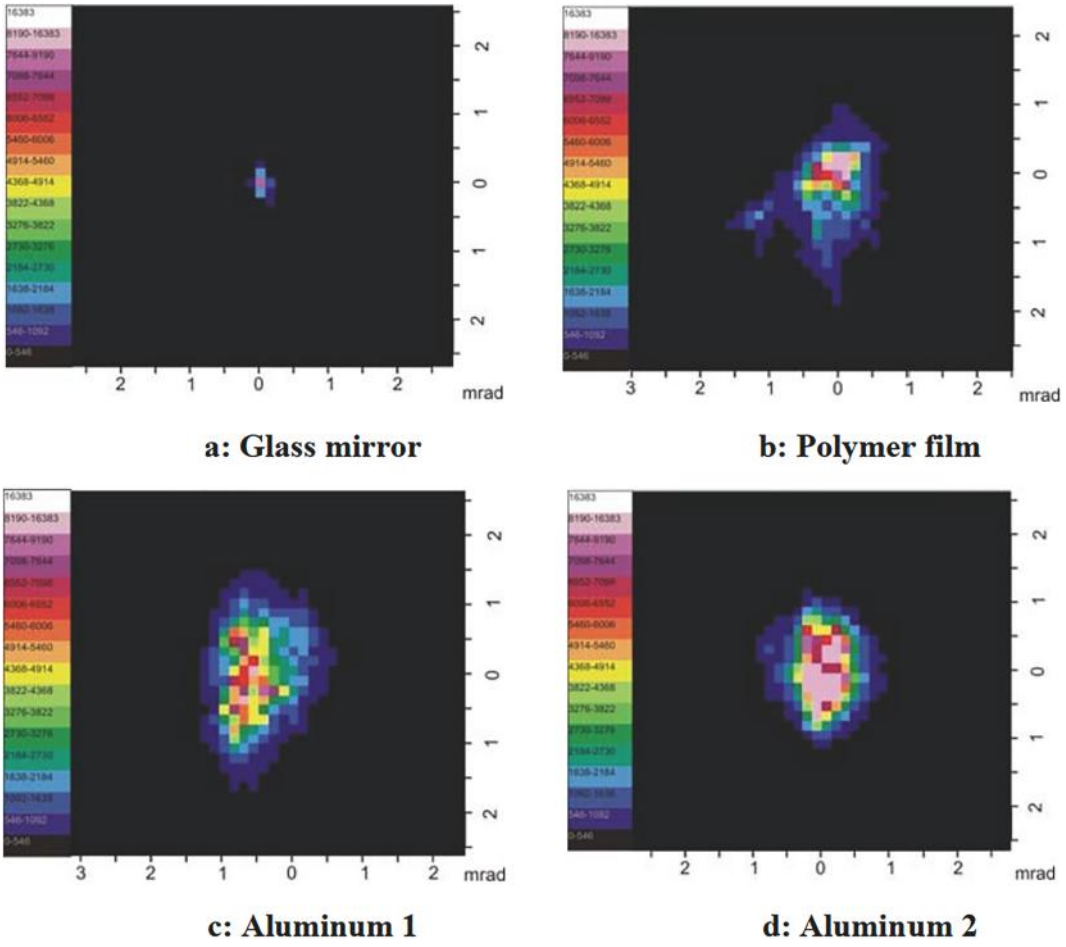

Fig. 49. Images of specular beam diversion of different material samples. Profile in the range of 3–4 mrad standard deviations respectively σ_{spec} in both directions to zero (Meyen et al., 2009).

Among the collector types, the peak optical efficiency ranges between 80.1% attributed to the UltimateTrough (Ruegamer et al., 2014) and 63% for the Heliovis collector (Bermadinger et al., 2019). In the case of the MS-Trough with 78% (Lüpfert, 2015) and Split Mirrors with 75% (Blümner, 2012), both innovations are reported on the basis of numerical results as an estimation for real scale modules. Other collectors present neither access on this parameter nor an estimation chance. Table 9 shows the values for each collector regarding the peak optical efficiency.

Incident angle modifier IAM(θ_i) and cosine lossescos(θ_i) – As the sun position varies from east to west and the elevation angle over the seasons, a parameter called Incident Angle Modifier IAM(θ_i) describes the angular dependent loss mechanism. For incident angles $\theta_i \neq 0^\circ$ the radiation does not hit the aperture area with its maximal intensity, but it does with the direct normal irradiance times the cosine of the incident angle$\cos(\theta_i)$. The cosine losses correspond to a greater loss fraction for non-perpendicular incident angles then the IAM (Eickhoff et al., 2014). Correlations of the incident angle modifier are based on measurement campaigns for each specific collector (Schenk & Eck, 2012). A detailed analysis of this factor is a limitation of the present study, since this corresponds to unique geometrical and structural properties of each collector. This information is relevant to simulate a more accurate collector performance. Despite this limitation, the study proceeds to observe the instantaneous collector efficiency, thus the factors are considered at $\theta_i = 0^\circ$. Subsequently IAM$(0^\circ) = 1$ and $\cos(0^\circ) = 1$ are set conditions for the present study. Future works may include this factor if technically disclosed by manufacturers.

Reflector type – A previous study for the characterization of the optical properties of reflector materials for concentrating solar power technologies, measured the specular reflectance $\rho_{spec}$and the surfacés degradation rate among other parameters. By using these results, it is possible to rank the reflector types according to the beam deviation of the reflected incident solar rays. The importance of the concentration of the light in a minor area (i.e. focus) is that of the interception accuracy at the focal point. The greater the beams diversion, the greater are the optical losses caused by the material or its surface.

Thick and thin glass, polymeric films and sputtered aluminium reflectors, are the state of the art. Results of the aforementioned study are presented in Fig. 49. The images show the measured specular beam profile and demonstrate the marginal size of specular beam diversion of all samples (Meyen et al., 2009). Even though thin glass mirrors were not measured, similar results to Fig. 49a) are assumed, due to the similar architecture and materials as thick glass.

Thin glass mirrors possess an enhanced reflectivity respective to thick glass. It also has the advantage of a thinner glass layer, which reduces transmission losses. It is therefore why thin glass is considered a more suitable alternative technology with a potential to enhance a collectors optical performance. Furthermore, degradation rates are higher in first-surface mirrors, which are the case for polymeric films and aluminium (Meyen et al., 2009). For the analysis, the reflector ranking is shown in Table 10.

4.1.2. Thermal performance

In an operational solar field, heat losses occur in the receivers and the connected piping system. These losses depend on the temperature difference between the heat transfer fluid and the surrounding. As mentioned previously in Chapter 2.3, large parts of the thermal losses occur in the receivers predominantly at high temperatures, where coating properties, vacuum insulation and absorber diameter have an important influence. For the theoretical comparison of the thermal aspects, assumptions are made, since the operating temperatures and heat capacity factors vary according to the implemented heat transfer fluid. Also depending on the collectoŕs concentration ratio, the heat gain is variable.

A challenge for this criterion is to compare the collectors and their components as they correspond in their commercial configuration. It may sound paradoxical that the comparison is not based on the same line of characteristics, but if this were the case, the analysis would be based on technologies that are not tangible and would rule out the possibility of highlighting practical technological attributes. If we observe an objective and arbitrary example, commercially there is: i) A EuroTrough loop with a length of 600 m, an aperture of 5.77 m, uses a receiver of 70 mm diameter and has an optical efficiency of 0.75 (Lüpfert et al., 2003). ii) An UltimateTrough loop with a length of 960 m, an aperture of 7.51 m, uses a receiver with a diameter of 90 mm and has an optical efficiency of 0.80 (Ruegamer et al., 2014). Both operating with thermal oil. If we compare the thermal aspect, we have to take into account the concentrated absorbed solar power depending on the amount of DNI per aperture area. In this case, the UltimateTrough has a larger area than the EuroTrough, and implies a higher proportion of solar energy collected and concentrated in the receivers. Respectively, the70 mm and 90 mm receivers have their emissivity and absorption properties that define the thermal losses at operational state.

With this example, if it were assumed that both collectors use 80 mm

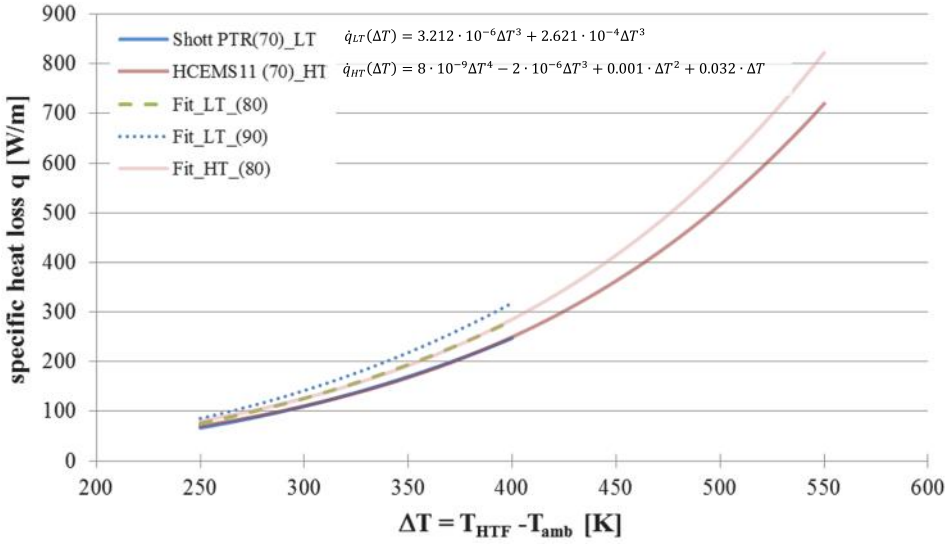

Fig. 50. Specific thermal losses of a low temperature receiver PTR70 (SCHOTT Solar CSP GmbH, 2013) and of a high temperature HCEMS11 receiver (Archimede Solar Energy, 2012).

receivers in order to introduce a general baseline of thermal losses, parameters would be induced that do not match the operational collectors. In this case, the geometric concentration value of the collectors would change, as well as the optical efficiency value. Consequently, the value of the mass flow at design point for each loop would be altered by the variation of the diameter and with this, the hydraulic power consumption and its pressure losses (i.e. parasitic losses). A practical example is the UltimateTrough operating with molten salts. The manufacturer's design for this medium integrates a special 70 mm receiver (instead of 90 mm) for which the optical efficiency sinks to 0.76 (0.04 points less than with oil) (Ruegamer et al., 2014). In order to analyse and evaluate the reality of each concept, the parameters of their commercial version are considered in order to identify its special attributes over others.

This study, however, uses a general description for the specific receiver heat losses $\dot{q}$ in W/m depending on the diameter. Departing from the losses given in the product data sheet of a low temperature PTR70 receiver at laboratory conditions, a curve $\dot{q}_{LT}(\Delta T)$ is interpolated with a 3rd order polynomial (SCHOTT Solar CSP GmbH, 2013). The same procedure is done for a high temperature receiver type HCEMS11 (70) with a curve $\dot{q}_{HT}(\Delta T)$. This curve will be specially use to simulate the case with molten salt HTF. Fig. 50 shows both curves of specific receiver thermal losses.

For simplification purposes, the ratio between receiver diameters is assumed as an increment factor to describe receiver losses with greater diameters compared to 70 mm. A greater receiver diameter, imply a greater receiver surface, thus greater losses are expected. It is estimated for a diameter ∅80 mm that receiver losses will at least be increased by a factor of 1.14 (80 ÷ 70), while for ∅90 mm by a factor of 1.29 (90 ÷ 70) as the ratio of the diameters is calculated.

Another challenge for the analysis of the thermal performance, (and in general), is to avoid analysing mixed criteria. For example, there are studies that raise the exergy efficiency as an indicator for the performance. The reason is that this factor describes the useful heat production as the maximum equivalent work that a Carnot thermal engine is able to produce (Bellos and Tzivanidis, 2018). At the same time, it considers the pressure drop along the absorber tube and the pumping work demand for the mass flow of the HTF. The exergy efficiency is defined as the ratio of the useful exergy production to the exergy flow of the solar irradiation (Bellos & Tzivanidis, 2017):

$$\eta_{ex} = \frac{E_u}{E_s} \tag{8}$$

This study, seeks to separate this criteria, since pumping power and thermal properties can be individually analysed. Even though, the exergy efficiency analysis is a valuable indicator, it is not used explicitly as a comparison criterion. If it were included, the same characteristic would be evaluated multiple times (i.e. thermal performance and parasitic consumption). Thus, the possibility of observing the individual technical aspects would be excluded. For this reason, two scenarios characterize the evaluation study for the thermal performance criterion: Scenario 1 compares all evaluable collectors using the same heat transfer fluid, in this case with a thermo-oil of type Therminol VP-1. Scenario 2 analyses only those collectors suitable for molten salts. The parasitic consumption is then discussed as individual criterion in the following subsection.

4.1.2.1. Scenario 1: Thermal power & performance with thermo-oil type Therminol VP-1. A loop for each respective collector type is considered with thermo-oil as HTF. This scenario aims to describe the performance at optimal conditions of a single loop of each collector. The factors of interest are respective loop thermal power gain and losses at operational design mass flow. The Eq. (9) shows the dependence of the effective thermal energy according to the properties of the fluid and operational temperatures.

$$\dot{Q}_{eff} = \dot{m}_{HTF} \cdot c_p \cdot (T_{out} - T_{in}) = \dot{Q}_{con,abs} - \dot{Q}_{loss} \tag{9}$$

The analysis is considered at optimal conditions for incident angle $\theta_i = 0°$, for which the cosine losses and IAM take the value of 1. For the cleanliness factor, brand new installed reflectors are assumed ($\eta_{clean} = 1$) at a design point of DNI = 800 W/m^2. According to Eq. (5) the solar thermal energy is computed as follows:

$$\begin{aligned} &\dot{Q}_{con,abs} = A_{eff} \cdot \mathrm{DNI} \cdot \eta_{opt} \\ \text{with} \quad &\mathrm{IAM}(0^\circ), \cos(0^\circ), \eta_{shad}, \eta_{endloss}, \eta_{clean} = 1 \end{aligned} \tag{10}$$

For the thermal losses following expression is used, where x is the loop length (Schenk & Eck, 2012):

$$\dot{Q}_{loss} = \int \dot{q}(\Delta T) dx = \int \dot{q}(T_{\mathrm{HTF}} - T_{\mathrm{amb}}) dx \tag{11}$$

See in Fig. 50 the values of $\dot{q}(\Delta T)$, where the low temperature curve is used for thermal oil scenario and the high temperature curve for the molten salt scenario. The collector thermal efficiency is calculated next as follows:

$$\eta_{col} = \eta_{opt} - \frac{\dot{Q}_{loss}(\Delta T)}{DNI \cdot A_{eff}} \tag{12}$$

Table 11
Simulation results of different PTC loops and relevant parameters for the computation with thermo-oil as HTF.

Collector Loop HTF: Therminol VP-1		Euro Trough	Ultimate Trough	SkyTrough	SkyTrough DSP	LAT73	SL4600	ConSol	GlassPoint	Heliovis	Split Mirrors	MS-Trough (600)
Loop length	m	600	960	460	592	576	720	576	360	440	576	600
Absorber diameter	m	0.07	0.09	0.08	0.08	0.07	0.07	0.07	0.07	0.07	0.07	0.07
Peak optical efficiency	–	0.75	0.801	0.76	0.75	0.77	0.75	0.67	0.68	0.63	0.75	0.78
Mass flow at loop design	kg/s	7.62	16.40	5.90	8.86	9.30	6.97	6.30	5.35	5.85	7.40	10.50
Thermal loss per loop	MW_{th}	0.10	0.21	0.09	0.11	0.15	0.12	0.10	0.06	0.08	0.10	0.10
Interconnection pipes losses	MW_{th}	0.006	0.008	0.007	0.007	0.007	0.006	0.006	0.002	0.006	0.003	0.001
Effective thermal energy	MW_{th}	1.97	4.40	1.58	2.37	2.43	1.86	1.68	1.43	1.64	1.97	2.82
Losses for each MW thermal power	$\%/MW_{th}$	5.1	4.7	5.6	4.8	6.2	6.5	5.7	4.2	4.9	4.9	3.6
Losses at interconnection pipes	$\%/MW_{th}$	0.32	0.18	0.44	0.31	0.28	0.31	0.37	0.17	0.38	0.18	0.02
Collector Efficiency	–	0.71	0.77	0.72	0.72	0.73	0.70	0.63	0.65	0.60	0.72	0.75
Solar-to-Electric Efficiency (power block efficiency η_{PB} = 38.5%)	%	0.27	0.29	0.28	0.28	0.28	0.27	0.24	0.25	0.23	0.28	0.29

Table 12
Simulation results of different PTC loops and relevant parameters for the computation with molten salt as HTF.

Collector Loop HTF: Molten Salt			Ultimate Trough	SkyTroughDSP	Split Mirrors	MS-Trough (800)
l_{loop}	Loop length	m	960	592	576	800
$\varnothing d_{abs}$	Absorber diameter	m	0.07	0.08	0.07	0.07
$\eta_{opt,peak}$	Peak optical efficiency	–	0.76	0.75	0.75	0.78
$\dot{m}_{design}$	Mass flow at loop design	kg/s	10.30	5.78	4.80	9.25
Q_{loss}	Thermal loss per loop	MW_{th}	0.32	0.20	0.20	0.27
$Q_{ip,loss}$	Interconnection pipes losses	MW_{th}	0.011	0.012	0.006	0.001
Q_{eff}	Effective thermal energy	MW_{th}	4.05	2.27	1.87	3.62
$Q_{loss} \div Q_{eff}$	Losses for each MW thermal power	$\%/MW_{th}$	8.0	8.8	10.4	7.4
$Q_{ip,loss} \div Q_{eff}$	Losses at interconnection pipes	$\%/MW_{th}$	0.28	0.53	0.30	0.03
η_{col}	Collector efficiency	–	0.70	0.69	0.68	0.73
$\eta_{solar\text{-}to\text{-}electric}$	Solar-to-Electric Efficiency (Power Block Efficiency, $\eta_{PB} = 43.3\%$)	%	0.30	0.30	0.29	0.31

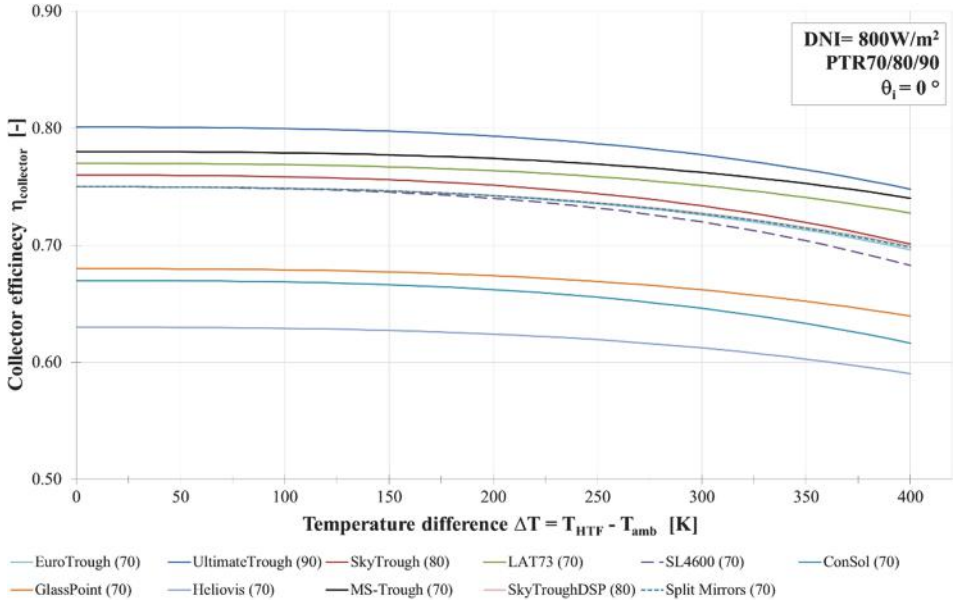

Fig. 51. Performance comparison of different PTC loops with Thermo-Oil as HTF.

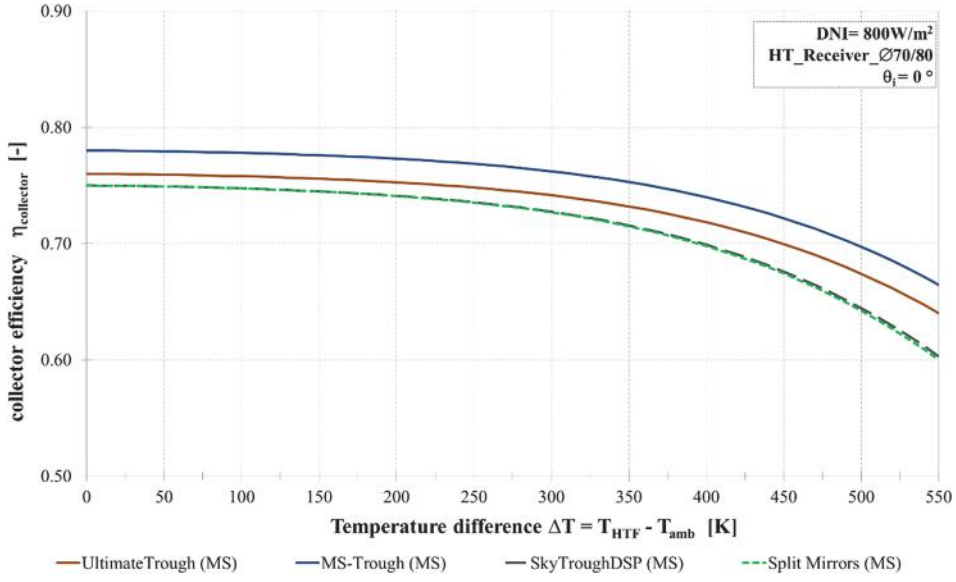

Fig. 52. Performance comparison of different PTC loops with Molten Salt as HTF.

which derives from the thermal balance in Eqs. (4)–(5) considering thermal losses in the system. Being this efficiency assumed as the solar field efficiency η_{SF}, it is possible to estimate the solar-to-electric efficiency of the solar power plant for each collector type according to Eq. (13) (Günter et al., 2011). A power block efficiency η_{PB} is generalized for the two HTF implementations. In this case, the value for thermo-oil operating solar fields is considered at 38.5% (Ruegamer et al., 2014):

$$\eta_{solar-to-electric} = \eta_{SF} \cdot \eta_{PB} = \eta_{col} \cdot \eta_{loss,pipe} \cdot \eta_{PB} \quad (13)$$

Pipeline thermal losses are neglected($\eta_{loss,pipe} = 1$) for this study, thus we induce an ideal energy conversion between the power generated by the collectors and by the power block. Since the format, size and solar multiple varies depending on the design of the power plant, this statement remain general for this studied collectors. Further research on the operational losses can benefit from the results of the collector efficiencies shown in Table 11 for collectors operating with a VP1 thermo-oil HTF and from Table 12 for collectors operating with molten salt as HTF.

To facilitate the comparison between the different collector types from a global point of view, three collectors have been adapted for the study.

- **GlassPoint:** The collector is specifically used for process heat generation with steam, more precisely for enhanced oil recovery (EOR). An operational assumption with thermo-oil as heat transfer fluid is set for this scenario.
- **SL4600:** Its main operational purpose is direct steam generation (DSG). Same assumption is met as the previous collector.
- **MS-Trough:** The collector is specifically designed to operate with the denser molten salt medium in comparison to thermal oil, which is the reason for its 800–1000 m continuous solar collector assembly length. The pressure drop in a collector loop of these dimensions represents an unrealistic deployment at approximately 20 bar. The loop length is therefore established at 600 m for oil operations.

Fig. 51 exposes the performance curve of the collector concepts with their respective receiver diameter. For this, Eqs. (9)–(12) are used. Table 11 sums up the computed parameters as well as the results for the respective collectors.

The UltimateTrough yields the best thermal performance at operational temperatures (T_{in} = 290 °C, T_{out} = 400 °C) with 77% followed by the MS-Trough with 75%. GlassPoint (65%), ConSol (63%) and Heliovis (60%), have the lowest thermal performance of this case. This result in specific percentual heat losses related to the generated thermal power output of 3.6%/MW_{th} for the MS-Trough, 4.2%/MW_{th} for GlassPoint, 4.7%/MW_{th} for the UltimateTrough, 4.8%/MW_{th} for SkyTroughDSP, 4.9%/MW_{th} for Heliovis and the Split Mirrors, 5.1%/MW_{th} for the EuroTrough, 5.6%/MW_{th} for SkyTrough, 5.7%/MW_{th} for ConSol, 6.2%/MW_{th} for the LAT73 and 6.5%/MW_{th} for the SL4600+. The table contains as well results of the solar-to-electric efficiency of the power plant according to Eq. (13) with a power block efficiency of 38.5% (Ruegamer et al., 2014).

These calculations were performed with heat losses data according to the receiveŕs manufacturer delivered at laboratory conditions (i.e. without wind influences, with completely new absorber tubes and optimal thermal holder insulation). In a real solar thermal power plant, these heat losses are higher, so that in reality the efficiencies calculated in this study tend to be optimistic. Nevertheless, these values can be used, as this study targets a tendency comparison and not of the absolute values. The tendency to positive efficiency determination has the same effect on all collectors, so that this effect has practically no significant influence once comparing the collectors to each other.

4.1.2.2. Scenario 2: Thermal power & performance with molten salt. This scenario only deals with collectors designed or adaptable to operate with molten salts, among them, the conventional collector UltimateTrough and three further innovations namely SkyTroughDSP, Split Mirrors and MS-Trough. They are declare by their manufacturers to be suitable for this fluid. The aim of this scenario is to remark the improvement potential of a power plant under the use of molten salts (vs. thermo-oils) as HTF. The power block efficiency with molten salt applications is considered at 43.3% (Ruegamer et al., 2014).

The comparison follows the same format as in "scenario 1", yet considering operational solar field temperatures at T_{in} = 290 °C and T_{out} = 550 °C. Results are shown in Fig. 52 and Table 12. Two collectors are adapted for the comparison as follows:

- **UltimateTrough:** Operational conditions for molten salt have been simulated in a previous study to optimize its performance. The computed parameters are based on it, including a ∅70 mm receiver and an optical efficiency of 75.5% (Ruegamer et al., 2014).
- **MS-Trough:** Once operating with molten salt the previous modification for "scenario 1" is no longer required. The collector length is considered at 800 m as designed.

4.1.3. Parasitic consumption

Another type of loss that is affected significantly by the collector loops and subsequently by its design, is the parasitic energy consumption of the power plant. These losses constitute the required electrical power to operate the plant. Normally this electricity demand is covered by the thermal power plant itself or by the grid-network, when the plant is offline (Schenk & Eck, 2012). The majority of this power is consumed by the pumping of the heat transfer fluid trough the extensive collector rows or through the storage tanks and by the tracking drives of the collectors. A percentage of the parasitic consumption occurs also due to further electrical components, like valves, ventilators, and BOP (balance of plant) equipment. The parasitic energy consumption amounts around 10% of the generated power or about 2% of the input solar power (Jones, 2001). This section focuses on the electric consumption of the solar field HTF-pumps mainly because this is directly affected by the

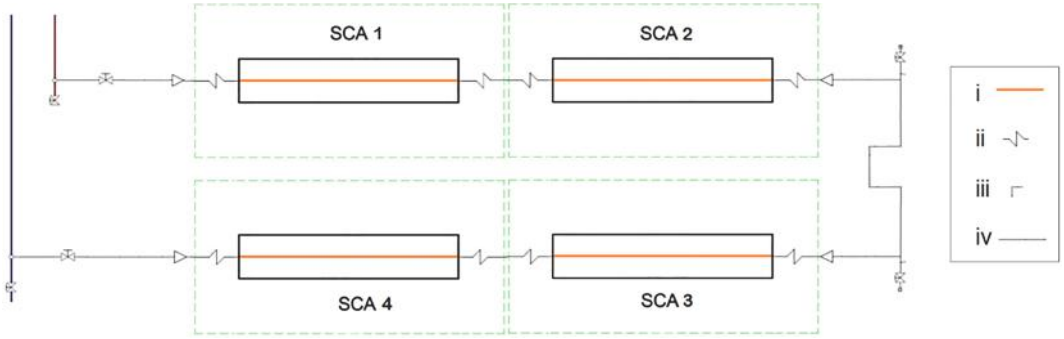

Fig. 53. Scheme of a conventional loop. (i) Receiver piping, (ii) ball-joints, (iii) 90°-elbows and (iv) straight piping.

Table 13
Parasitic power consumption of the HTF pump in a solar field with thermo-oil as HTF.

Pressure Drop with HTF: Therminol VP-1			Euro Trough	Ultimate Trough	Sky -Trough	SkyTrough DSP	LAT73	SL4600	ConSol	Glass -Point	Heliovis	Split Mirrors	MS-Trough (600)
$\Delta p_{receiver}$	Pressure drop on receiver tubes	bar	4.4	6.9	1.0	2.9	6.3	4.4	2.9	1.3	1.9	4.0	8.4
$\Delta p_{crossover+}\Delta p_{obstacle}$	Pressure loss on cross-over pipes and obstacles	bar	3.4	2.9	0.9	2.2	5.2	2.7	2.3	0.3	0.8	0.7	0.2
$\sum \Delta p$	Total pressure loss per loop	bar	7.8	9.9	1.9	5.1	11.5	7.2	5.2	1.6	2.8	4.7	8.6
Parasitic Consumption													
$P_{pump,el}$	Electric power consumption of the HTF pump	kW_{el}/ Loop	9.8	26.4	1.9	7.3	17.4	8.2	5.3	1.4	2.6	5.7	14.8
P_{el}	Thermal-to-electric power	MW_{el}/ Loop	0.70	1.51	0.54	0.81	0.84	0.63	0.57	0.50	0.54	0.68	0.98
$\eta_{parasitic}$	Parasitic Power consumption due to HTF pumping	%	1.4	1.8	0.3	0.9	2.1	1.3	0.9	0.3	0.5	0.8	1.50

collector loop design. Other power consumers like ventilators, valves and BOP pumps for instance, are not included. The parasitic consumption for the tracking systems of the collectors can be assumed to be about the same and is therefore negligible for the comparison of the collector concepts (Schenk & Eck, 2012).

Departing from the previous scenarios for the thermal performance estimation in scenario 1 and 2, the electrical parasitic consumption for the solar field is evaluated for both thermo-oil and molten salt application separately. For these cases, a single loop design of each collector is analysed, where piping cross-overs units, flexible joints and receivers are taken into account to calculate the respective pressure drop.

The heat transfer fluid pumps efficiency (η_{pump}) ranges between 0.8 and 0.9 depending on the manufacturer. The electric consumption of this pump is estimated with Eq. (14) (Schenk & Eck, 2012):

$$P_{pump,el} = \frac{\dot{V}_{HTF} \cdot \Delta p_{HTF}}{\eta_{pump}} \tag{14}$$

Considering the mean density of the fluid, the volumetric flow is written as follows:

$$\dot{V}_{HTF} = \frac{\dot{m}_{Design}}{\rho_{mean}} \tag{15}$$

The values for the mass flow design are taken from Table 11 and Table 12. This only leaves the determination of the HTF pressure drop over the whole loop open to calculate the parasitic power consumption. This study provides an emphasis on the pressure drop in a loop attached to the receivers ($\Delta p_{receiver}$), cross-over sections over the pipeline length ($\Delta p_{crossover}$), as well as of ball joints and elbow elements ($\Delta p_{obstacle}$). Fig. 53 shows the conventional format of a collector loop and the piping segments. The loops of those innovative collectors that differ from this format are calculated according to their design as for the cases of Heliovis, GlassPoint, Split Mirrors and MS-Trough.

The pressure drop in the HTF is calculated with the following equation:

$$\Delta p_{HTF} = \Delta p_{receiver} + \Delta p_{crossover} + \Delta p_{obstacle} \tag{16}$$

where the pressure drops due to the straight receiver tubes $\Delta p_{receiver}$ is given as follows:

$$\Delta p_{receiver} = \lambda \cdot \frac{8 \cdot L \cdot \dot{m}^2}{d^5 \cdot \pi^2 \cdot \rho} \tag{17}$$

The friction coefficient for turbulent streams ($\lambda = 0.015$) is considered to be constant as a simplification for the cases. To calculate the pressure drop in the ball-joint assemblies and in the obstacles like elbows, following equation is used:

$$\Delta p_{crossover} + \Delta p_{obstacle} = \left(n \cdot \xi + \frac{\lambda \cdot L}{d}\right) \frac{8 \cdot \dot{m}^2}{d^4 \cdot \pi^2 \cdot \rho} \tag{18}$$

The the pressure loss coefficient for 90° elbows is $\xi_{90°} = 0.35$ and n is the number of ball-joints and elbow elements. The two later are considered to cause the same pressure loss. The parasitic power consumption due to the heat transfer fluid pumps can be described as

Table 14
Parasitic power consumption of the HTF pump in a solar field with molten salt as HTF.

Pressure Drop HTF: Molten Salt			Ultimate Trough	SkyTroughDSP	Split Mirrors	MS-Trough (800)
$\Delta p_{receiver}$	Pressure drop on receiver tubes	bar	5.4	0.5	0.7	3.6
$\Delta p_{crossover} + \Delta p_{obstacle}$	Pressure loss on cross-over pipes and obstacles	bar	2.7	0.4	0.1	0.1
$\sum \Delta p$	Total pressure loss per loop	bar	8.1	1.4	0.8	3.7
Parasitic Consumption						
$P_{pump,el}$	Electric power consumption of the HTF pump	kW_{el}/Loop	5.7	0.5	0.2	2.4
P_{el}	Thermal-to-electric power	MW_{el}/Loop	1.35	0.74	0.62	1.22
$\eta_{parasitic}$	Parasitic Power consumption due to HTF pumping	%	0.42%	0.06%	0.03%	0.19%

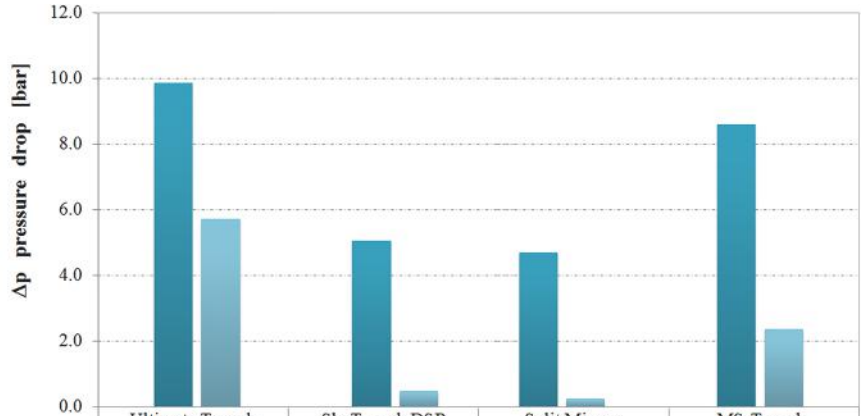

	Ultimate Trough	SkyTrough DSP	Split Mirrors	MS-Trough
Themo Oil VP-1	9.9	5.1	4.7	8.6
Molten Salt	5.7	0.5	0.2	2.4
Parasitics ThermoOil	1.8%	2.1%	0.8%	1.5%
Parasitics Molten Salt	0.42%	0.06%	0.03%	0.19%

Fig. 54. Pressure drop and parasitic consumption of different PTC loops with Thermo-Oil (VP-1) vs. Molten Salt as HTF.

follows (Schenk & Eck, 2012):

$$\eta_{\text{parasitic}} = \frac{P_{\text{pump,el}}}{P_{\text{el}}} \tag{19}$$

Finally, it is necessary to use the electric power gained by the simulated loops to estimate the parasitic consumption in relation to the produced power. The effective thermal output $\dot{Q}_{eff}$ multiplied by the efficiency factor of the solar power plant η_{PB}, previously given in Table 11 and Table 12, result in the generated electric power (Schenk & Eck, 2012):

$$P_{el} = \dot{Q}_{eff} \cdot \eta_{loss,pipe} \cdot \eta_{PB} \tag{20}$$

Also here, the pipeline thermal losses are neglected ($\eta_{loss,pipe} = 1$) as in Eq. (13). The results on the parasitic consumption of the heat transfer fluid pump are summed up in Table 13.

Power plants count with a designed pressure drop of about 10 to 14 bar, which in operation may be influenced by the design of the piping and interconnection elements. In addition, the length of the collector influences significantly the value for the pressure drop on the receiver $\Delta p_{\text{receiver}}$ significantly. The assumed length modification of 600 m instead of 800 m for the MS-Trough exemplifies this behaviour, which results in an increased pressure drop from 8.4 bar to 19.9 bar (42% difference) on the straight receiver tubes by just varying the length of the receiver tube. A possible alternative to reduce the pressure drop is the variation of the tubes to a greater diameters, as can be deduced from Eq. (17) and Eq. (18). In the case of the MS-Trough, GlassPoint and Split Mirrors, the absence of ball joints leads to lower pressure losses ($\Delta p_{\text{crossover}} + \Delta p_{\text{obstacle}}$) ranging from 0.7 and 0.2 bar. Compared to that, the other collectors show a pressure drop between 5.2 and 0.9 bar, for the computed loop conditions.

For the scenario with molten salts as heat transfer fluid, Table 14 shows the results. The SkyTroughDSP and the Split Mirrors collectors require the lowest mass flow as shown before in Table 12. These collectors have also the shortest collector loops compared to the UltimateTrough and the MS-Trough, which is the main reason for their low parasitic consumption. All four collectors represent an evident enhancement on the pressure losses and subsequently on the parasitic consumption. Fig. 54 shows the pressure drop using thermal oil vs. molten salts HTF.

4.1.4. Costs scenario

In a parabolic trough power plant, the investment cost of the solar

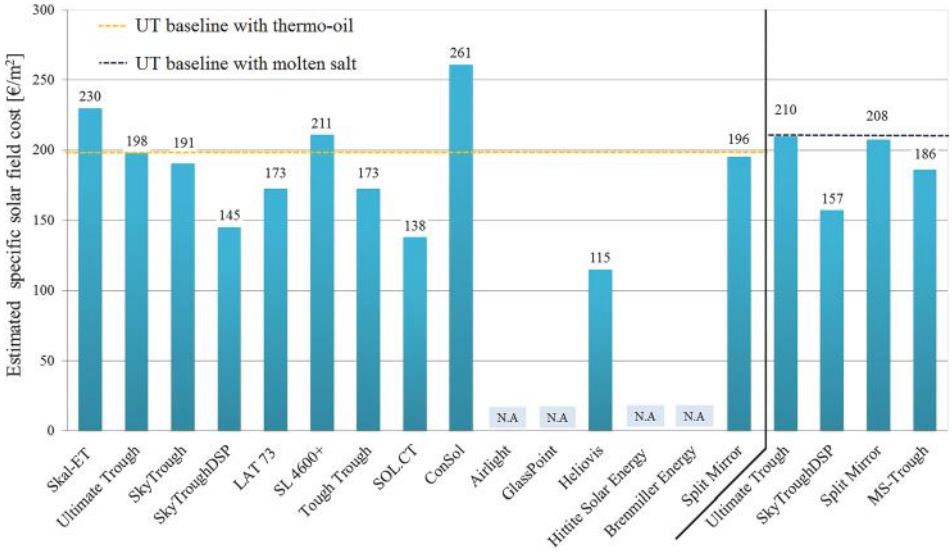

Fig. 55. Specific solar field cost estimate for different parabolic trough collectors. Supplement Table 15.

Table 15
Specific solar field cost estimation with different parabolic trough collectors.

HTF: Thermo-Oil Category	Collector	Solar Field Costs €/m²	Estimate difference to Baseline 1	HTF: Thermo-Oil Category	Collector	Solar Field Costs €/m²	Estimate difference to Baseline 1	HTF: Molten Salt Category	Collector	Solar Field Costs €/m²	Estimate difference to Baseline 2
A	EuroTrough	230	Baseline 1[1]	D	Airlight	n.a.	–	A	Ultimate Trough	210	Baseline 2 [2]
	Ultimate Trough	198	↓14% [2]		GlassPoint	n.a.	–	B	SkyTrough DSP	157	↓ 25% *
B	SkyTrough	191	↓17% [2,3]		Heliovis	115	↓50% [9]	E	Split Mirror	208	↓ 1.2% *
	SkyTrough DSP	145	↓37% [4]	E	Hittite Solar Energy	n.a	–		MS-Trough	186	↓ 11% [1]
	LAT 73	173	↓ 25% [5]		Brenmiller Energy	n.a	–				
C	SL 4600+	211	↓ 8% [6]		Split Mirror	196	↓ 15% [10]				
	ToughTrough	173	↓ 25% [7]		MS-Trough	172	↓ 25% [1]				
	SOL.CT	138	↓ 40% [8]						Currency conversion: (2.12.2019)	1.00€	⇔ 1.10 $
	ConSol	261	+↑ 12% [6]								

Sources: (Lüpfert, 2015)[1], (Ruegamer et al., 2014)[2], (Kurup and Turchi, 2015)[3], (Schuknecht et al., 2018)[4], (3M & Gossamer SpaceFrames, 2012)[5], (Krüger et al., 2018)[6], (Stancich, 2012)[7], (Alto.Soultions, 2018)[8], (Bermadinger et al., 2019)[9], (Prahl & Pfahl, 2009)[10].

field amounts about 31% with a 7.5 h storage system that adds further 11% to the total costs as described for the Andasol plant in Spain (IRENA, 2012). This means that the parabolic trough collectors and the supplementary operational equipment (e.g. drives, pylons, electric components, inter loop piping, header piping, among others), are carriers of one third of the costs of a solar plant. The heat transfer fluid carries between 5% and 8% of the costs including the medium of the storage block (IRENA, 2012).

A solar field with molten salts as heat transfer fluid requires a constant higher thermal state to avoid the solidification of the salt in the pipelines, including receivers and cross-over elements. Thus, the requirements on the piping material, isolation material and antifreeze heating system are also higher and therefore higher in cost. The piping needs to be first made of stainless steel as a corrosion resistant material and secondly, it should be fully equipped, for instance, with induction heaters for the receivers and heat tracing systems through the kilometres of solar field piping. Also the heating of movable components i.e. ball-joints or swivel joints, comprehend on a cost intensive character. That causes an increase of the solar field costs, but on the other hand significant reductions on the storage and adjacent blocks can be achieved. The application of the same transfer fluid in the solar field and storage system enables a more effective use of the higher temperature difference between the two storage thanks, increasing the capacity of their given volume (Ruegamer et al., 2014). The specific cost of the thermal storage block is reduced by almost a factor of three considering an overall molten salt implementation and an upscale from a 50 MW to a 100 MW solar plant (Ruegamer et al., 2014).

The present study contains a rough estimate overview of the specific solar field costs for the collectors, some of them departing from manufacturers' specifications and others by technical argumentations or case studies. The analysis of these collectors presents practical boundaries that need to be established. One is the limitation of information and the other is that in most of the cases no real solar field has been deployed aside from theoretical studies. The specific baseline for a 50 MW EuroTrough solar field was considered at around ≈228 €/m² (Ruegamer et al., 2014). For the sake of introducing a common reference for the specific solar field costs the current baseline is considered at 230 €/m² for the conventional collector, EuroTrough. This enables a qualitative representation of the collectors endorsed by the given sources.

The diagram in Fig. 55 presents the results of the study focused on two baselines. First, Baseline 1 is represented by the value of the EuroTrough as the known conventional collector, which operates with thermo-oil as HTF. The solar field costs of the UltimateTrough were previously estimated with a cost reduction of −23% vs. the EuroTrough, due to the scaling of the aperture and reduction of elements (Riffelmann et al., 2013). This was later rectified in a case study by the manufacturers with only 14% reduction, thus deferring from the starting calculations by 9% (Ruegamer et al., 2014).

A comparison study between the UltimateTrough and SkyFuel collector, points out the sensibility of the collector price just depending on variations of the aluminium alloys. Thus a SkyFuel collector solar field could amount 152 €/m² for an aluminium alloy cost of 2.04 /kg, while the cost would increase to 187 €/m² for an alloy price of 3.36 /kg (Kurup and Turchi, 2015). This represents about 19% increase of the total costs. Therefore, with the acknowledgement of this scenario, it is to understand that given numbers could also be influenced by this effect.

Baseline 2 is introduced to differentiate those collectors operating with molten salts as heat transfer fluid. Aforementioned requirements include the material selection and the auxiliary pipe-heating system. Structural steel is holding somewhere between 0.6 /kg to 1.6 /kg, while stainless steel is at least around 5.9 /kg (Wallace, 2018). This specially affects interconnection piping and ball joint assemblies. In the case of an EuroTrough solar field, the cost for the ball joints are valued at 3.6 €/m² (Krüger et al., 2018). Considering a 44% reduction of these elements in a solar field with UltimateTrough collectors, 1.6 €/m² are estimated. In the case of molten salts, the implementation of swivel joints is more susceptible to withstand the operating conditions, rather than ball joints assemblies. The price of the swivel joints alone is estimated at 14.2 €/m² (Krüger et al., 2018). The heat transfer fluid itself represents also a cost reduction, where a solar salt type Hitec® approximately amounts 1.34 /kg compared to 4.01 /kg of a synthetic oil (Turchi & Mehos, 2010).

Complement for Table 15, baseline 1: Thermo-Oil as heat transfer fluid

- **SkyTrough.** The specific collector costs are estimated at 170 $/m² (155 €/m²) (Kurup and Turchi, 2015). To approximate the solar specific field cost it is necessary to consider additionally the HTF-piping costs. For a rough estimate of a SkyTrough solar field, the specific HTF-piping costs of an UltimateTrough solar field of similar size are used, which result from the specific Ultimate Trough solar field costs (198 €/m²) (Riffelmann et al., 2013) and the specific UltimateTrough collector costs (162 €/m²), (Kurup and Turchi, 2015). Thus the estimated total specific solar field costs for SkyTrough is estimated at 191 €/m².
- **SkyTroughDSP**. This collector is a scaled model of the previous SkyTrough with 30% larger dimensions. The SkyTroughDSP aims reductions to up to 50 $/m² (45,50 €/m²) (Schuknecht et al., 2018). To follow up the estimation, this amount is reduced from the total

Table 16
Specific total weight and maximal operational wind speed.

Category	Collector	Specific total weight [kg/m^2]	Wind speed (operational) [m/s]	Category	Collector	Specific total weight [kg/m^2]	Wind speed (operational) [m/s]
A	SKAL-ET	30.0 [1]	14.0 [1]	D	Airlight	–	16.6 [9]
	UltimateTrough	28.0 [2]	–		GlassPoint	40 [10]	zero wind environment
B	SkyTrough	15.5 [2]	12.0 [3]		Heliovis	–	–
	SkyTroughDSP	–	13.0 [4]	E	Hittite Solar Energy	–	–
	LAT 73	–	12.5 [5]		Brenmiller Energy	–	–
C	SL 4600+	19.8 [2]	14.0 [6]		Split Mirror	14.3 [2]	10.0 [2]
	Tough Trough	–	–		MS-Trough	–	–
	SOL.CT	–	37.5 [7]				
	ConSol	–	10.0 [8]				

Sources: (CIEMAT et al., 2001)[1], (Prahl, 2009)[2], (SkyFuel, 2017a)[3], (SkyFuel, 2017b)[4], (Chen et al., 2012)[5], (Solarlite GmbH, 2010)[6], (Alto.Soultions, 2018)[7], (Krüger et al., 2018)[8], (Airlight Energy, 2015a,b)[9], (Bierman et al., 2013) [10].

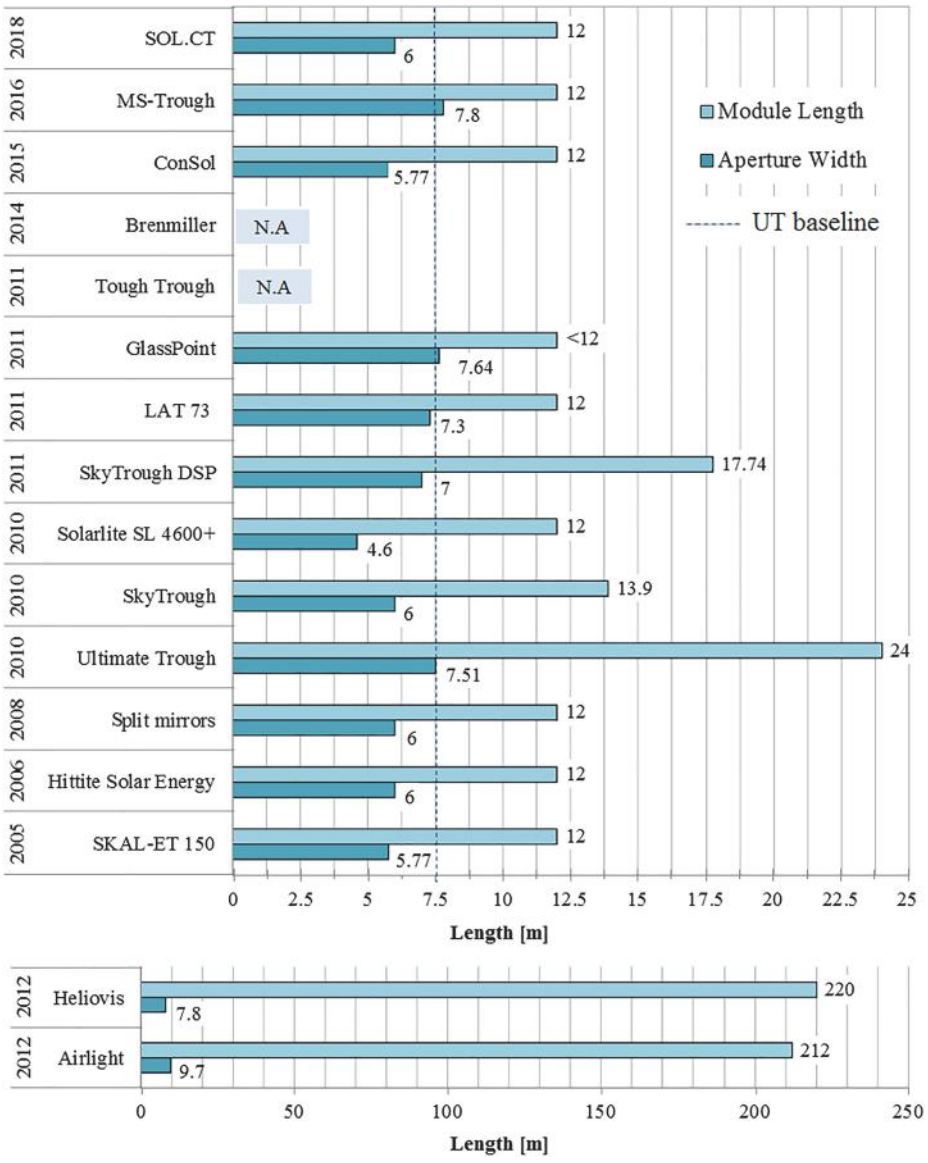

Fig. 56. Dimensions comparison of innovative parabolic trough collector modules and timeline of innovations.

specific solar field costs of the already stated SkyTrough costs. Finally a 145 €/m^2 is the result for the solar field costs.

- **SOL.CT and ConSol.** While the Sol.CT concrete collector waits for the first demonstration, the ConSol collector was built and evaluated. The latter aimed significant cost reduction due to the implementation of concrete. The manufacturing, transportation and assembly adjustments demonstrated, nevertheless, a total increase of 12% to baseline 1. The Sol.CT concept suggests a similar approach for which

Fig. 57. Estimate aperture area per loop and evaluation marks.

the manufacturer assures a 40% reduction to the baseline 1 (Alto. Soultions, 2018). The potential of implementing concrete for the whole structure is feasible, but it requires further research.

- **Airlight.** The cost information is not available. A hypothesis based on the ConSol experience, leads to the assumption that the cost must be significantly higher than the baseline of the EuroTrough. The massive structure requires as well steel materials and the mechanical tracking system a series of robust drive components.
- **GlassPoint.** The cost information is not available. To encounter an estimate, first the evident 6 m high greenhouse glass should be considered and multiplied by the number of implemented modules. In addition, the simplification of the tracking and bearing system can mean a reduction, but the lightweight application of the honeycomb aluminium based parabolic concentrators, might raise the price again.
- **Heliovis.** A reduction of the solar field cost by 30% compared to the Skal-ET is currently estimated (Bermadinger et al., 2019). This reference also points out that due to the future full-automated production line the total cost with this collector will profit from up to a 50% reduction of the solar field. Thus the total amount considered in this study will be 115 €/m^2 compared to the 230 €/m^2 of the Skal-ET.
- **Brenmiller.** The cost information is not available for this collector.

Complement for Table 15, baseline 2: Molten Salt as heat transfer fluid

- **UltimateTrough.** An increase of 12 €/m^2 can be seen from the UltimateTrough baseline 1 to baseline 2, corresponding on a 10% increase of the costs. The authors included the costs for the heat tracing system and the stainless steel materials for a doubled in size solar field (Ruegamer et al., 2014). It is also to point out that the receivers are smaller ∅70 mm once operating with molten salt vs. ∅90 mm with thermo-oil, which also reduces the share of its costs.
- **SkyTroughDSP.** To follow the tendency shown in the case of the UltimateTrough, 12 €/m^2 are assumed and added to the costs once operating with thermo-oil. In this case a 157 €/m^2 are estimated for a molten salt solar field application.
- **Split mirrors.** Also here the addition of 12 €/m^2 approach is used to estimate the total value. Thus the specific solar field cost result in height of 208 €/m^2.
- **MS-Trough**. About 14 €/m^2 for the heat tracing system are considered in this concept (Lüpfert, 2015). Thus the total solar field costs result 11.4% lower than the baseline 2. This reduction is influenced by the elimination of interconnecting pipes between and at the end of the solar collector assembly. The new design allows also less robust drives, where single drive could control a 200 m long collector segment. The metal structure is reduced to the torque tubes, the continuous heat collector element support rail and the lighter pylons.

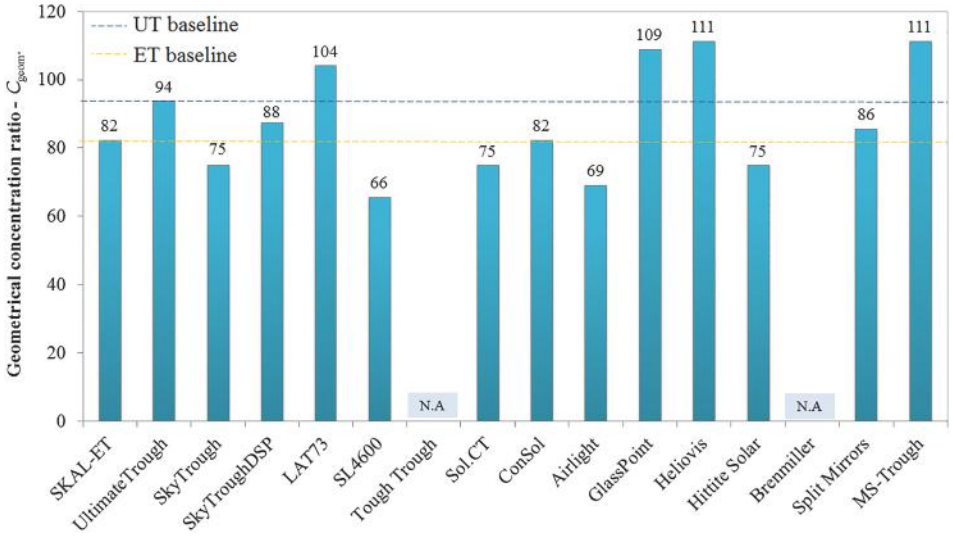

Fig. 58. Designed concentration ratio of innovative parabolic trough collectors.

The sandwich material facets with thin glass mirrors might lead to an increase of the costs.

Together Fig. 55, Table 15 and the comments give an overview from low-cost to cost-intensive collectors. There is an evident tendency to less expensive specific solar field costs targeted with the innovations presented in this review (see Table 16).

4.1.5. Concentration potential of a loop

This criterion compares the dimensional characteristics of the studied collectors. Larger apertures mean an enhanced capability to collect the solar light, but this alone is not all, since the intensity of the concentrated solar energy also depends on the implemented receivers. Therefore, not only the dimensions, but also the possible concentration ratios are compered in this section.

Particularly the module length of the innovative parabolic trough concepts with inflatable polymeric films, namely Heliovis and Airlight, exceed by almost 10 times the continuous module length of the conventional longest baseline of the UltimateTrough. Regarding the aperture width, other two collectors surpass as well this baseline, namely the MS-Trough and GlassPoint. Fig. 56 summarizes the dimensions of the innovations referred to in the study.

The scalability can be evaluated by means of the aperture area at operative scale. This aspect is reduced to consider only the segment area of one single loop simplified as follows:

$$A_{loop} = l_{loop} \cdot a \tag{21}$$

The UltimateTrough and the MS-Trough result to have the greatest aperture areas per single loop as seen Fig. 57. The remarkable difference among these both is the configuration. The UltimateTrough loop on one hand is composed of parallel rows and has its respective cross-over pipelines. On the other hand the MS-Trough possesses a continuous 800 m solar collector assembly.

Regarding the concentration ratio of the collectors, it might vary according to the implemented receiver diameter. This, on further considerations modifies the collectorś intercept factor and subsequently the optical efficiency. The Fig. 58 shows the practical values as result of the literature research and is the base for the evaluation on this criterion.

The baseline is again set on the conventional collector, UltimateTrough, which possess a concentration ratio of 94 with a receiver diameter of ∅80 mm. The Brenmiller collector's dimensions are not available.

These two criteria highlight the collectorś capability to achieve improvements regarding its structural and performance design. On the one hand, wider apertures enable the construction of shorter collectors without reducing the aperture area. Shorter modules in this format require less receivers, thus the investment costs and thermal losses of the elements are reduced. On the other hand a too wide aperture might have an impact on the structureś rigidity requirements, thus the possible increment of the structural cost can be the consequence. Mainly the alignment of the outer reflectors has to be precise, since a greater distance to the focal point gives also more space for the light beams to spread away and not hit the absorber. These two criteria can however benefit from up scaling effects in financial and performance terms.

4.1.6. Structure

The structure criterion is analysed by qualitatively comparing aspects as lightweight, wind resistance and longevity.

Category A – A 50 MW solar field with EuroTrough collectors corresponded to a specific total weight of 30 kg/m^2, accounting the steel structure, glass mirrors, receivers and bearings (CIEMAT et al., 2001). An estimation by C. Prahl for the UltimateTrough accounts with 28 kg/m^2 (Prahl, 2009). The collectorś receivers, reflectors and structures with the proper maintenance suppose a life time of 25 years. In the case of the UltimateTrough, due to the great aperture, wind fences need to be implemented. The wind load on it is however reduced by 30% due to the gaps on the parabolic aperture (Riffelmann et al., 2013).

Category B – These collectors specially target cost reductions through lightweight and standardized structures. In case of the SkyTrough a mass reduction of about 50% was achieved compared to the EuroTrough. The successor SkyTroughDSP is assumed to have a similar value in analogy between the EuroTrough and UltimateTrough. For the LAT73, due to the similar structural approach and the aluminium frame, a value slightly higher than 15.5 kg/m^2 can be expected, yet lower than the EuroTrough baseline. Reasons for this assumption are the additional longitudinal girders for the reflectors support and the reflector panels themselves.

Category C – The SL4600+ achieves thanks to the sandwich composite structure a 30% reduction in specific weight compared to the EuroTrough. It implements a robust torque tube, yet uses only three pairs of stamped sheet arms. The ToughTrough collector might have a similar weight as the SL4600+, since it uses a similar material and structural approach (toughTrough, 2018). The concrete collectors do not offer a value on the total specific weight. An assumption is that both of them are significantly heavier than the EuroTrough collector. In an example with the ConSol collector, only one of four supports bases weights 1995.0 kg per piece (Krüger et al., 2018). The continuous parabolic shell for two modules bring further weight into the structure. Regarding the operational wind resistance, the value given for the SOL.CT is evidently superior as the ConSol, which is still to be demonstrated.

Category D – For the GlassPoint collector a reduction of 84% in concrete, 56% in metal and an estimate of 12 kg/m^2 in glass elements were stated compared to Andasol 1 (Bierman et al., 2013). The final specific weight results higher than the EuroTrough. Remarkable is, nevertheless, the zero wind environment of operation, which distinguishes it over the other studied collectors. In the case of the Airlight collector, the weight is assumed to be the greatest of all given, due to its piecés dimensions, which are full concrete with steel body. Heliovis instead, represents a lightweight inflatable body made of plastic membranes. The factor that increases its weight, nevertheless, is its bearing structure. Regarding the longevity, these three collectors have a common significant risk, namely the breakage of its enclosing element. Possible hazards are strong winds, flying sharp rocks, sand/dust abrasion or degradation due to ultra-violet radiation on the surface. An example of a degraded inflatable collector, due to a possible crack of the plastic film can be seen under the coordinates: 30°13′01.7″N 9°08′57.5″W in satellite images (e.g. Google.Maps).

Category E – Regarding these aspects the Brenmiller collector can be close to the baseline of the EuroTrough, due to the steel structure and the use of mirror facets. The Hittite instead is assumed to be higher in weight mainly because of its massive counter weight, yet similar regarding wind resistance and longevity. The Split Mirrors collectorś specific weight of 14.4 kg/m^2 was estimated and it was preliminary analyzed for wind speeds of 10 m/s (Prahl & Pfahl, 2009). The MS-Trough is assumed to have similar or slightly higher specific weight values than the Split Mirrors collector, due to the thin glass and sandwich composite structures. Regarding the wind loads, its large aperture means also a mayor exposed area to the wind. At strong wind position, the MS-Trough is nevertheless horizontally orientated and the load is therefore reduced to one third. In all categories, longevity between 20 and 25+ years should be fulfilled, as it is state of the art.

4.2. Evaluation matrix

The recurred method evaluates a row of different solutions from an economic and technical point of view. The VDI 2225 guideline is a design engineering method that allows a comparative analysis of several configurations versus a theoretical ideal solution, regarding performance and capital costs. After the evaluation section, a so-called *s-diagram* (*s* for *strength*) can be derived from the results to illustrate the innovative and conventional collectors versus an ideal solution.

The results of this method are strongly depended on the evaluation scale and the weight of the defined criteria. Since the categories and

Table 17
Evaluation metrics of the criteria and sub-criteria.

VDI 2225 guideline scale	Very Good (Ideal)	Good	Sufficient	Acceptable	Unsatis-factory	
Punctuation	**4**	**3**	**2**	**1**	**0**	
Optical Performance						Reference
Peak Optical Efficiency	82–78	77–73	72–68	67–60	n.a	Table 9
Reflector Type	Thin glass	Thick glass	i. enclosed coated aluminium ii. polymeric reflector	i. enclosed polymeric reflector ii. coated aluminium	n.a	Table 1 & 10
Thermal Performance						
Scenario 1: Loop Power Losses per produced Megawatt (HTF: Thermo-Oil)	<4%	4%–5%	> 5%–6%	>6%	n.a	Table 11
Scenario 1: Interconnection Thermal Losses	0%–0.15%	>0.15%–0.30%	>0.30%–0.45%	>0.45%	n.a	Table 11
Scenario 2: Loop Power Losses per produced Megawatt (HTF: Molten Salt)	<8%	8%–10%	>10%–11%	>11%	n.a	Table 12
Scenario 2: Interconnection Thermal Losses	0%–0.15%	>0.15%–0.30%	>0.30%–0.45%	>0.45%	n.a	Table 12
Parasitic Consumption						
With Thermo-Oil vs. Molten Salt	0%–0.5%	>0.5%–1.5%	>1.5%–2%	>2%	n.a	Tables 13 and 14
Concentration potential of a loop						
Effective Aperture	Mark 4	Mark 3	Mark 2	Mark 1	n.a	Fig. 57
Concentration Ratio	>100	<100–90	<90–75	<75	n.a	Fig. 58
Structure						
Operational Wind Speed [m/s]	zero environment	17–12	12–10	10–5	n.a	Section 4.1.6
Lightweight [kg/m^2]	10–20	20–30	30–40	> 40	n.a	Section 4.1.6
Longevity	Objective argumentation in Section 4.1.6; State of the art baseline are 25 years					Section 4.1.6

technologies of this study possess specific strengths, it is practically contradictory to weight each criterion, since some of them could be systematically undervalued. Therefore, to avoid arbitrary results all considered criteria are weighted with the same importance as suggested in the guideline. The global scale is simplified from 0 (unsatisfactory) to 4 (ideal).

Technical Value X – The technical value evaluates those criteria that determine aspects like performance, structure and longevity. From the analysis in Chapter 4.1, 10 criteria are selected to evaluate the concepts. Each criteria can be valued with a maximum of 4 points, thus the ideal concept amounts a total of 40 points for those 10 criteria. The ideal solution is represented at a value of X = 1.0 according to Eq. (22), when all criteria have the maximum punctuation. In the case, that 0 points are marked, it means that there are limitations from the value analysis chapter. To calculate the technical value of each collector according to the VDI 2225 method, following equation is used (VDI-Richtlinie, 1998)

$$X = \frac{p_1 + p_2 + p_3 + \cdots + p_x}{n_c{}^{*} p_{max}} = \frac{\overline{p}_x}{p_{max}} \tag{22}$$

A technical value above X = 0.8 is generally to be considered as very good, for X = 0.7 as good and X = 0.6 or below as unsatisfactory. Results of the technical value X aim to give a general overview of the different concepts and it only expresses, whether the chosen solutions promise success at least in technical terms (VDI-Richtlinie, 1998).

The Economic Value Y – This parameter concentrates on the specific solar field costs, which are taken from Section 4.1.4 in Fig. 55 and Table 15. Also here an ideal scenario based on a market survey is set. One strategy is to identify current low costs with a conventional state of the art collector and to put them in relation to the innovations specific costs. For this comparison, the UltimateTrough was set as the commercial baseline of conventional collectors ($H_{baseline}$). To define an evaluation range for Y, it is necessary to identify the economic value of the lowest solar field costs found among the studied innovations. According to the VDI 2225 guideline the economic value is defined as followed:

$$Y = \frac{H_{M,min}}{H} = \frac{\beta \cdot H_{baseline}}{H} \tag{23}$$

The cost levelling factor (β) is the ratio between the solar field cost baseline reference (i.e. UltimateTrough's solar field cost equal 198 €/m^2) and that of the market lowest achievable costs. In this study, Heliovis results to be the reference case ($H_{M,min}$) with specific solar field costs of 115 €/m^2. Thus the cost levelling factor is equal to β = 0.58 by calculating the ratio. This means that the economic value of the UltimateTrough collector, as the conventional baseline of costs, is 0.42 points below the best cost performing reference of the study, namely the Heliovis collector with an economic value of Y = 1.0.

With this method, it is necessary to establish the metric guideline to evaluate each criteria. Table 17 sustains the technical aspects and it includes optical performance, thermal performance, parasitic energy consumption, loop concentration potential and structure as criteria. To enable a comprehension of the values, references are given to the analysis results conducted in Chapter 4.1. The evaluation matrix from this methodical approach shows the results for the technical value X and for the economic value Y for each collector in Table 18.

4.3. Evaluation results

The *s-diagram* in Fig. 59 is the tool to sum up the results of the present study. The s-diagram computes the X and Y values of each collector concept from Table 18, which indicate the techno-economic strength 's' of their respective design. The development line of concepts ranges from point (0.0|0.0) to s_i(1.00|1.00), which describes an equal technical and economic value growth until the ideal solution. The results close to the development line represent an ideal feasibility of the concept, yet stronger, the closer they are to the ideal points$_i$ (i.e. the top right corner). Fig. 59 includes also the state of the art development line, which is approximated by observing the UltimateTrough and the Skal-ET. This indicates a roughly estimate of the current conventional collectors development tendency.

The economic value Y of the concepts ranges in the graphic from the lowest to the highest limit. On one hand the Heliovis collector shows the

Table 18
Evaluation matrix of innovative parabolic trough collector concepts for large-scale application.

Category		A - Conventional		B - Alternative Structures & Sheet Reflectors			C - Non-Metallic Materials				D - Enclosed Aperture			E - Fixed Focus				A	B	E	E
Criteria and respective sub-criteria	Ideal Collector	Euro Trough	Ultimate Trough	Sky Trough	Sky Trough DSP	LAT 73	SL 4600+	Tough Trough	SOL. -CT	Con -Sol	Air -light	Glass -Point	Heliovis	Hittite Solar	Bren-miller	Split Mirrors	MS-Trough	UT (MS)	SkyTr. -DSP (MS)	Split Mirrors (MS)	MS-Tr. (MS)
Optical Performance	**8**	**6**	**7**	**5**	**5**	**5**	**7**	**4**	**1**	**2**	**2**	**4**	**2**	**4**	**3**	**7**	**8**	**6**	**5**	**7**	**8**
Peak Optical Efficiency	4	3	4	3	3	3	3	0	0	1	1	2	1	0	0	3	4	3	3	3	4
Reflector Type	4	3	3	2	2	2	4	4	1	1	1	2	1	4	3	4	4	3	2	4	4
Thermal Performance	**8**	**4**	**6**	**4**	**5**	**4**	**3**	**0**	**0**	**4**	**0**	**6**	**5**	**0**	**0**	**6**	**8**	**7**	**4**	**5**	**8**
Loop Power Losses per produced	4	2	3	2	3	1	1	0	0	2	0	3	3	0	0	3	4	4	3	2	4
Interconnection Thermal Losses	4	2	3	2	2	3	2	0	0	2	0	3	2	0	0	3	4	3	1	3	4
Parasitic Consumption	**4**	**3**	**2**	**4**	**3**	**1**	**3**	**0**	**0**	**3**	**0**	**4**	**4**	**0**	**0**	**3**	**3**	**4**	**4**	**4**	**4**
Concentration potential of a loop	**8**	**4**	**7**	**4**	**5**	**7**	**4**	**1**	**2**	**4**	**2**	**6**	**6**	**2**	**0**	**4**	**8**	**8**	**5**	**4**	**8**
Effective Aperture	4	2	4	2	3	3	2	0	0	2	1	2	2	0	0	2	4	4	3	2	4
Concentration ratio	4	2	3	2	2	4	2	1	2	2	1	4	4	2	0	2	4	4	2	2	4
Structure	**12**	**10**	**10**	**9**	**9**	**9**	**11**	**11**	**5**	**5**	**4**	**9**	**7**	**7**	**9**	**10**	**10**	**10**	**9**	**10**	**10**
Wind load resistance	4	3	3	3	3	3	3	3	2	2	2	4	2	2	3	3	3	3	3	3	3
Lightweight	4	3	3	4	4	4	4	4	1	1	1	2	3	2	3	4	4	3	4	4	4
Longevity	4	4	4	2	2	2	4	4	2	2	1	3	2	3	3	3	3	4	2	3	3
Sum:	**40**	**27**	**32**	**26**	**27**	**26**	**28**	**16**	**8**	**18**	**8**	**29**	**24**	**13**	**12**	**30**	**37**	**35**	**27**	**30**	**38**
Technical Value X	**1.00**	**0.68**	**0.80**	**0.65**	**0.68**	**0.65**	**0.70**	**0.40**	**0.20**	**0.45**	**0.20**	**0.73**	**0.60**	**0.33**	**0.30**	**0.75**	**0.93**	**0.88**	**0.68**	**0.75**	**0.95**
Economic Value Y	**1.00**	**0.50**	**0.58**	**0.60**	**0.79**	**0.67**	**0.55**	**0.67**	**0.89**	**0.44**	**0.00**	**0.00**	**1.00**	**0.00**	**0.00**	**0.59**	**0.67**	**0.55**	**0.73**	**0.55**	**0.62**

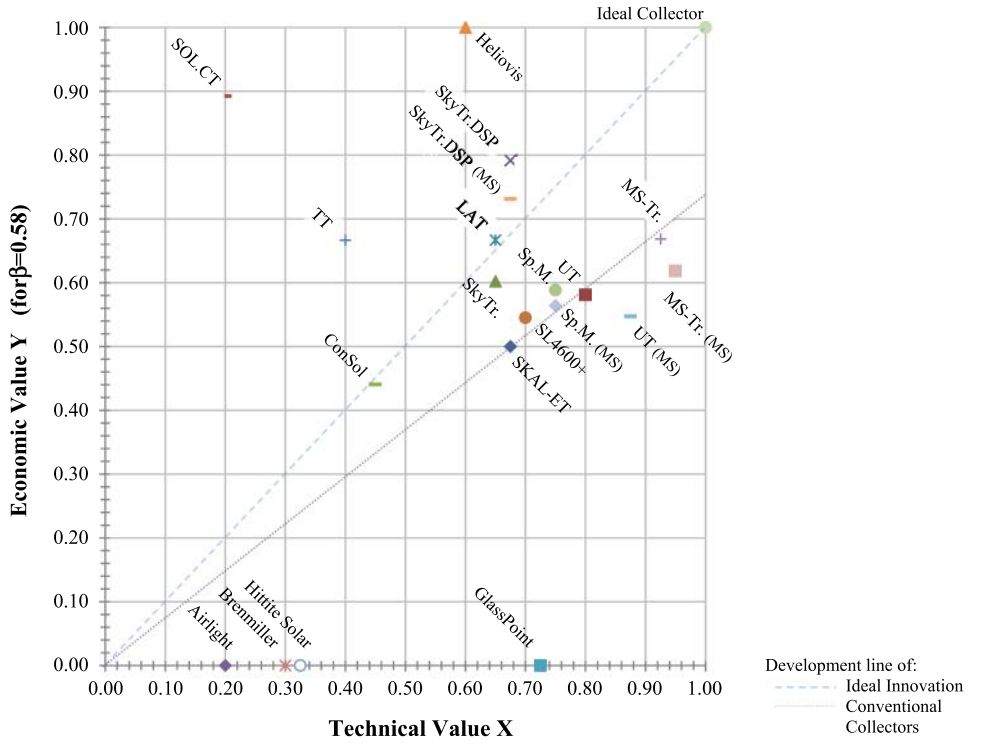

Skal-ET"=EuroTrough; "UT"=UltimateTrough; "Sky.Tr."=SkyTrough; "Sky.Tr.DSP"=SkyTroughDSP; "Sp.M"=Split Mirrors; "TT"=ToughTrough; "MS-Tr."=MS-Trough; "(MS)" = collector operating with molten salt as HTF

Fig. 59. S-Diagram for the evaluation of innovative parabolic trough collectors.

best economic performance punctuation (Y = 1.0) since it has the lowest specific solar field costs within the studýs scope and it is set as lowest price basis. On the other hand Hittite Solar, Brenmiller, Airlight, and GlassPoint collectors result on the lowest values for Y = 0.0 due to the lack of accurate information about their solar field costs. Assumptions for the two latter collectors could expect lower Y values than the Skal-ET or even lower than the ConSol collector (see 4.1.4 Costs Scenario). The graph also shows that the innovations tend to improve the specific costs of the solar field compared to conventional collectors. This is marked by the higher Y values, which are greater for example than Y = 0.50 of the Skal-ET and higher than Y = 0.58 of the UltimateTrough. From all concepts, 50% are above the UltimateTroughs economic value.

The technical value X is not as widespread as the economic value. It ranges from X = 0.20 for the Airlight and SOL.CT collectors, to X = 0.95 for the MS-Trough operating with molten salt as heat transfer fluid. In this range, 70% of the concepts are better than the unsatisfactory

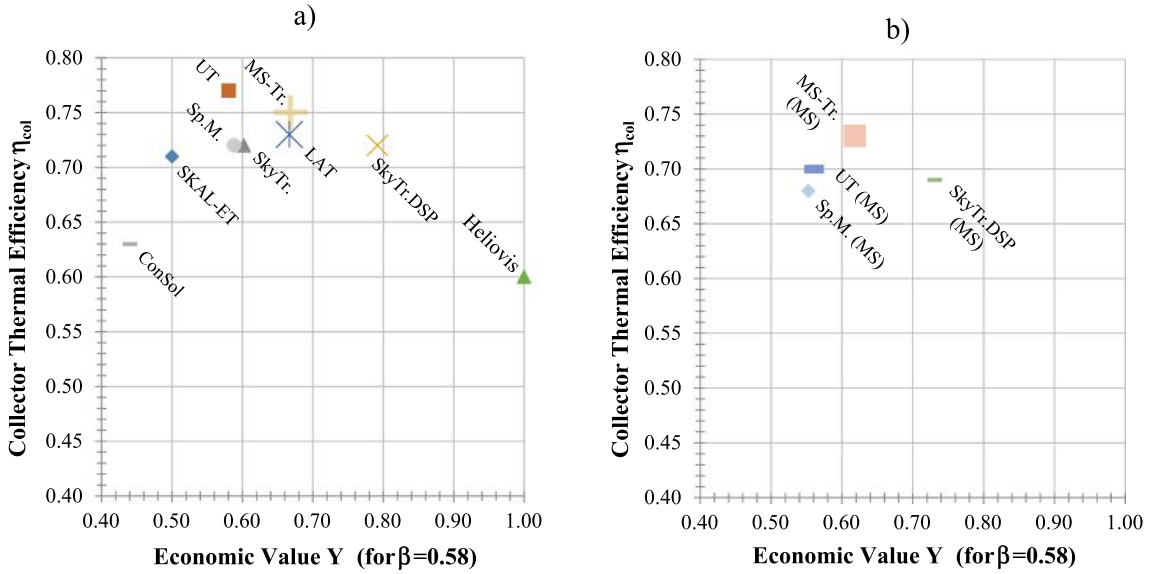

"Skal-ET"=EuroTrough; "UT"=UltimateTrough; "Sky.Tr."=SkyTrough; "Sky.Tr.DSP"=SkyTroughDSP; "Sp.M"=Split Mirrors; "MS-Tr."=MS-Trough; "(MS)" = collector operating with molten salt as HTF

Fig. 60. Evaluable extract of the collector thermal performance vs. the economic value. a) With thermo-oil type Therminol VP-1 as HTF and b) with molten salt of composition 60%$NaNO_3$, 40%KNO_3 (i.e. Solar Salt) as HTF.

technical value X = 0.6 and 1% results in a higher than the optimal value of X ≤ 0.9. A result of the graph is also that only few concepts surpass the technical value of the UltimateTrough (X = 0.80) operating with thermo-oil. One of them is the MS-trough operating with both heat transfer fluids and the other again the UltimateTrough, but with molten salts.

There is a concentration of collectors around the development line, which mainly includes Category B collectors. Among them, the SkyTroughDSP with thermo-oil has a better technical value, than the SkyTrough and the LAT73 with the same fluid. The implementation of the SkyTroughDSP (MS) with molten salt equalizes its technical performance and drops its economic value by 5 points. In fact, all collectors operating with molten salt as heat transfer fluid equalize or enhance the technical value compared to their versions operating with thermo-oil. Nevertheless at the expense of increasing costs expressed by a lower economic value.

Results of the collectors below the economic and technical value of the Skal-ET do not necessarily express the inferiority of the concepts. The method rather aims to show the direction of development to which a concept should be steered following the evaluated criteria. To summarize, the results in Fig. 59 show two outstanding concept. On one hand, the most salient economical variant for the considered specific solar field costs is the Heliovis collector (Y = 1.00) with its enclosed aperture from Category D. On the other hand, the fixed focus MS-Trough collector operating with molten salts from Category E approaches the most with X = 0.95, the ideal technical value.

The assignation of the technical criteria has a strong influence on the results obtained. For this study, the evaluated criteria were optical performance, collector thermal performance, parasitic energy consumption of the respective loop designs, concentration potential and structural properties. Each of these aspects was compared with a hypothetical ideal solution under the established metric guidelines of Table 17. Whilst it is true that a main technical interest in general is the collector thermal performance, it is possible to extend the evaluation to observe this key aspect. For this, the implemented method is convenient, since it allows the use of the previous economic frame.

Fig. 60 takes into account the collector thermal efficiency of each concept as calculated for both heat transfer fluids (i.e. thermal-oil and molten salts) in Section 4.1.2 (Table 11 and Table 12). Both thermal oil and molten salt collectors have been simulated on the basis of the established baseline, which is the respective commercial version. In other words, each concept is analysed with its corresponding reflectors, receivers, dimensions and loop design. The differentiation of heat transfer fluid is made, with the intention of demonstrating innovative concepts that fit into a new horizon of solar thermal plants that aim to use molten salts in the solar field.

Fig. 60a) and b) show the concepts that have been able to be evaluated both in the technical and economic framework. Therefore, Fig. 60a) leaves out collectors such as the ToughTrough, SOL.CT, GlassPoint, Airlight, Brenmiller and Hittite Solar because of missing economic and technical data. The limitations for each concept are explained in detail in chapter 4.1. In both figures, the ideal collector tends to the point (1.00|1.00). On Fig. 60a), the economic efficiency of the Heliovis (1.00|0.60) and the thermal efficiency of the UltimateTrough (0.58|0.77) are therefore emphasized. The economic advantage of the Heliovis over the UltimateTrough is by 0.42 points and the collector thermal efficiency advantage of the UltimateTrough over the Heliovis is of 0.17. These two collectors stand out from the other collectors. Despite this, it is also to remark the tendency balance of both parameters of the SkyTroughDSP (0.79|0.72). In Fig. 60a) one can also note the economic improvement proposed by the innovations in relation to the UltimateTrough baseline.

In Fig. 60b) of molten salt collectors, the MS-Trough peaks in terms of thermal efficiency (0.62|0.73) and in the economic aspect the SkyTroughDSP (0.73|0.69). By comparing both figures, it can be seen that collectors with molten salt show lower thermal efficiencies than those with thermal oil. It should be remembered that molten salt enables a solar field outlet temperature of $T_{out,SF}$ = 550 °C and thermo-oils at $T_{out,SF}$ = 400 °C. This means that molten salts can increase the efficiency of the electricity generation process in the power block, according to Carnoťs principle. At the same time, operations at higher temperatures cause greater thermal energy losses, which influence in the decrease of the collectors' efficiencies. It is also worth noting the technical-economic advantage of the thermal storage efficiency favored due to the use of the same transfer fluid in the solar field and in the storage block. These aspects are important for the reader to consider and it is recalled that these results in Fig. 60 are based on the efficiencies with a focus only on the solar field.

4.4. Evaluation discussion

The evaluatioń s results highlight the technical-economic degree of current conventional and innovative parabolic trough collector concepts. The panorama presented in Fig. 59 shows partial results considering that the evaluation does not include all possible criteria, but it does contain those within the framework of requirements attributed to innovations as mentioned in Chapter 3. Hence, it is possible to identify which collectors are of interest for utility scale power generation according to the evaluated criteria.

For the analysis and evaluation, collectors suitable for two heat transfer fluids were previously differentiated. On one hand, those state of the art collectors operating with thermo-oils as heat transfer fluid and on the other hand, those operating with molten salts. In the comparison, collectors with molten salts possess heat transfer fluid specific advantages in anticipation on two points. One of them is the higher operating temperatures from up to 550 °C or 580 °C, which enable an increase of the solar power planťs global efficiency. The second is that the parasitic power consumption of the cycle decreases due to density and viscosity of the fluid. The calculated parasitic power values are lower with molten salts compared to thermal-oils. This could be observed at the UltimateTrough loop example, where the change from thermo-oil to molten salts result on parasitic power values going from 1.8% to 0.42% as seen in Section 4.1.3 Parasitic Consumption.

These collectors also have a practical disadvantage in the framework of the evaluation, since only the specific solar field costs were included to establish a common baseline. It is important to have the awareness that the same fluid in the solar field and in the thermal storage block can reduce the costs of the overall solar power plant. The specific costs of the storage block could be reduced by up to a factor of 3 and also up to 23% less costs of the adjacent blocks together (i.e. BOP, power block, HTF system) (Ruegamer et al., 2014). These numbers consider the upscale effect of the solar plant from 50 MW to 100 MW with UltimateTrough collectors. The present review demonstrates the certain increase of the solar field costs with this medium, however it is necessary to emphasize that the true cost-efficient factor is defined together with the thermal storage block. These aspects represent the reason why it was necessary to differentiate both operating fluids.

About the UltimateTrough reference base line, it can be seen that its techno-economic relevance is already relatively competent even among the innovations. If its economic factor could be improved, an ideal concept would be approached. Unlike this one, Category B collectors that implement space frames do have an enhanced economic scenario at equally robust structures. On the one hand, the installation of standardized elements in the main structure has a significant influence on the manufacturing, assembly and installation costs, reducing on the specific solar fields costs. On the other hand, the implementation of polymeric reflectors clearly favours the lightweight of the concept. However, it is also its weak point in terms of durability and optical performance.

Close to that category there are the sandwich composite structures collectors (see Fig. 59). Collectors from Category C have the strong advantages of their robust structure, good optical performance and

longevity, but at the expense of high manufacturing costs that can result at utility scale. In the case of the SL4600+ a disadvantage is also the concentrating potential, which is limited by its aperture and concentration ratio. Its installation would require a larger number of modules in a solar field and also of absorber tubes. This not only affects the thermal efficiency of the solar field, but also causes higher investment costs. It should be noted that this technology has been industrially approved and that the approach with sandwich composite materials will be optimized with a wider aperture and thinner facets, in order to save on material and weight. The latter aspect is precisely addressed with the Split Mirrors fixed focus collector of Category E, which proposes the use of similar facets to those of the SL4600+. The proposal of this collector is certainly innovative. However, it has structural technical challenges that need to be projected, by means of the torque body and heat collector element support bearings.

Following Category E collectors, the MS-Trough specially designed for the operation with molten salts at high temperatures, sustains the most outstanding technical value of the study. In response to the current demand of optical efficient collectors for, the MS-Trough has features that favour both the cost-efficiency and performance of the solar plant. Its fixed focus design enables the elimination of flexible interconnection elements, thus eliminating components with a tendency to frequent breakdowns (e.g ball- or swivel-joints). As far as the optical design is concerned, a value is estimated between the conventional EuroTrough and UltimateTrough collectors. The other collectors in this category, Hittite and Brenmiller, are fairly similar designs to each other in structure and result in a similar technical value due to constrains in information and the discontinuation of the models by the manufacturers. However, an important feature that differentiates them is the mass distribution. On one hand, Hittite employs a counterweight in its structure which facilitates the fixation of the receiver, while the centre of mass is placed on the absorber axis. This design avoids static torsional deformations due to structurés imbalance around the rotary axis. However, it is achieved at the expense of heavier modules for the drives to sustain. On the other hand, the centre of mass does not coincide with the focal line in the Brenmiller collector; it is rather bellow. It implements for this reason a drive on each single module to compensate all static torsional deformations along the assembly.

From Category D, the Heliovis collector has the economic superiority over the concepts of the study. It proposes an extreme lightweight with its inflatable collector tube and a flexible implementation for industrial process heat, enhanced oil recovery and electricity generation. In analogy to the Airlight collector, a reduction in the intensity of the incident energy flux through the top membrane can be expected. Light deviations due to reflection effects by the cover and reflector layers disadvantage the modulés intercept factor. It is also assumed that the enclosing membrane is susceptible to frequent breakage caused by flying sharp objects taken strong winds.

Among the innovations, the least salient collectors are those with a concrete structure. Of the three included in the study, only two have been built: the Airlight and the ConSol collectors. The third concept and yet to be demonstrated is the SOL.CT. A main advantage of these concepts is the universal accessibility of the material. As far as the structure is concerned, the concepts do not support a good optical performance, mainly due to the shrinking of the material in the hardening process and creep deformation. The ConSol project demonstrated nevertheless the possibility of building this type of collectors and it can be considered as a milestone for the development process of these collector types.

All in all the evaluation of the various collector technologies is to be understood only as a trend assessment, since an onerous evaluation is not feasible mainly due to three aspects. One is the lack of some collector data, second is the limited selection of criteria and third are the perhaps too optimistic collector properties given by the manufacturers, especially of those that have not had practical tests.

5. Conclusion and outlook

This review presents the state of the art of parabolic trough collectors suitable for large-scale application. First, a description of the main components that define the optical and thermal performance was presented (e.g. receivers, geometry, heat transfer fluid and reflectors). Secondly, a classification of conventional and innovative collector concepts was included, with a review of each collector and their technical data. Throughout the review, the main focus are entire solar collector assemblies; however some hints to further technological advances are mentioned (e.g. secondary reflectors, booster reflectors, alternative receivers, nano fluids, plant operation designs with molten salts in the solar field and with supercritical CO_2-Brayton power cycle). The review goes then though the simulation and analysis of technical criteria with both thermal oil and molten salt heat transfer fluids in their respective loop dimensions for which the collected technical data was used. It is important to emphasize that the calculations could be optimized in a future work, by including the values of the Incident Angle Modifier of each collector (factor that was a limitation for this study and more accurate results could be expected).

The review paper proposes a comparison evaluation method according to VDI 2225 guidelines and defines a metric table of technical criteria, an evaluation matrix and a strength-diagram, which sums up the technological and economic tendencies of the reviewed collectors. One goal of the evaluation was to identify those collector concepts with a potential to enhance the overall efficiency of the power plant. Results showed that the UltimateTrough collector operating with molten salts achieves a solar-to-electric efficiency of 30% and of 29% operating with thermal oils as heat transfer fluid. Only superior in this sense, the MS-Trough reaches a solar-to-electric efficiency of 31% with molten salts. Both cases were assumed without pipeline thermal losses. Under this hypothesis, the UltimateTrough and the MS-Trough are the most salient concepts of the study in terms of performance.

Another goal was to estimate the collectorś economic importance on the solar field. Regarding this, the Heliovis collector is found to be the representative concept proposing the highest specific costs reduction of 50% compared to the EuroTrough baseline (Bermadinger et al., 2019). These left the baseline of the specific solar costs at 115 €/m^2. However, its technical performance is distant from the UltimateTrough and MS-Trough, mainly because it combines polymeric reflectors and a transparent membrane, which reduce the intercept factor onto the receivers and with it, the optical performance. Overall 50% of the innovations included in the review show an economic improvement in comparison to the conventional collector baselines.

The study highlights the potential of operating with molten salts as heat transfer fluid. This implies a significant reduction of the solar power plantś investment by up to a factor 3 of the storage block and of 23% less of the costs in the adjacent blocks together (i.e. balance of plant, power block and heat transfer fluid system) (Ruegamer et al., 2014). However, this configuration not only benefits from the properties of molten salts, but it is also attached to operational boundaries. Current technologies can maintain the temperature of the solar salts in its liquid phase above 270 °C in the pipes, receivers and storage tank by means of heat tracing and auxiliary heaters at expense of great power consumption. This is cost intensive, thus a roadblock for the technological breakthrough in the market. Studies regarding the molten salts HTF are being undertaken to reduce their solidification temperature properties and to counterbalance the risks during operation. In the solar field, especially the sealing of flexible interconnection elements such as ball-joints or swivel hoses mean a weak point for the salt medium and a high risk of salt solidification. For this purpose, only two concepts mitigate this risk, namely the MS-Trough and the Split Mirrors. Because of their fixed focus design both collectors can eliminate these components allowing a fixed interconnection between the modules and the header piping to the storage tanks. This property is only found in Category E collectors.

In conclusion, this study analysed and evaluated conventional and

innovative parabolic trough collectors from a techno-economic perspective to investigate those development tendencies and the progress of their implementation potential. Collectors capable of operating with molten salts demonstrated superior technical relevancy, among them the MS-Trough, the UltimateTrough and the SkyFuelDSP. That is mainly for their performance and second for their economic impact on the overall cost of a solar power plant. The three collectors benefit from the scale-up effects of their wide apertures, but more importantly they have the potential to integrate the cycle of the solar field with that of the thermal storage block in one. The review offers a widespread overview of parabolic trough collectors for utility energy generation. The content can be used as a market survey of current concepts, which highlights those technologies with the potential to have a major breakthrough in the sector. The objective is, in fact, that of incentivizing the prevalence and competitiveness of the technology within the framework of sustainable renewable energies.

Declaration of Competing Interest

The authors declare that they have no known competing financial interests or personal relationships that could have appeared to influence the work reported in this paper.

Acknowledgments

The work conducted for this publication was carried out under the mentoring of experts from the Institute for Solar Research of the German Aerospace Centre (DLR) and from professors of the Department of Engineering and Natural Sciences of the University of Applied Sciences Wildau.

References

3M & Gossamer Space Frames, 2012. Large Aperture Trough (LAT) 73 - engineered by Gossamer Space Frames and 3M, St. Paul: 3M.

3M & Gossamer SpaceFrames, 2012. 3M and Gossamer Space Frames to Inaugurate World's Largest Aperture Parabolic Trough Installation - A New Benchmark in Solar Collectors, St. Paulo: 3M.

Abengoa Solar, 2013. A New Generation of Parabolic Trough Technology, Phoenix: SunShot CSP Programm Review.

Adel, A., 2015. TU Wien. [Online] Available at: https://www.tuwien.ac.at/fileadmin/t/tuwien/fotos/news/inventum2015_3_Modell.JPG [Accessed 20. 03. 2019].

Adel, A., 2018. Development of a New Generation of Parabolic Trough Collectors to Maximize the Local Content in Developing Countries - from Idea to Business. Technische Universität Wien, Vienna.

Ahn, Y., et al., 2015. Review of supercritical CO2 power cycle technology and current status of research and development. Nucl. Eng. Technol. 47–6, 647–661.

Airlight Energy, 2015. Concentrated Solar Power Thermal Collector Data Sheet, Biasca: Airlight Energy.

Airlight Energy, 2015. CSP Plant, Ait-Baha, Morocco. [Online] Available at: http://www.airlightenergy.com/csp-gallery/ [Accessed 13. 12. 2018].

Alto.Soultions, 2018. High performance and highly cost-competitive parabolic trough, s.l.: s.n.

AltoSolution, 2018. High performance & high cost-competitive Parbolic-Trough (Technical Data Sheet), s.l.: SOL.CT.

Ambrosini, A., 2015. High-Temperature Solar Selective Coating Power Tower Recievers. [Online] Available at: energy.gov/sunshot [Accessed 07.12.2018].

ArchiemedeSolarEnergy, 2019. www.archimedesolarenergy.com. [Online] Available at: http://www.archimedesolarenergy.com/molten_salt_vs_oil.htm [Accessed 31. 10. 2020].

Archimede Solar Energy, 2012. HCEMS11 Molten Salt Receivers Datasheet. [Online] Available at: http://www.archimedesolarenergy.it/en_hcems-11-sali-fusi.htm [Accessed 23. 02. 2019].

Bader, R., 2011. Optical and Thermal Analyses of an Air-Based Solar Trough Concentrating System. ETH Zurich Research Collection, Zurich.

Balz, M., Schweitzer, A., 2015. UltimateTrough - Aufgabestellung [Interview] 2015.

Baudis, U., 2001. Technologie der Salzschmelze. Wärmebehandlung, Härtetechnick, Wärmeübertragung, Reinigung, Lech: Landsberg.

Bellos, E., Tzivanidis, C., 2018. Alternative Designs of Parabolic Trough Solar Collectors. In: Process in Energy and Combustion Science. Elsevier, pp. 81–117.

Bellos, E., Tzivanidis, C., 2017. A Detailed Exergetic Analysis of Parabolic Trough Collectors. Energy Conversion and Management, Athens, Greece.

Bellos, E., Tzivanidis, C., 2019. Investigation of a booster secondary reflector for a parabolic trough solar collector. Solar Energy, Febraury, pp. 174–185.

Bellos, E., Tzivanidis, C., Antonopoulos, K., Gkinis, G., 2016. Thermal enhancement of solar parabolic trough collectors by using nanofluids and converging-diverging absorber tube. Renew. Energy 25 (03), 213–222.

Bermadinger, S., Steinmair, M., Tiefenbacher, F., 2019. HELIOtube: An industrially realized reinvention of a CSP collector. Austria, AIP Conference Proceedings 2126.

Bierman, B., Al-Lawatia, H., DiFilippo, M., O'Donnell, J., 2017. Deploying Enclosed Trough for Thermal EOR at Commercial Scale. Sultanate of Oman, Muscat.

Bierman, B., Treynor, C., O'Donnell, J., Lawrence, M., Chandra, M., Farver, A., von Behrens, P., Lindsay, W., 2013. Performance of an enclosed trough EOR system in South Oman. Energy Procedia 49, 1269–1278. https://doi.org/10.1016/j.egypro.2014.03.136.

Blümner, R., 2012. Development and Testing of a Design Optimization Routine for Concentrating Solar Power Collectors. Berlin Institute of Technology, Almería.

Bortolato, M., Dugaria, S., Col, D.D., 2016. Experimental study of a parabolic trough solar collector with flat bar-and-plate absorber during direct steam generation. Energy 1 December, pp. 1039–1050.

Brenmiller Energy, 2019. A Thermal Storage Company. [Online] Available at: https://www.bren-energy.com/technology/ [Accessed 11. 08. 2019].

Brenmiller, A., et al., 2016. Modular Solar Field. United States of America, Patent No. US 2016/0003496 A1.

Chen, D. T., Reynolds, G., Gray, A., 2012. Nest Generation Parbolic Trough Solar Collectors fro CSP. St. Paul, s.n.

Chen, F., Li, M., Zhang, P., Luo, X., 2015. Thermal performance of a novel linear cavity absorber for parabolic trough solar concentrator. Energy Convers. Manage. 90, 292–299. https://doi.org/10.1016/j.enconman.2014.11.034.

CIEMAT, et al., 2001. Development of a new Low Cost European Parabolic Trough Collector. Non Nuclear Energy Programme, Tabernas.

DLR, 2019. MS-Trough Collector Module. [Online] Available at: https://www.dlr.de/sf/de/desktopdefault.aspx/tabid-10649/18658_read-43431/ [Accessed 01. 08. 2019].

DLR, et al., 2018. Ergebnisbericht: ConSol - Concrete Solar Collector. DLR, Germany.

Dyreby, J., Klein, S., Nellis, G., Reindl, D., 2014. Design considerations for supercritical carbon dioxide brayton cycles with recompression. J. Eng. Gas Turbines Power, University of Wisconsin–Madison, October, Volume 136(10), p. 101701.

Edevane, G., 2016. mashable.com. [Online] Available at: https://mashable.com/2016/02/06/moroccan-solar-plant/?europe=true [Accessed 02 02. 2019].

Eduardo Zarza, M., 2012. Parabolic-trough concentrating solar power (CSP) systems, s.l.: Concentrating Solar Power Technology.

Eickhoff, M., 2010. U4: Parabolic Trough and Fresnel Collectors - Capacity Building Course eM-CB01, s.l.: DLR, enerMENA.

Eickhoff, M., 2018. Parabolic Trough Collector Module Unit and Solar Thermal Power Station. United States of America, Patent No. US 2018/0023845 A1.

Eickhoff, M., et al., 2014. Guidelines for CSP yield analysis - optical losses of line focusing systems; definitions, sensitivity analysis and modeling approaches. Energy Prceedia (49), 1318–1327.

Eickhoff, M., Meyer-Grünefeldt, M., Keller, L., 2015. New operating strategies for molten salt in line focusing solar fields - Daily drainage and solar receiver preheating. Tabernas, s.n.

Energy Globe World Award 2017, 2017. Energy Globe. [Online] Available at: https://www.energyglobe.info/awards/project/awdid/227922/year/2017/.

Enriquez, L.C., 2017. Nueva generacion de centrales termosolares con colectores solares lineares acoplados a ciclos supercriticos de potencia, Madrid: Universidad Politecnica de Madrid, tésis doctoral.

European Academies Sciences Advisory Council (EASAC), 2011. Concentrating solar power: its potential contribution to a sustainable energy future. The Clyvedon Press Ltd, Cardiff, Halle.

Fairly, P., 2016. Spectrum. [Online] Available at: https://spectrum.ieee.org/at-work/innovation/profile-hittite-solar-energy.

Feldhoff, J.F., et al., 2014. Status and first results of the DUKE project – Component qualification of new receivers and collectors. Energy Procedia, Elsevier, 49 (SolarPACES 2013), p. 1766–1776.

GIZ, 2014. Solar Thermal Heat & Power - Parabolic Trough Technology for Chile. GIZ Brasil, Santiago de Chile.

Glass Point Solar, 2013. Fact Sheet GlassPoint Collector, California: s.n.

GlassPoint, 2019. [Online] Available at: glasspoint.com [Accessed 25. 01. 2019].

Good, P., et al., 2013. Towards a Commercial Parabolic Trough CSP System using Air as Heat Transfer Fluid. Elsevier, Las Vegas.

Günter, M., Joemann, M., Csambor, S., 2011. Advanced CSP Teaching Materials - Chapter 05: Parabolic Trough Technology, -: EnerMENA and German Aerospace Center [DLR].

HeliosCSP, 2015. Concentrated Solar Power SkyFuel Completes Efficiency Testing of the SkyTrough DSP Collector. [Online] Available at: http://helioscsp.com/concentrated-solar-power-skyfuel-completes-efficiency-testing-of-the-skytrough-dsp-collector/.

HelioTrough, 2019. http://www.heliotrough.com/. [Online] [Accessed 01. 06. 2019].

Heliovis, A.G., 2018. Frequently Asket Questions. Heliovis, Wiener Neudorf.

IRENA, 2012. Renewable Energy Technologies. International Renewable Energy Agency, Vol. 1(2/5), p. 48.

ISE, 2015. Current and Future Cost of Photovoltaics. Long-term Scenarios for Market Development, System Prices and LCOE of Utility-Scale PV Systems. Agora Energiewende & ISE Fraunhofer Institute, Ettlingen.

Jähning, D., 2005. Entwicklung und Optimierung eines Parabolrinnekollektosystems zur Erzeugung von Prozesswärme für industrielle Produktionsprozesse, Fabrik der Zukunft. [Online] Available at: www.aee-intec.at/0uploads/dateien26.pdf [Accessed 06. 08. 2019].

Janotte, N., 2012. Requirements for Representative Acceptance Tests for the Prediction of the Annual Yield of Parabolic Trough Solar Fields. Shaker Verlag, Germany.

Jones, S., 2001. TRNSYS Modeling of the SEGS VI Parabolic Trough Solar Electric Generating System. s.l., s.n.
Jung, C., Dersch, J., Nietsch, A. & Senholdt, M., 2015. Technological perspectives of silicone heat transfer fluids for concentrated solar power. Energy Procedia, Volume 69 SolarPACES 2014, p. 663–671.
Kearney, D., 2003. Assessment of a Molten Salt Heat Transfer Fluid in a Parabolic Trough Solar Field. J. Sol. Energy Eng. 125, 170–176.
Krüger, D., et al., 2018. Ergebnisbericht: ConSol - Concrete Solar Collector, Germany: DLR, TU Kaiserslautern, RUB, Solarlite, Almeco, Stanecker, Pfeifer.
Kurup, P., Turchi, Craig S., 2015. Parabolic Trough Collector Cost Update for the System Advisor Model (SAM). National Renewable Energy Laboratory (NREL), Denver.
Laezman, R., 2009. https://www.ecmag.com/. [Online] Available at: https://www.ecmag.com/section/miscellaneous/breakthrough-technology-could-heat-market-concentrated-solar-power [Accessed 18. 09. 2019].
Liang, H., et al., 2018. Study on the thermal performance of a novel cavity receiver for parabolic trough solar collectors. Appl. Energy 15 July, Volume 222, pp. Pages 790–798.
Lipman, E., 2019. Vice President of the R&D Department, Brenmiller Energy [Interview] (18. 03. 2019).
Lüpfert, E., 2015. MS-Trough Marktbetrachtung. DLR - Institut für Solarforschung, Köln.
Lüpfert, E., et al., 2003. EuroTrough collector qualification complete - performance test results from PSA. DLR, CIEMAT, Flagsol GmbH, sbp, Almeria.
Maccari, A., et al., 2015. Archimede Solar Energy Molten Salt Parabolic Trough Demo Plant: A Step Ahead towards the New Frontiers of CSP. Energy Procedia, 05 June, Volume 69, pp. 1643–1651.
Mason, A., Reitze, E., 2013. Establishing bankability for high performance, cost reducing SkyTrough parabolic trough solar collector. s.l., s.n.
McMullen, P., 2016. Using Molten Salts as a Heat Transfer Fluid and Thermal-Storage Medium. [Online] Available at: https://www.process-heating.com/articles/91918-using-molten-salts-as-a-heat-transfer-fluid-and-thermal-storage-medium [Accessed 01. 10. 2020].
Meyen, S., Lüpfert, E., Pernpeintner, J., Fend, T., 2009. Optical Characterisation of Reflector Materials for Concentrating Solar Power Technology. Berlin, Germany, s.n.
Mwesigye, A., Zhongjie, H., Meyer, P.J., 2015. Thermodynamic optimisation of the performance of a parabolic trough receiver using synthetic oil–Al2O3 nanofluid. Appl. Energy 15 (10), 398–412.
Neises, T., Turchi, C., 2014. A comparison of supercritical carbon dioxide power cycle configurations with an emphasis on CSP applications, 01. 06 Energy Procedia 49, 1187–1196.
O'Rourke, D., et al., 2015. Improved Large Aperture Collector Manufacturing. Abengoa Solar LLC, Lakewood.
Own Creation, 2013. Wikipedia. [Online] Available at: https://commons.wikimedia.org/wiki/File:Parabolic_trough_at_Harper_Lake_in_California.jpg.
Perers, B., 2016. A CSP plant combined with biomass CHP using ORC-technology in Brønderslev Denmark. International Solar Energy Society, Lyngby.
Pitz-Paal, R., et al., 2007. Development steps for parabolic trough solar power technologies with maximum impact on cost reduction. J. Sol. Energy Eng. 129, 8. https://doi.org/10.1115/1.2769697.
Prahl, C., 2009. Solar Power Plant Costs Estimation with differnt Modells, s.l.: s.n.
Prahl, C., 2015. Strukturoptimierung einer Parabolrinne mit ortsfester Brennlinie. s.l., s.n.
Prahl, C., 2019. Inventor of the Fixed Focus Split Mirror Collector [Interview] (15. 02. 2019).
Prahl, C., Pfahl, A., 2009. A New Concept For Line-Concentrating CSP Collectors. SolarPaces, Tabernas.
Price, H., et al., 2002. Advances in parabolic trough solar power technology. J. Sol. Energy Eng. 120, 17. https://doi.org/10.1115/1.1467922.
Raush, J.R., Chambers, T.L., 2014. Initial field testing of concentrating solar photovoltaic (CSPV) thermal hybrid solar energy generator utilizing large aperture parabolic trough and spectrum selective mirrors. Int. J. Sustain. Green Energy 3 (6), 123–131.
Reuters, 2014. The Voice of the Orthodox Jewish Community. [Online] Available at: https://www.vosizneias.com/194194/2015/02/09/jerusalem-israeli-company-to-build-20-hour-per-day-solar-power-plant/ [Accessed 20. 03. 2019].
Riffelmann, K.-J., et al., 2009. HelioTrough-A New Collector Generation for Parabolic Trough Power Plants. Flagsol, Cologne.
Riffelmann, K., Richert, T., Nava, P., Schweitzer, A., 2013. Ultimate Trough® – A significant step towards cost-competitive CSP. Cologne, s.n.
Röger, M., Potzel, P., Pernpeintner, J., Caron, S., 2014. A Transient thermography method to separate heat loss mechanisms in parabolic trough receivers. J. Sol. Energy Eng. 136 (011006–1), 9.
Ruegamer, T., et al., 2014. Molten salt for parabolic trough applications: system simulation and scale effects. Energy Procedia, Elsevier 49, 1523–1532.
sbp, 2012. Schlaich bergemann and partner. [Online] Available at: https://www.sbp.de/en/project/ultimate-trough-testloop/ [Accessed 08. 11. 2019].
sbp, Ultimate Trough, 2013 [Accessed 3 July 2020].
Schenk, H., Eck, M., 2012. Yield Analysis for Parabolic Trough Solar Thermal Power Plants - A Basis Approach. DLR, Cologne.
Schiel, W., 2011. Next Generation Parabolic Trough. Jülich, s.n.
SCHOTT Solar CSP GmbH, 2013. Data sheet PTR®70 Receivers, Mainz: s.n.
Schuknecht, N., McDaniel, J., Filas, H., 2018. Achievement of the $100/m2 Parabolic Trough. SkyFuel Inc, Lakewood.
Sener, 2018. SenerTrough-2: New Optimized Solar Collector. Sener, Fact Sheet, s.l.
Skyfuel, 2017. ReflechTech Product Information (Data Sheet). [Online] Available at: http://www.skyfuel.com/downloads/brochure/Brochure_ReflecTech.pdf [Accessed 30. 11. 2018].
SkyFuel, 2017. SkyTrough Product Information (Data Sheet). [Online] Available at: http://www.skyfuel.com/downloads/brochure/SkyTroughBrochure.pdf [Accessed 29. 11. 2018].
SkyFuel, 2017. SkyTroughDSP Product Information (Data Sheet). [Online] Available at: http://www.skyfuel.com/downloads/brochure/SkyTroughDSPBrochure.pdf [Accessed 30. 11. 2018].
Solar Millenium AG, 2008. Die Parabolrinnen-Kraftwerke Andasol 1 bis 3, Erlangen: Solar Millenium.
Solarlite GmbH, 2010. Solar Trough Technology - SL4600, Technical Datasheet, Duckwitz: Solarlite.
SolarPaces & IEA, 2019. https://www.solarpaces.org/. [Online] Available at: https://www.solarpaces.org/wp-content/uploads/status.jpg [Accessed 08. 05. 2019].
Soleval Termosolar, 2016 [Accessed 04 Dec 2020].
Speciality Structures and Installations, 2017. Boulder City, Nevada. [Online] Available at: http://specialty-structures.com/portfolio-reader/nevada-solar-one.html [Accessed 11. 08. 2019].
Stancich, R., 2012. toughTrough: From renewable to invincible. CSP Today 18 (05), 3.
Subramani, J., et al., 2017. Experimental study on the thermal performance and heat transfer characteristics of solar parabolic trough collector using Al2O3 nanofluids. Environ. Progress Sustain. Energy 2018, p. 37(3):114 (03.10).
toughTrough, 2018. Fact Sheet: Innovative Solar Mirror Technology. [Online] Available at: www.toughtrough.com [Accessed 03. 12. 2019].
Turchi, C., Mehos, M., 2010. Current and Future Costs for Parabolic Trough and Power Tower Systems in the US Market. National Renewable Energy Laboratory (NREL), Perpignan.
Usmani, B., & Harinipriya, S., 2015. Chapter 15: High-Temperatur Solar Selective Coating. In: Systems Thinking Approach for Social Problems: Proceedings of 37th National Systems Conference, December 2013 (pp.9). s.l.:Springer.
VDI-Richtlinie, 1998. VDI2225 - Konstruktionsmethodik, Technisch-Wirtschaftliches Konstruieren, Technisch-Wirtschaftliche Bewertung (Blatt 3). Verein Deutscher Ingenieure, Düsseldorf.
Vignolini, M., 2009. A new approach to concentrating solar plant (CSP) by ENEA. ENEA - DESERTEC, Italy.
Vijayan, S.N., Kumar, S.S., 2017. Theoretical Review on Influencing Factors in the Design of Parabolic Trough Collectors. Int. J. Mech. Mater. Eng. 11 (11), 6.
Wagner, P.H., 2012. Thermodynamic simulation of solar thermal power stations with liquid salt as heat transfer fluid. Technisch Universität München, Lehrstuhl für Energiesysteme, München.
Wallace, D., 2018. Sciencing. [Online] Available at: https://sciencing.com/about-6711987-price-steel-vs–stainless-steel.html [Accessed 05. 07. 2019].
Wang, Z., 2019. Design of the Concentration System, s.l.: Design of Solar Thermal Power Plants.
Yokohama, P., 2010. Archiemede Solar. [Online] Available at: http://www.archimedesolarenergy.it/events_archive.asp?pagina=2 [Accessed 07. 12. 2018].